

**Satellite Remote Sensing of *Nereocystis luetkeana* (Bull Kelp) and the
use of Kelp by Juvenile Salmon in the Salish Sea.**

By

Sarah B. Schroeder

B.Sc., University of Victoria, 2016

A Thesis Submitted in Partial Fulfilment of the Requirements for the Degree of

MASTER OF SCIENCE

in the Department of Geography

©Sarah B. Schroeder, 2019
University of Victoria

*All rights reserved. This thesis may not be reproduced in whole or in part by
photocopy or other means, without the permission of the author.*

**Satellite Remote Sensing of *Nereocystis luetkeana* (Bull Kelp) and
the use of Kelp by Juvenile Salmon in the Salish Sea.**

By

Sarah B. Schroeder

B.Sc., University of Victoria, 2016

Supervisory Committee

Dr. M. Costa, Co-supervisor (Department of Geography)

Dr. F. Juanes, Co-supervisor (Department of Biology)

Dr. C. Robinson, Member (Department of Geography)

Abstract

The macro-algae *Nereocystis luetkeana* or bull kelp is an important canopy-forming species in the rocky nearshore ecosystems of the Salish Sea. It provides structural habitat for many fish and invertebrates including juvenile salmon. In the Pacific Northwest, major declines in Chinook and Coho salmon populations have led to increased scientific efforts to determine the causes behind these losses. High mortality of juvenile salmon during their first months in the marine environment may be linked to loss of habitat such as kelp beds, which can provide shelter, concentration of prey and energetically favorable conditions. This work seeks to understand the role of kelp habitat in the early marine growth period of juvenile salmon. Initially, methods using satellite imagery were developed for mapping the location of kelp beds adjacent to a salmon bearing river in Cowichan Bay, on the West Coast of British Columbia. These methods were then applied to a time series of imagery from 2004 to 2017, to determine how kelp beds are changing over time and the possible drivers of those changes. The results found spatial and temporal variability in kelp beds with a decline from a high in 2015 to the lowest levels in 2017. The observed changes were over a short period considering the natural variability of *Nereocystis* and continued long term monitoring will help to determine if the declines are permanent. Spatial and temporal variability were found to relate to substrate type, current strengths and potential lag effects of declines due to warmer than average sea surface temperatures. Lastly, the maps created through satellite-based methods served to inform surveys investigating the importance of kelp habitat to the declining populations of Chinook and Coho salmon. To address this, remote underwater video and visual snorkel surveys were used to determine the presence and absence of juvenile salmon in paired kelp and no-kelp sites throughout the season when the fish are known to be present in the region. Higher densities of

juvenile salmon were detected in kelp-associated areas; however, this effect was detected both before kelp growth in early spring and during kelp presence. Transects conducted on the inner edge of kelp beds, adjacent to rocky shorelines were determined to have the highest salmon densities indicating that physical factors such as substrate type and wave energy associated with these areas may be preferential to juvenile salmon.

Table of Contents

Supervisory Committee	ii
Abstract	iii
Table of Contents	v
List of Tables	viii
List of Figures	ix
Acknowledgements	xi
Co-authorship Statement	xii
1.0 Introduction	1
1.1 Overview	1
1.2 Research Objectives	2
1.3 Thesis Structure	3
2.0 Passive Remote Sensing Technology for Mapping Bull Kelp (<i>Nereocystis luetkeana</i>): A Review of Techniques and Regional Case Study	4
2.1 Abstract	4
2.2 Introduction	4
2.3 Optical Remote Sensing of Bull Kelp: Principles	6
2.3.1 Optical Properties of Kelp Beds	6
2.3.2 Bull Kelp Morphology and Growth	8
2.4 Methods for Optical Remote Sensing of Macro Algae	10
2.4.1 Imagery Acquisition	11
2.4.2 Ground-truthing Data	14
2.4.3 Image Processing	17
2.4.4 Classification	21
2.4.5 Validation and Accuracy Assessment	24
2.4.6 Products	25
2.5 Case Study: Remote Sensing of Bull Kelp in the Salish Sea	26
2.5.1 Study Site	26
2.5.2 Methods	26
2.5.3 Results and Discussion	29
2.6 Conclusion	35

3.0 Spatial and Temporal Persistence of Nearshore Kelp Beds on the West Coast of British Columbia, Canada using Satellite Remote Sensing.....	37
3.1 Introduction	37
3.2 Methods.....	39
3.2.1 Study Area	39
3.2.2 Imagery database	40
3.2.3 In situ dataset	41
3.2.4 Image Processing and Classification	43
3.2.5 Classification	45
3.2.6 Change Analysis	46
3.3 Results	48
3.3.1 Image Reliability	48
3.3.2 Spatial Patterns of Persistence	51
3.3.3 Temporal Change	53
3.3.4 Spatial Drivers	54
3.4. Discussion	56
3.4.1 Limitations of Satellite Imagery	56
3.4.2 Spatial Drivers	57
3.4.3 Temporal Change	58
3.5. Conclusion.....	60
4.0 Investigating the Use of Kelp Habitat by Juvenile Salmon during Early Marine Residency. 62	
4.1 Introduction	62
4.2 Methods.....	63
4.2.1 Study Area	63
4.2.2 Field Methods	64
4.2.3 Snorkel Data	65
4.2.4 Video Data.....	66
4.3 Data Analysis	67
4.3.1 Snorkel Data	67
4.3.2. Video Data.....	68
4.4 Results	68
4.4.1 Snorkel Data	68
4.4.2 Video Data.....	71

4.5 Discussion	72
4.5.1 Snorkel vs video survey.....	72
4.5.2 Juvenile salmon: kelp vs no-kelp habitat.....	73
4.6 Conclusion.....	76
5.0 Summary and Conclusions	78
6.0 References	81

List of Tables

Table 1. Remote sensing of floating macro algae studies relevant to the detection of bull kelp. Note that this table is not a comprehensive list of all studies, but presents a sample of relevant techniques from the literature.	15
Table 2. Remote sensors used for floating macro algae detection	17
Table 3. Indices used for enhancing detection of floating Macro Algae where R = reflectance, SWIR, NIR, Red, Green, Blue indicate the bands from the sensors being used. For full variable definitions, refer to the literature cited.	20
Table 4. Error matrices for Minimum Distance (MD), ISODATA (ISO), Decision Tree (DT) spectral unmixing SU, and OBIA classification results for bull kelp in the Salish Sea.	31
Table 5. Selection of classification methods based on quality of input parameters.	35
Table 8. Validation error matrix for the 2016 Image using a subset of concurrent field data.	49
Table 9. Wilcoxon tests for differences between field data from 2016 base image and other imagery.	50
Table 10. Results of Paired Wilcoxon Signed Rank Test for Salmon Density measured by Snorkel Survey	70
Table 11. Results of Paired Wilcoxon Signed Rank Test for maxN of Kelp and Nok areas calculated from stationary video data.	72

List of Figures

Figure 1. Reflectance of dense (>50% of 1m ² covered), sparse (<50% of 1m ² covered), submerged kelp (all plants slightly below water surface) and ocean water measured with a Fieldspec Pro® spectroradiometer in the coastal waters of British Columbia, Canada.....	8
Figure 2. (a) Overhead view (satellite view) of floating bull kelp, with the bulb and part of the stipe emerged, and the blades submerged in water. (b) Bull kelp bed cross-section. The length of the stipe and the height of the tide affects whether kelp is submerged or emerged.	10
Figure 3. Generalized workflow for mapping floating macro algae with optical imagery, following previous research.	11
Figure 4. Left: Regional context of study area (black box) Cowichan Bay and Sansum Narrows on the east coast of Vancouver Island, British Columbia, Canada. Right: extent of study area, covering Cowichan Bay and Sansum Narrows.	26
Figure 5. Result of minimum distance (MD) supervised classification with total accuracy of 90.7.....	32
Figure 6. Classification results for the MD, DT, SU, OBIA, and ISO classifications on a subset of the true colour WorldView 3 image for bull kelp in the Salish Sea.	33
Figure 7. Errors in classification methods for submerged vegetation, shadow, bright objects, sparse kelp beds, and dense kelp beds in the Salish Sea.....	34
Figure 8. Study area including Cowichan Bay and Sansum Narrows on the East Coast of Vancouver Island, British Columbia, Canada. Red polygons are kelp beds delineated by a kayak-based field survey in August 2016. Hatched lines indicate the total area covered by the kayak-based field survey in August 2016.	40
Figure 9. Representative reflectance of dense (>50% of FOV), sparse (<50% of FOV), submerged kelp and ocean water measured with a Fieldspec Pro® spectroradiometer in the coastal waters of British Columbia, Canada.....	43
Figure 10. Example of normalization for water based on the 2016 corrected image (2016 Reference), and results before (RrsATM) and after normalization (RrsNorm) for each image year. Note the generalized decreased reflectance in band 1 (blue spectra) between RrsATM and RrsNORM showing improved Rayleigh correction, and the expected low and high band 4 (NIR) reflectance for water and kelp, respectively.	45
Figure 11. Boxplots of the relative distributions of sampled kelp pixels (n=500), for the classification results of each image year and the reference.	49
Figure 12. Classification results for the five images with each year's image extent shown in dashed lines. Note the difference in coverage area for the 2004 image which did not cover East Sansum.	50
Figure 13. Persistence of kelp beds in Cowichan Bay and Sansum Narrows from 2004 to 2017. Shaded grey areas indicate the Sub regions of SC= South Cowichan, NC= North Cowichan, WS= West Sansum, ES= East Sansum, OP= Octopus point, MB= Maple Bay, N= North channel.	52

- Figure 14.** Percentage of total shoreline units with persistence of kelp by sub-region and entire region. East Sansum units are calculated from only four images (2012, 2015, 2016, and 2017) due to differences in number of images. For region definitions, see Figure 13..... 53
- Figure 15.** Percent of Kelp Units containing kelp each year by sub region and overall. Sub regions are: East Sansum (ES), North Cowichan (NC), South Cowichan (SC), and West Sansum (WS). Note OP, MB and N were not included as no units had kelp in any year. No data were available for ES in 2004 due to imagery coverage. 54
- Figure 16.** Kelp persistence across substrate types (top) and RMS tide (bottom), where RMS 0.1 is low current and 0.9 is high current..... 55
- Figure 17.** Coastal class (Top) and RMS tidal speeds (bottom) by Region. SC=South Cowichan, NC=North Cowichan, WS=West Sansum, ES=East Sansum, OP=Octopus Point, MB=Maple Bay, N=North..... 56
- Figure 18.** Location of sampling sites on the north side of Cowichan Bay, East Coast of Vancouver Island, British Columbia, Canada. Green polygons indicate kelp beds mapped by kayak in 2016. 64
- Figure 19.** Location of snorkel transects, remote camera's and kelp and no-kelp areas within the four sampling sites. 66
- Figure 20.** Image and diagram of remote underwater video tripod. Two cameras facing opposite directions adjustable up to 3.5m vertically and 360 degrees depending on orientation of kelp and direction of sun. 67
- Figure 21.** Snorkel data for average salmon density per m^3 error bars indicate one standard deviation by a) Habitat, and Habitat by b) Transect, c) Site and d) Week. Star indicates time when kelp was present at surface. Arrows indicate weeks of hatchery salmon release. April 17th and May 24th. Note: The different scales for the y-axis due to the range of values included with the error bars. 70
- Figure 22.** Average MaxN and one standard deviation by habitat type (A, D), site (B, E) and week (C, D) for video data and the analogous average salmon density from the middle transect of snorkel data. Note: Different scales are used for the y-axis due to the range in values when including error bars. 72

Acknowledgements

I would like to express my sincere gratitude to my supervisory committee –Dr. Maycira Costa, Dr. Francis Juanes and Dr. Cliff Robinson for their support and guidance throughout the journey of developing my research goals, implementing field surveys and thesis writing. I would also like to thank all of the collaborators on this project including the SeaChange Marine Conservation Society, including Leanna Boyer for providing her knowledge, skills, and leadership with kayak-based kelp mapping. Many thanks to Colleen Dupont for being an excellent and enthusiastic field and research assistant. To my colleagues in the Spectral lab, you provided much needed support guidance and encouragement throughout my master's studies. Finally, I would like to thank my partner and my family members and for their support and patience.

Funding for this research was provided by the Pacific Salmon Foundation through the Salish Sea Marine Survival Project.

Co-authorship Statement

This thesis contains the manuscripts for three scientific papers, published or submitted to academic journals as part of the goals of this project in partnership with the Pacific Salmon Foundation and SeaChange under the Salish Sea Marine Survival Project. For these manuscripts, I led all the research, fieldwork, data preparation, analysis, and writing. Dr. Costa and Dr. Juanes provided support through input into developing research questions, understanding research results and editorial comments incorporated into the final manuscripts. Ms. Boyer and Ms. Dupont provided assistance with fieldwork including the previous development of kayak-based mapping protocols and preliminary literature review respectively.

1.0 Introduction

1.1 Overview

The Salish Sea is a body of water encompassing the Strait of Georgia, Puget Sound, and the Strait of Juan de Fuca on the west coast of North America. This biodiverse region is home to many iconic marine organisms and important habitats. It is also home to over seven million people with several large cities and coastal developments in the region (Gaydos et al., 2008). This has impacts on the marine environment through shipping, mining, forestry, urban and industrial activities (Dethier et al., 2016; Springer, Hays, Carr, & Mackey, 2007). Anthropogenic influences and changing environmental conditions such as sea surface temperature, dissolved oxygen levels, and alteration in stream flows cause disturbances to the intricate connections between trophic levels in the ecosystem (Beamish, Sweeting, Neville, & Lange, 2005; Riche, Johannessen, & Macdonald, 2014). These disturbances have varying effects on all aspects of the Salish Sea ecosystem, including Pacific salmon species, which are crucially important to marine and terrestrial food webs as well as a commercially significant (Gislason, Lam, Gunnar, & Guettabi, 2017; Schindler et al., 2003). Changing and deteriorating habitat and environmental conditions are a concern in maintaining a healthy functioning ecosystem in the Salish Sea (Mumford, 2007).

One example of potential impacts is changes in the distribution and persistence of bull kelp (*Nereocystis luetkeana*) and the effect of these changes on fish species that interact with them (Springer et al., 2007). Bull kelp is an important habitat forming macro algae in the nearshore region of the Salish Sea (Carney, 2005). This canopy forming kelp provides structural habitat, which is utilized by a variety of organisms including juvenile salmon (Shaffer, 2004; Thom & Hallum, 1990). Further, dense growth of kelp beds can dampen the effects of waves on the shoreline, create nutrient entrainment and acts as a source of carbon to detrital food webs (Duggins, Eckman, Siddon, & Klinger, 2001; Duggins, 1988; Krumhansl & Scheibling, 2012).

Reports of declining kelp beds have been increasing in the Salish Sea and along the west coast of North America (Berry, Mumford, & Dowty, 2005; Van Wagenen, 2015). Factors contributing to this decline may include increase in average sea-surface temperature, higher levels of turbidity, unchecked herbivory due to predator loss and changes in the light and nutrient availability in the

region (Foster & Schiel, 2010; Halpern, Cottenie, & Broitman, 2006; Steneck et al., 2002). Loss of this important habitat, among others, has been identified as a contributor to the decline in Pacific salmon populations (David et al., 2016; Ruff et al., 2017). In particular, high mortality of juvenile salmon in their first months in the marine environment has been identified as a key driver of population decline (Kemp, 2014; Preikshot, Beamish, Sweeting, Neville, & Beacham, 2012). As salmon smolt grow they move away from the estuary and forage along the nearshore region where kelp habitats are common (Duffy, Beauchamp, Sweeting, Beamish, & Brennan, 2010).

To understand the impacts that changes in habitat availability and quality may have on juvenile salmon, it is essential to have accurate knowledge of the habitat distribution. Accurate maps of nearshore habitats including kelp and continuous temporal data are needed to discern changes to its extent and potential drivers of these changes (Van Wagenen, 2015). Satellite-based mapping can provide important information on changing kelp beds given the large areas that can be mapped that may not be accessible to field-based methods such as boats (Jensen, Estes, & Tinney, 1980). Satellite imagery also covers a large temporal period extending back to the 1980s allowing a time series of changes in kelp distribution over time to be created using the known spectral reflectance of kelp (Cavanaugh, Siegel, Kinlan, & Reed, 2010; Stekoll, Deysher, & Hess, 2006).

Mapping kelp is the first step in understanding how the health of this habitat may influence the species that use them. While there is much anecdotal evidence, there is a gap in scientific literature regarding the importance of kelp beds to juvenile salmon and, specifically, in BC, few studies have been published on bull kelp extent (Sutherland, Karpouzi, Mamoser, & Carswell, 2008), spatial temporal changes (Watson & Estes, 2011) and the use of kelp by juvenile salmon (Shaffer, 2004) due to difficulties in sampling this complex habitat.

1.2 Research Objectives

This goal of this thesis is to detect and map changes in the extent and persistence of kelp habitat and evaluate the use of kelp by juvenile salmon with the following specific objectives:

- (1) Develop methods for the accurate mapping of kelp distribution using high resolution satellite imagery in the fringing nearshore kelp beds of the Salish Sea;

- (2) Apply methods to a time series of historical satellite images to define kelp persistence over time; and
- (3) Evaluate the use of kelp habitats by juvenile Pacific salmon using non-invasive techniques of remote underwater video and snorkel surveys.

1.3 Thesis Structure

This thesis is organized into three individual papers to address the research objectives. The first paper (Chapter 2) provides a literature review on the methods used in the remote sensing of floating macro-algae using high-resolution satellite imagery and demonstrates how they can be applied to the detection of bull kelp through a case study (Schroeder, Dupont, Boyer, Juanes, & Costa, 2019). The second paper (Chapter 3) applies the methods developed for detecting kelp to a time series of historical imagery and explores the potential issues and results of change analysis and the drivers of kelp persistence (Schroeder, Boyer, Juanes, & Costa, In Press). The third and final paper (Chapter 4) discusses the process and methods of surveying kelp beds in relation to its importance to the survival of juvenile Pacific salmon. As these papers were prepared as independent publications there is some repetition of background information pertaining to the subject of kelp beds and remote sensing. The thesis concludes with a summary of the key findings of each paper (Chapter 5).

2.0 Passive Remote Sensing Technology for Mapping Bull Kelp (*Nereocystis luetkeana*): A Review of Techniques and Regional Case Study

2.1 Abstract

The distribution and abundance of the canopy-forming kelp *Nereocystis luetkeana* is of increasing concern for environmental management and conservation in coastal regions due to its importance as a foundation species. Mapping kelp forests aids in understanding their health, productivity, and response to environmental conditions. Remote sensing using satellites is an increasingly accessible tool for mapping nearshore habitats allowing for applications such as long-term monitoring and large- and small-scale surveys. This paper provides a review of passive optical remote sensing techniques for detection and mapping of floating macro-algae, and adapts these techniques for detecting *Nereocystis luetkeana*, demonstrating their application through a comprehensive case study, from imagery acquisition to map validation. This review with associated case study communicates to non-remote sensing experts a road map to use remote sensing technology for mapping kelp habitats.

2.2 Introduction

Bull kelp (*Nereocystis luetkeana*) is a brown algae in the order Laminariales, and represents one of two important canopy-forming kelp species found in marine nearshore habitats on the west coast of North America, along with giant kelp (*Macrocystis pyrifera*) (Druehl, 1970). Although the two species have similar ranges, extending from Alaska to California, there are differences in local scale distribution due to variations in tolerance to temperature and wave exposure. Often referred to as a foundation species, beds of bull kelp form structural underwater forests that offer habitat for fish and invertebrates (Christie, Norderhaug, & Fredriksen, 2009; Trebilco, Dulvy, Stewart, & Salomon, 2015), and provide nutrients to grazers and to detrital food webs as wrack (Duggins et al., 2001). Also, the three-dimensional structure of beds acts as a physical barrier, reducing coastal erosion and dampening wave action (Eckman, Duggins, & Sewell, 1989). The importance of this species in nearshore ecosystems makes its abundance and distribution of great concern to environmental monitoring and management (Krumhansl et al., 2016; Mumford, 2007; Springer et al., 2007; Teagle et al., 2017).

Several factors determine bull kelp distribution and abundance. Natural factors include grazing pressure (Taylor & Schiel, 2018), physical disturbance from wave action (Reed et al., 2011), and natural variations of light availability, nutrients, and temperature (Bell, Cavanaugh, Reed, & Siegel, 2015; Pfister, Berry, & Mumford, 2018). Anthropogenic factors include direct harvest (Sutherland et al., 2008), increase in herbivores through removal of predators by fisheries (Halpern et al., 2006; Ling, Johnson, Frusher, & Ridgway, 2009), coastal pollution through wastewater (Foster & Schiel, 2010), increased turbidity from shoreline development (Deiman, Iken, & Konar, 2012; Dethier et al., 2016). Larger scale impacts include climate change-induced sea temperature change, ocean acidification, and increased storm activity (Byrnes et al., 2011; Hernández, Sangil, Fanai, & Hernández, 2018; Vergés et al., 2016). For instance, there have been reports of bull kelp decline following abnormally high temperature disturbances and local scale losses attributed to regions with high anthropogenic stress (Pfister et al., 2018; Schiel, Steinbeck, & Foster, 2004). In many regions, however, data on the spatial temporal distribution and abundance of bull kelp are lacking, making it difficult to define the impact of human activities and environmental drivers on this ecologically important foundation species.

Remote sensing technology, including aerial, drone, and satellite imagery, is becoming a key component of kelp monitoring programs (Bell, Cavanaugh, & Siegel, 2015; Casal, Kutser, Domínguez-Gómez, Sánchez-Carnero, & Freire, 2013; Cavanaugh et al., 2010; Pfister et al., 2018). Specifically, satellite data is advantageous for mapping large areas as it provides multi-temporal data in both visible and infrared wavelengths, and requires less time and labour than traditional boat- or diver-based surveys (Casal, Sánchez-Carnero, Sánchez-Rodríguez, & Freire, 2011). Furthermore, remote sensing technologies have the potential to improve spatial and temporal coverage through automation and repeatability (Augenstein, Stow, & Hope, 1991; Nijland, Reshitnyk, & Rubidge, 2019). Through the use of remote sensing technology, we now have a better understanding of regional kelp community dynamics, temporal trends, and oceanographic effects in these communities (Bell, Cavanaugh, & Siegel, 2015; Cavanaugh, Siegel, Reed, & Dennison, 2011).

There is a growing body of research using remote sensing for detecting several species of floating algae, including giant kelp (Augenstein et al., 1991; Bell, Cavanaugh, Reed, et al., 2015; Cavanaugh et al., 2010, 2011; Deysher, 1993; Donnellan & Foster, 1999; Fyfe et al., 1999; Kim, Olsen, Lee, & Jablonski, 2010), *Sargassum* (Dierssen, Chlus, & Russell, 2015; J Gower, Hu,

Borstad, & King, 2006; Jim Gower & King, 2008; Marmorino, Miller, Smith, & Bowles, 2011; Wang & Hu, 2016), and green algae (Cui et al., 2012; Keesing, Liu, Fearn, & Garcia, 2011; Ma, Li, Lan, & Li, 2009; Shi & Wang, 2009). In comparison, relatively few studies have used satellite remote sensing to map bull kelp due to the challenge of detecting the generally smaller beds found in close proximity to rocky shorelines (Stekoll et al., 2006). Although key differences exist between various species of floating macro algae, the general principles for detection with remote sensing are similar. Therefore, the methods for detecting giant kelp, green algae, and *Sargassum* are a foundation for developing methods for remote sensing of bull kelp. The objectives of this paper are to (1) outline the principles for optical remote sensing of bull kelp, (2) review methods used by studies to map macro algae and their relevance to bull kelp mapping, and (3) illustrate a methodology for optical remote sensing of bull kelp with a case study in British Columbia, Canada.

2.3 Optical Remote Sensing of Bull Kelp: Principles

The principles for optical remote sensing of bull kelp are based on the algae's morphology and growth patterns, along with the spectral properties of the algae, surrounding seawater, and its optical constituents.

2.3.1 Optical Properties of Kelp Beds

Bull kelp beds are composed of many kelp sporophytes, which grow at or near the water's surface; they may form a dense or sparse canopy, depending on the number and proximity of individuals. The reflectance from kelp beds is composed of signals from the kelp plants floating on the water's surface, as well as water and its optical constituents. As Figure 1 shows, the above-water reflectance signal corresponding to different densities of kelp is generally most prominent at the visible (VIS) and near infrared (NIR) spectra, similar to vascular plants (Cavanaugh et al., 2010; Jensen et al., 1980), and is a result of its physiological and morphological characteristics.

Kelp reflectance at visible wavelengths is largely due to the photosynthetic pigments chlorophyll-a, chlorophyll-c, and fucoxanthin present in the chloroplasts (Wheeler, Smith, & Srivastava, 1984). Dominant pigments are chlorophyll-a with peak absorption at 435 and 675 nm, chlorophyll-c with peak absorption around 460 and 633 nm, and fucoxanthin, absorbing between 500 and 550 nm (Anderson, Barrett, Wolstenhome, & Fitzsimons, 1979; Kotta, Remm,

Vahtmäe, Kutser, & Orav-Kotta, 2014). The absorption characteristics of these pigments result in the brownish colour of the kelp (Charrier, Le Bail, & de Reviers, 2012); note in Figure 1 the lower reflectance in the blue and green wavelengths due to the higher absorption by pigments and slightly higher reflectance towards the red wavelengths. Higher reflectance in the near infrared spectra between 700 and 900 nm is mostly due to the internal cellular structure of the central tissues, which refract and strongly reflect these longer wavelengths (Liew, Chong, Li, & Asundi, 2008). Pure water, on the other hand, is characterized by low reflectance across all wavelengths and very high absorption in the near infrared due to the absorption properties of water molecules (Mobley, 1994).

When kelp beds are sparse or partially submerged, the detected near infrared reflectance is a combination of the high signal from kelp and low signal from the highly absorbing surrounding water. This reduces the overall signal of both the red and infrared wavelengths (see sparse and submerged kelp vs dense kelp spectral signatures in Figure 1). Furthermore, optical constituents present in the seawater can reduce contrast between the beds and surrounding water, decreasing the detectability of kelp beds. For example, phytoplankton may form dense blooms and increase the near infrared reflectance of seawater (Babin et al., 2003), and suspended sediments generally increase visible and near infrared reflectance, especially red wavelengths (Roesler & Perry, 1995). Coloured dissolved organic matter (CDOM) strongly absorbs visible light, resulting in decreased reflectance in blue wavelengths (Brezonik, Olmanson, Finlay, & Bauer, 2015).

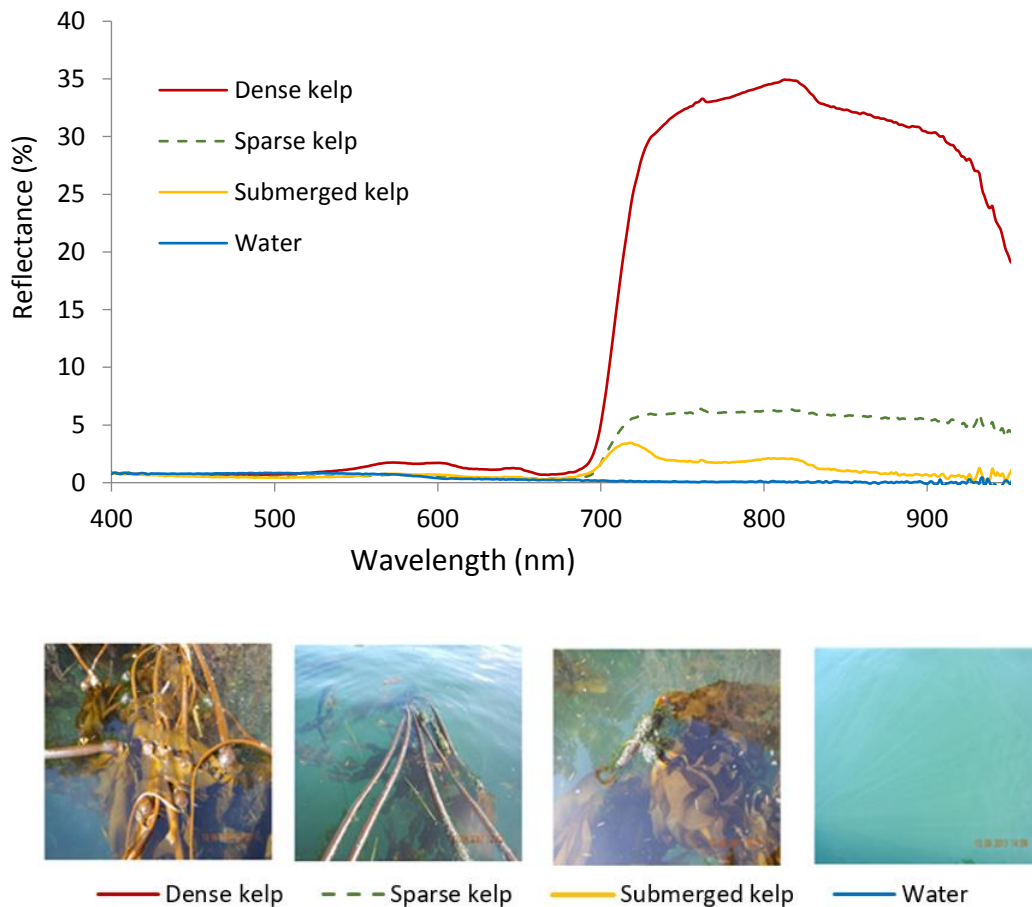


Figure 1. Reflectance of dense (>50% of 1m² covered), sparse (<50% of 1m² covered), submerged kelp (all plants slightly below water surface) and ocean water measured with a Fieldspec Pro® spectroradiometer in the coastal waters of British Columbia, Canada.

2.3.2 Bull Kelp Morphology and Growth

Growth of the bull kelp sporophytes begins in early spring, after which plants grow rapidly and can reach sizes greater than 10 metres in height at their maximum extent by late summer. The physical condition of the sporophyte deteriorates due to prolonged exposure to high currents and temperatures, resulting in dislocation and removal of the plant by fall and winter (Mumford, 2007). Because of its annual growth cycle, late summer is generally the best period for mapping bull kelp.

Each kelp plant is composed of a root-like holdfast that anchors to hard rocky substrate, a long, hollow stem-like stipe, and an air-filled bulb called a pneumatocyst up to 15 cm in diameter (Amsler & Neushul, 1989) from which multiple blades or lamina grow (Figure 2b). The

buoyancy of the bulb and stipe allow the plant to stand upright in the water column and the blades to form a canopy. The portion of kelp canopy floating on the surface or just below the surface allows remote sensing platforms to detect the macro algae (Figure 2a). However, the proportion of kelp canopy at the water's surface can change depending on the length of the kelp, tidal height, currents, bathymetry, and water conditions (Figure 2b).

The density of kelp canopy at the surface will also affect the reflectance detected by a sensor and its ability to discriminate kelp from water. While there is no standard measure to define dense or sparse beds, the distinction may be based on the objective of the study. Aerial-based methods such as Kelp Inventory Monitoring (KIM-1) and its modifications used in British Columbia to quantify kelp extent and biomass (Foreman, 1975; Sutherland et al., 2008) calculate *Nereocystis* density directly from imagery using a point intercept method, and define dense beds as greater than 10 plants per 10 square meters, and sparse as fewer than 10 plants. Other methods have defined density by the percent coverage of plants or fronds visible at the surface, where low density is less than 15% and high density is greater than 15% of a given area (Sutherland et al., 2008). These methods are well suited to remote sensing-based detection where only the reflectance of surface plants can be detected.

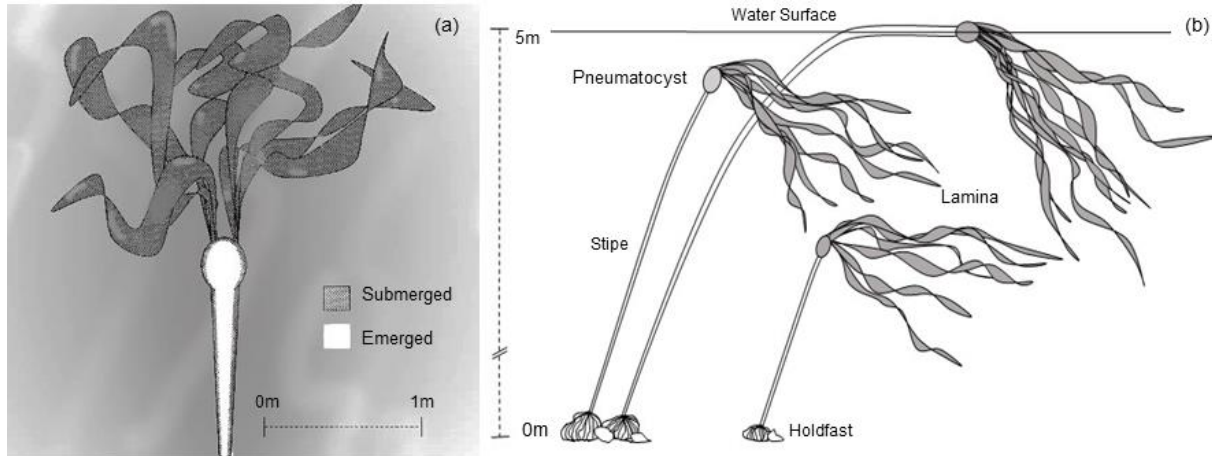


Figure 2. (a) Overhead view (satellite view) of floating bull kelp, with the bulb and part of the stipe emerged, and the blades submerged in water. (b) Bull kelp bed cross-section. The length of the stipe and the height of the tide affects whether kelp is submerged or emerged.

2.4 Methods for Optical Remote Sensing of Macro Algae

We compiled a literature review of studies on the subject of remote sensing of macro algae species including *Nereocystis luetkeana*, *Macrocystis pyrifera*, canopy-forming Laminariales, and other species of floating macro algae, aiming to summarize the methods applicable to the detection of bull kelp. Although the reviewed methods focus on various macro algae species such as *Ulva*, *Sargassum*, and *Macrocystis*, which all have differences in their morphological, temporal, spatial, and spectral characteristics, the remote sensing-based mapping protocols follow the same basic steps and techniques (workflow illustrated in Figure 3).

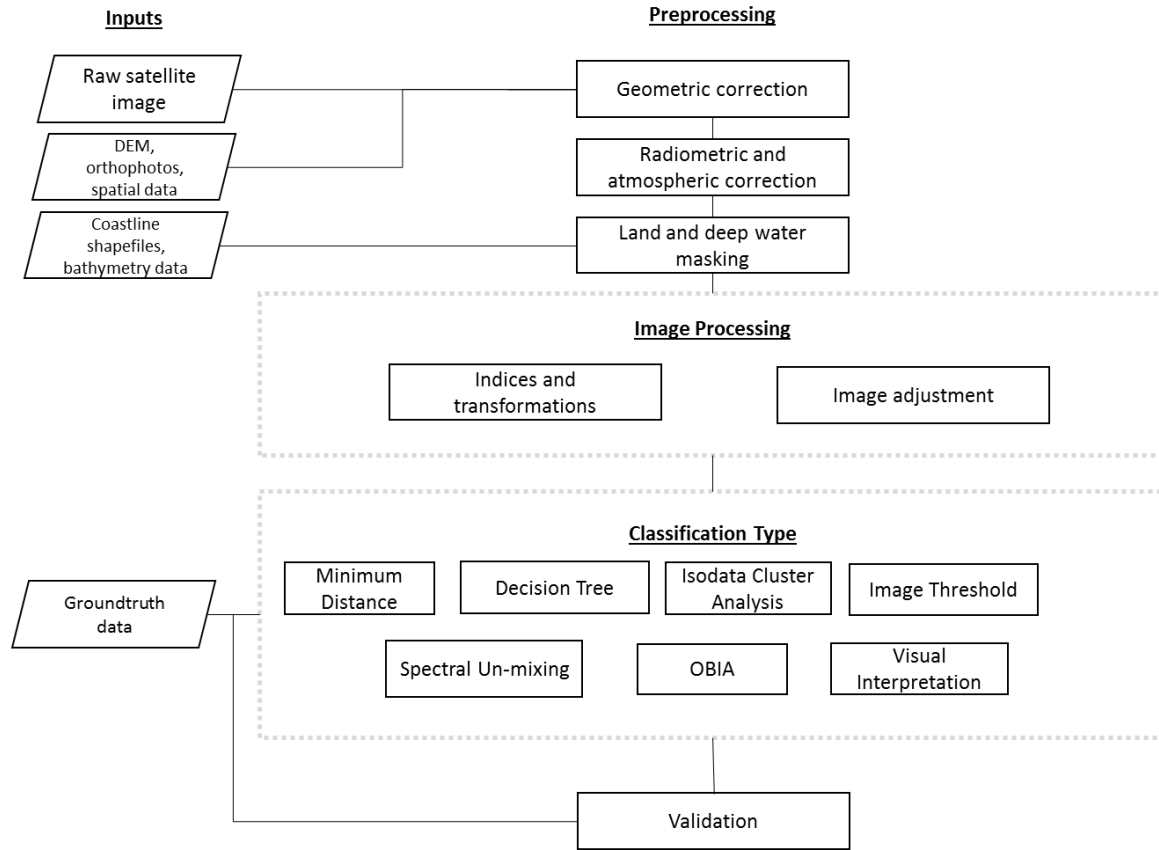


Figure 3. Generalized workflow for mapping floating macro algae with optical imagery, following previous research.

2.4.1 Imagery Acquisition

One of the first steps in remote sensing-based mapping projects is imagery acquisition. The optimal sensor to employ depends on the relationship between the spectral, spatial, and temporal characteristics of the target species and the sensor. Aerial cameras (Donnellan & Foster, 1999; Fyfe et al., 1999; Hu, Feng, Hardy, & Hochberg, 2015; Nezlin, Kamer, & Stein, 2007), airborne hyperspectral (Hu et al., 2015; Stekoll et al., 2006) and multispectral imaging systems (Stekoll et al., 2006), space-borne multispectral sensors (Casal et al., 2011; Cavanaugh et al., 2010; Garcia, Fearn, Keesing, & Liu, 2013; Jim Gower & King, 2008; Hu, 2009; Kim et al., 2010), and more recently, unmanned aerial vehicles (Duffy, Pratt, Anderson, Land, & Shutler, 2018; Nahirnick et al., 2019) have been used in macro algae detection. Along with choosing an appropriate sensor, timing of imagery acquisition is crucial for successful mapping of macro algae. While some macro algae, such as pelagic *Sargassum* and *Ulva*, float freely on the surface and are therefore not affected by tidal height, other macro algae, such as bull kelp, is most exposed during low tide and weak currents, thus defining optimal conditions for imagery acquisition. Furthermore, cloud

cover, water roughness, sun angle, and water column constituents also affect the visibility of macro algae. Rough waters, such as those with breaking waves, can obscure the reflectance of the underlying kelp. Waves and ripples alter the angle between incoming solar radiation and the surface of the water, causing glint, which results in high reflectance across visible and NIR wavelengths and may obscure kelp (Hedley, Harborne, & Mumby, 2005). In practice, it is difficult to time surveys and conditions perfectly; consequently, data are often acquired under sub-optimal circumstances (Casal et al., 2011; Kay, Hedley, & Lavender, 2009).

Aerial Sensors

Aerial imagery utilizes sensors fixed on aircraft to collect overlapping images covering the study area. Images are then used to create orthophotos for delineating kelp beds and deriving products. RGB cameras, near infrared, or hyperspectral sensors may be used depending on the objectives of the project. Near infrared (NIR) aerial imagery has been used since the 1930s for mapping kelp resources, for instance, in California for monitoring giant kelp (Deysher, 1993; North, James, & Jones, 1993), in British Columbia to inventory kelp resources (Foreman, 1975; Sutherland et al., 2008), and in Washington State to map kelp aerial extent, species, and density (Pfister et al., 2018; Van Wagenen, 2015). Beyond NIR imagery, airborne hyperspectral imagers such as AVIRIS, CASI, AISA, and PRISM collect spectral information in very narrow bands over many wavelengths, and provide both high spatial and spectral resolutions, which is beneficial in discriminating between similar species (Dierssen et al., 2015; O'Neill & Costa, 2013). A major benefit of aerial sensors on aircraft is the control of survey timing, temporal, and spatial resolutions so that data acquisition can be optimized, however the costs can be high (R. J. Anderson, Rand, Rothman, Share, & Bolton, 2007). There are private companies that can be contracted to fly and collect images, some of which may process the data into orthophotos for use in classification.

Unmanned Aerial Vehicles (UAV)

The use of unmanned aerial vehicles or drones is becoming increasingly common for all types of habitat mapping (Duffy et al., 2018; Hardin & Jensen, 2011; Kislik, Dronova, & Kelly, 2018; Murfitt et al., 2017; Nahirnick et al., 2019). This method is the most flexible in terms of controlling for environmental variables and flight times; however, it is limited to small areas of spatial coverage. Depending on the altitude of data collection, imagery resolution can be

extremely high (<1cm) (Murfitt et al., 2017), allowing visual counts of individual plants and discrimination of species (Murfitt et al., 2017; Nahirnick et al., 2019). Site-specific studies aiming to estimate parameters such as kelp biomass may be well served by this method. Costs will include the purchase of an appropriate UAV able to carry the sensor of choice (RGB cameras such as a GoPro® or higher-end NIR, multispectral and hyperspectral) and GPS; further requirements are related to country-dependent license and air space limitations. Alternatively, several UAV-based contracting companies are available. In order to accurately process the images, users will need access to appropriate software to create orthomosaics and georeference the images for use in classification (see Kislik et al., 2018).

Satellite Sensors

Spaceborne multispectral imagers are a feasible choice for detecting floating macro algae due to their relatively low cost, high spatial coverage, and available archived data. The various satellite sensors used in previous research (Table 6 and 7) have differing specifications, and therefore different applications for macro algae detection. Coarse spatial resolution imagery from MODIS (250-1000 m) has been used to create indices for large floating macro algae blooms such as *Sargassum* and *Ulva* in the open ocean (Cui et al., 2012; Garcia et al., 2013; J Gower et al., 2006; Jim Gower & King, 2008; Hu, 2009; Hu et al., 2015; Keesing et al., 2011; Shi & Wang, 2009). Medium spatial resolution data from sensors such as Landsat (30m) and SPOT (6m) have been used for detecting giant kelp (Bell, Cavanaugh, & Siegel, 2015; Casal et al., 2011; Cavanaugh et al., 2010, 2011; Deysher, 1993). On the other hand, mapping of nearshore, fringing bull kelp beds requires sensors with meter to sub-meter spatial resolution, such as the QuickBird and WorldView series. Hyperspectral sensors are being planned for the future, and will provide high spectral resolution imagery, which may be necessary to differentiate among species, but have coarser spatial (60 m) and temporal resolutions (Bell, Cavanaugh, & Siegel, 2015). A proof of concept was the HICO sensor onboard the International Space Station, which has proven to be effective for differentiating *Sargassum* from garbage, oil, and other algae (Hu et al., 2015).

There are various procedures for acquiring satellite imagery depending on whether it is freely available or provided by proprietary satellites. Free imagery, such as the Landsat series and Sentinel, can be downloaded from the United States Geological Survey (USGS) and European Space Agency (ESA) (<https://earthexplorer.usgs.gov/>, <https://scihub.copernicus.eu/dhus/>). Several

generations of Landsat satellites have been in operation from 1972 to the present. Older sensors had lower spatial resolution and differing spectral bands, however, the data is a valuable resource and has been utilized by numerous macro algal studies to understand drivers of change over long periods (R. J. Anderson et al., 2007; Bell, Reed, Nelson, & Siegel, 2018; Nijland et al., 2019). MODIS and MERIS are also freely available; images cover large areas (185-100km) but with coarse spatial resolution ($\geq 250\text{m}$). Higher spatial resolution satellites such as the WorldView Series, GeoEye, and QuickBird are proprietary, and imagery can be bought from archived databases or tasked for a specific time and location. The cost of a tasked mission is typically a few thousand dollars (\$27-45 USD per km^2) as there is a minimum order size required.

2.4.2 Ground-truthing Data

For floating macro algae studies, field observations are required to validate remote sensing classifications (Richards & Congalton, 2001), to train supervised classifications (Casal et al., 2011), and to inform product creation such as biomass estimates (Cavanaugh et al., 2010; Stekoll et al., 2006). Ground-truth surveys of kelp are often undertaken by boat, and may involve using divers if biological parameters such as lengths and weights are needed (Stekoll et al., 2006). Basic requirements for ground-truth data are an accurate record of where kelp is located in at least a subset of the area to be imaged. Additional data collected can help with understanding variability within a scene and may include: other species present; physical conditions such as wind speed, surface conditions, tide height, depth of kelp, Secchi depth, or water turbidity; and bed density estimates. More detailed data such as individual plant location, length, and wet/dry weights may also be recorded if products such as biomass are being derived from imagery. For biomass estimates, the location and number of sampling sites may also have an effect on results. For instance, plots placed in the center of beds may be more representative of site-wide biomass than those at the edges (Cavanaugh et al., 2010). A key consideration for field surveying is to acquire field data concurrently with imagery acquisition. However, it is often difficult to achieve simultaneous collection, so the time between acquisitions should be minimized and considered during image processing and interpretation (McCoy, 2005).

Although collecting field data is important for training and for validating a model for classification, it is not always feasible due to inaccessibility of a study area or when using historical imagery. Alternatively, some studies use data from historical maps, classified aerial

photography, and algae harvesting records (Casal et al., 2011; Cavanaugh et al., 2010; Deysher, 1993; Donnellan & Foster, 1999). In some cases, such as the pelagic *Sargassum* survey by Marmorino et al., (2011) alternatives for field data were not available and accuracy assessment was omitted. Similarly, several studies of the *Ulva* bloom in the Yellow Sea proceeded without field data (Keesing et al., 2011; Ma et al., 2009), however, local knowledge was used as the bloom was observed by many vessels during the 2008 Olympic sailing preparations. For the same bloom, another study (Cui et al., 2012) compared satellite-estimated drifting velocity to modelled surface currents as a validation technique in the absence of formal field observations. In all instances, when field data are omitted or substituted, results should be interpreted with caution due to increased uncertainty.

Table 1. Remote sensing of floating macro algae studies relevant to the detection of bull kelp. Note that this table is not a comprehensive list of all studies, but presents a sample of relevant techniques from the literature.

Species	Sensor(s)	Image Processing	Classification	Study
<i>Ecklonia maxima</i> , <i>Laminaria pallida</i>	Colour infrared aerial photography, Landsat 7, Landsat 5	Bispectral and principal component (PC) analysis	Spectral Angle Mapper, supervised classification	(Anderson et al., 2007)
<i>Macrocystis pyrifera</i>	HypIRI, Landsat 5, AVIRIS	MESMA: multiple endmember spectral mixing analysis	MESMA threshold	(Bell et al., 2015b)
<i>Laminariales</i> spp.	SPOT 4	Histogram equalization, band ratios	Supervised angular, unsupervised cluster, visual	(Casal et al., 2011)
<i>Macrocystis pyrifera</i>	SPOT 5	NDVI, PC analysis	NDVI threshold	(Cavanaugh et al., 2010)
<i>Macrocystis pyrifera</i>	Landsat 5	MESMA	MESMA threshold	(Cavanaugh et al., 2011)
<i>Macrocystis pyrifera</i>	SPOT 1, 2	NIR:RED ratio	Density thresholds	(Augenstein et al., 1991)
<i>Enteromorpha prolifera</i>	HJ-1 A/B, ASAR, MODIS	NDVI backscattering interpretation	NDVI threshold	(Cui et al., 2012)
<i>Macrocystis pyrifera</i>	SPOT 1, ADAR	Histogram normalization, contrast enhancement, band ratios	Unsupervised cluster, CLUST analysis	(Deysher, 1993)
<i>Macrocystis pyrifera</i>	Colour infrared aerial photography	N/A	Visual interpretation	(Donnellan and Foster, 1999)
<i>Sargassum</i> spp., <i>Syringodium filiform</i>	PRISM	Spectral resampling, NDVI	Custom stepwise classification	(Dierssen et al., 2015)

<i>Zostera noltii</i>	Colour aerial photography (UAV)	RGB and texture of green band	Unsupervised and OBIA	(Duffy et al., 2018)
<i>Macrocystis pyrifera</i>	Colour aerial photography	N/A	Unsupervised classification	(Fyfe et al., 1999)
<i>Enteromorpha prolifera</i>	MODIS	Modified SAI on NDVI	SAI threshold	(Garcia et al., 2013)
<i>Sargassum</i> spp.	MERIS, MODIS	MCI, FLH	Visual interpretation	(Gower et al., 2006)
<i>Enteromorpha prolifera</i>	MODIS, Landsat	FAI	FAI threshold	(Hu, 2009)
<i>Sargassum</i> spp.	MODIS, Landsat, WorldView-2, HICO, AVIRIS, airborne digital photos	FAI, NDVI, MCI, SI, LD	Stepwise classification including index thresholds	(Hu et al., 2015)
<i>Macrocystis pyrifera</i>	Landsat, colour infrared aerial photography, radar	Near Infrared Band	Supervised Classification	(Jensen et al., 1980)
<i>Enteromorpha prolifera</i>	MODIS	SAI: scaled algae index	SAI threshold	(Keesing et al., 2011)
<i>Macrocystis pyrifera</i>	QuickBird	NDVI, panchromatic band	Brightness threshold	(Kim et al., 2010)
<i>Enteromorpha prolifera</i>	MODIS	Ratio bands 1 and 2, analysis of chlorophyll-a product	Index threshold	(Ma et al., 2009)
<i>Sargassum</i> spp.	CASI, thermal infrared imagery	Spectral and thermal interpretation, red-edge calculation	Red-edge threshold	(Marmorino et al., 2011)
<i>Macrocystis pyrifera</i> , <i>Nereocystis luetkeana</i>	Colour infrared aerial photography	Near infrared reflectance, contrast enhancement	Visual interpretation	(Pfister et al., 2017)
<i>Enteromorpha prolifera</i>	MODIS	NDAI (normalized difference algae index)	NDAI threshold	(Shi and Wang, 2009)
<i>Nereocystis luetkeana</i> , <i>Alaria fistulosa</i>	Colour infrared aerial photography	Log transformed, normalized difference using blue and NIR bands	ISODATA unsupervised classification	(Stekoll et al., 2006)
<i>Laminaria digitata</i> , <i>Saccharina latissima</i>	Custom airborne hyperspectral imager	N/A	Bayesian supervised classification, differential histogram equalization	(Volent et al., 2007)

Table 2. Remote sensors used for floating macro algae detection

Sensor	Spatial Resolution (m)	Spectral Range (nm)	Number of Bands	Swath	Revisit Time	Cost
<i>Satellite Sensors</i>						
Landsat 8	15 panchromatic, 30 multispectral, 100 thermal	430 - 12510	11	185 km	16 days	Free
Landsat 7	15 panchromatic, 30 multispectral, 60 thermal	450 - 12500	8	185 km	16 days	Free
Landsat-5 (TM)	30 multispectral, 120 thermal	450 - 12500	7	185 km	16 days	Free
SPOT-5	2.5 panchromatic, 10 multispectral, 20 SWIR	480 - 1750	5	60 km	2 - 3 days	\$
SPOT-6/7	1.5 panchromatic, 6 multispectral	455 - 890	5	60 km	1 - 3 days	\$
Sentinel 2	10, 20 60	490 - 1375	13	290km	5 days	Free
WorldView-2	0.46 panchromatic, 1.84 multispectral	400 - 1040	9	16.4 km	1 - 3 days	\$
MODIS	250, 500, 1000	405 - 14385	36	2330 km	1 - 2 days	Free
MERIS	300	390 - 1040	15	1150 km	3 days	Free
QuickBird	0.65 panchromatic, 2.62 multispectral	445 - 900	5	16.8 km, 18 km	1 - 3.5 days	\$
HICO*	90	350 - 1080	128	45 km	Irregular	\$
HJ-1 A/B	30	430 - 900	4	360	2 days	\$
<i>Airborne Sensors</i>						
AVIRIS	Altitude dependent	400 - 2500	224	Altitude dependent	N/A	\$
ADAR	Altitude dependent	400 - 1000	4	Altitude dependent	N/A	\$
CASI	Altitude dependent	380 - 1050	288	Altitude dependent	N/A	\$
DMSC	Altitude dependent	Varied	Varied	Altitude dependent	N/A	\$
PRISM	Altitude dependent	350 - 1050	> 200	Altitude dependent	N/A	\$

2.4.3 Image Processing

Image processing generally consists of preprocessing, processing, classification, validation, and a generated product. Several software programs are available for imagery processing, including ENVI, PCI Geomatica, ERDAS imagine, eCognition, for spatial data ArcGIS, open source free

software packages are also available: QGIS, GRASS, ILWIS, SNAP, and Google's Earth Engine.

Preprocessing

Image preprocessing is the correction of systematic errors and calibration of remotely sensed imagery to produce consistent and comparable data (Schowengerdt, 2012). For macro algae detection, preprocessing steps may differ slightly among studies, but generally include geometric, radiometric, atmospheric correction (for satellite images), and masking of land. These steps are fundamental principals in remote sensing techniques, and thorough descriptions can be found in texts such as Jensen's *Introductory Remote Sensing* (Jensen, 2005).

Processing

After images have been corrected and masked, information can be extracted with various processing methods. For macro algae detection, common techniques are development of indices, band ratios, and principal component analysis.

Indices and Band Ratios

Band ratios and spectral indices (Table 3) aid in macro algae detection by enhancing the differences in spectral responses (Dierssen et al., 2015). The normalized difference vegetation index (NDVI), developed for terrestrial vegetation, is also used for macro algae detection due to the spectral similarities between algae and vegetation. NDVI emphasizes the "red-edge" in vegetation and macro algae, and reduces environmental influences (Rouse, Haas, Schell, & Deering, 1974). This index has been used for detection of *Enteromorpha* blooms in the Yellow Sea (Cui et al., 2012), floating *Sargassum* (Dierssen et al., 2015), and *Macrocystis* biomass (Cavanaugh et al., 2010). Despite the success of NDVI in the aforementioned studies, this index is limited due to its sensitivity to atmospheric effects that can vary throughout the field-of-view (Garcia et al., 2013; Shi & Wang, 2009). Several studies have proposed modified indices to improve upon this limitation (Garcia et al., 2013; Hu, 2009; Huete, Justice, & Van Leeuwen, 1999; Shi & Wang, 2009). Building on indices developed to reduce atmospheric effects and improve the signal from high biomass terrestrial vegetation, Hu, (2009) developed the Floating Algae Index (FAI) (Table 3) to detect floating algae with MODIS and Landsat imagery, and found it less sensitive to changes in conditions such as aerosol type, sun glint, and solar geometry compared to other indices.

Similarly, the Normalized Difference Algae Index (NDAI) was developed to detect *Enteromorpha* (Shi & Wang, 2009). NDAI takes into account the NIR and Red reflectance, while also accounting for atmospheric effects by including the influence of Rayleigh scattering. Although FAI and NDAI succeeded in detecting floating macro algae, their use is limited to situations where the effect of Rayleigh scattering can be identified and corrected. To improve upon this limitation, the Scaled Algae Index (SAI) was developed to detect *Ulva* (Keesing et al., 2011). SAI uses a kernel filter to remove a localized background signal that includes turbidity, sun-glint, and atmospheric variation from each pixel, resulting in non-algae pixels having near-zero values, and algae pixels having high contrast with their surroundings.

The FAI, NDAI, and SAI were developed to mitigate the effects of atmospheric and environmental variation throughout large study areas. As such, these indices are especially suited for large-scale studies that target macro algae covering areas in the hundreds of meters, capable of being detected with medium to coarse spatial resolution imagery such as MODIS. Due to the growth patterns of bull kelp, which limit its distribution to relatively small areas close to the coastline, atmospheric differences throughout the study area are not as significant as those in the large, open-ocean areas typical of MODIS imagery. However, coastal areas may experience large spatial variations in turbidity, which may be reduced using the SAI index derived from high-resolution imagery, and modifications of FAI and NDAI using alternative bands on high-resolution sensors may be useful for detecting bull kelp.

Depending on the characteristics of the survey area, indices created for other applications have been useful for detecting floating macro algae. Casal et al. (2011) experimented with multiple band ratio combinations to detect submerged kelp using a band ratio of Red over Green.

Augenstein et al. (1991) used a simple ratio of NIR over Red, and Deysher (1993) used NIR over Green band to detect *Macrocystis*. Depending on the site conditions and band availability of the sensor used, substitutions of bands from established indices may produce better results such as in Stekoll et al. (2006) using the Blue band instead of the Red band in the NDVI to detect *Nereocystis* and *Alaria*.

Table 3. Indices used for enhancing detection of floating Macro Algae where R = reflectance, SWIR, NIR, Red, Green, Blue indicate the bands from the sensors being used. For full variable definitions, refer to the literature cited.

Index	Equation	Species	Use	Limitations	Study
NDVI: Normalized Difference Vegetation Index	$NDVI = \frac{R_{NIR} - R_{RED}}{R_{NIR} + R_{RED}}$	<i>Enteromorpha prolifera</i> , <i>Sargassum</i> , <i>Macrocystis</i>	Emphasize red edge	Sensitive to atmospheric variation in scene	(Cavanaugh et al., 2010; Cui et al., 2012; Dierssen et al., 2015)
FAI: Floating Algae Index	$FAI = R_{rc,NIR} - R'_{rc,NIR}$ $R'_{rc,NIR} = R_{rc,RED} + (R_{rc,SWIR} - R_{rc,RED}) \times (\lambda_{NIR} - \lambda_{RED}) / (\lambda_{SWIR} - \lambda_{RED})$	<i>Sargassum</i>	Detect floating algae with MODIS and Landsat	Limited to sensors with certain bands	(Hu, 2009)
NDAI: Normalized Difference Algae Index	$NDAI = \frac{[R_{NIR} - Rayleigh_{NIR}] - [R_{RED} - Rayleigh_{RI}]}{[R_{NIR} - Rayleigh_{NIR}] + [R_{RED} - Rayleigh_{RI}]}$	<i>Enteromorpha prolifera</i>	Similar to NDVI also takes influence Rayleigh scattering into account	Need SWIR bands at 1240nm and 2130nm	(Shi and Wang, 2009)
SAI: Scaled Algae Index	$SAI = NDVI_{POI} - medianNDVI_{kernel}$	<i>Ulva prolifera</i>	Removes background signal from turbidity, sun-glint, and atmospheric effects	Sensitive to the size of the processing kernel	(Keesing et al., 2011)
GNDVI: Green Difference Vegetation Index	$GNDVI = \frac{R_{NIR} - R_{GREEN}}{R_{NIR} + R_{GREEN}}$	Cyanobacteria Bloom	Uses green band instead of red for NDVI. Sensitive to chlorophyll variation	Best suited for “green” vegetation	(Goldberg et al., 2016)
EVI- Enhanced vegetation index	$EVI = Gain Factor \times \frac{(NIR - RED)}{(NIR + C1 \times Red - C2 \times Blue + L)}$	<i>Ulva</i>	Sensitive to canopy variations	More sensitive to green algae	(Son et al., 2012)
MCI- Maximum Chlorophyll Index	$MCI = R_{rc709} - R_{rc681} - (R_{rc754} - R_{rc681})(709 - 681)/(754 - 681)$	<i>Sargassum</i>	Measures red-edge reflectance of water column chlorophyll and floating vegetation	Designed for MERIS	(Gower et al., 2006; Hu et al., 2015)
Simple Ratio: NIR/Blue	$SR = \frac{R_{NIR}}{R_{BLUE}}$	<i>Nereocystis luetkeana</i> , <i>Alaria</i>	Detect floating	Unable to distinguish	(Stekoll et al., 2006)

Simple ratio: Red/Green	$SR = \frac{R_{RED}}{R_{GREEN}}$	<i>Submerged laminaria species</i>	laminaria biomass Enhances submerged vegetation	h between species Less effective for canopy detection	(Casal et al., 2011)
-----------------------------------	----------------------------------	--	---	---	----------------------

Principal Component Analysis

Principal component analysis (PCA) is a statistical technique used to reduce variance and dimensionality of a data set by transforming image bands into a set of uncorrelated output products, each composed of a combination of the original bands. The first principal component (PC1) represents the maximum proportion of variance from the data, and each subsequent PC represents the maximum of the remaining variance. This allows patterns in the data to be identified by accentuating similarities and differences (Gupta, Reet, Saini, & Srivastava, 2013). For the purpose of macro algae detection, PCA is beneficial for reducing spectral noise, and increasing separability between macro algae and its surroundings, which ultimately aids in image classification. Cavanaugh et al. (2010) found useful information in the different principal components of SPOT 5 imagery: the PC1 accounted for variations in atmosphere, suspended particles, whitecaps, and waves, and PC2 showed a signal that was inversely consistent with the expected kelp reflectance and could be used to delineate the canopy.

2.4.4 Classification

Classification of image data results in a spatial representation of kelp aerial extent, which can then be used to derive products such as biomass, productivity or temporal change, or persistence trends. There are several methods of classification that have been applied in previous research: supervised and unsupervised classification algorithms, thresholds, object-oriented segmentation, spectral un-mixing, and manual visual classification. Finally, the results of a classification may need to be adjusted to remove errors caused by speckling or noise. The final classification results are validated using ground-truth-based accuracy assessments.

Supervised Classification

Supervised classification uses ground-truth data provided by the user to train a classifier according to the classes of interest. This method is best used when the user has high quality field data and wishes to classify several cover types. Various supervised classification techniques have

been used in macro algae studies, including Spectral Angle Mapper (SAM) and maximum likelihood. The SAM method groups pixels into classes based on the angle in spectral space between the value of a given pixel and the class spectra (R. J. Anderson et al., 2007). The maximum likelihood classification calculates the probability that a given pixel belongs to a class previously characterized with training data, with the assumption that each class is normally distributed (Casal et al., 2011; Hogland, Billor, & Anderson, 2017). Minimum distance classification is similar to maximum likelihood except that it allows for the use of classes that are not normally distributed (Richards, 2013).

Image Threshold

Using image thresholds is a simple technique where threshold values are defined based on the separability of the features of interest. For example, a threshold value from an original band, PC product, or index is applied to the image, resulting in a binary product wherein each pixel is identified as either above or below that value. The threshold value may be determined through defining the value that produces the best output, as compared to validation data or visual interpretation of the satellite image (Cui et al., 2012; Kim et al., 2010), based on sensitivity analysis (Garcia et al., 2013) or spatial gradient analysis (Hu, 2009). A basic threshold will produce a binary product of either “kelp” or “not kelp.”

Threshold-based approaches may also consider a stepwise or decision tree procedure that can identify floating macro algae by ruling out other spectral features (Hu et al., 2015). For example, to discriminate *Sargassum* from floating seagrass wrack, Dierssen et al. (2015) applied a stepwise rule with multiple index/band thresholds to first isolate pixels containing floating vegetation (“vegetation” or “not vegetation”), and then applied a second index threshold to the vegetation class to differentiate between *Sargassum* and seagrass. In any threshold approach, a major challenge is threshold variability throughout the image, which can sometimes be dealt with by scaling image pixels using a kernel-based approach and then applying a global threshold (Garcia et al., 2013).

Spectral Un-mixing

Due to limitations in spatial resolution of images acquired by satellite and the small size of some floating macro algae beds, pixel reflectance may represent a mixture of signals composed of the target algae and the surrounding seawater. For example, in a binary classification of floating

macro algae, a mixed pixel would be classified as either algae or water, and therefore inaccuracy in canopy extent and biomass estimations may occur. Cavanaugh et al. (2011) and Bell et al. (2015b) used Multiple Endmember Spectral Mixture Analysis (MESMA) to address this problem by modelling each pixel in a Landsat image as a linear combination of giant kelp and seawater using one kelp pixel and multiple representative water pixels. MESMA was then used to determine the percent of kelp in each pixel. Uhl et al., (2013) used hyperspectral data to determine whether various species of macro algae could be detected within a mixed pixel and found that, while species level un-mixing was not possible due to the similarities in reflectance, higher taxonomic levels could be distinguished. For bull kelp detection, spectral un-mixing approaches may be especially advantageous given the small size of the kelp beds compared to the spatial resolution of available satellite imagery.

Object Based Image Analysis

Object Based Image Analysis (OBIA) is a method of classification in which pixels are first grouped into image objects (Blaschke, 2010). This technique is especially useful in conditions where the spatial resolution of an image is very high compared to the scale of the target of interest, such as in aerial, UAV, or high resolution satellite images (Blaschke, 2010; Nahirnick et al., 2019). Instead of classifying images on a pixel-by-pixel basis, image objects are created from groups of adjacent pixels based on information from spectral bands and contextual information, such as shape, scale, and compactness. This method can also include other spatial information, such as benthic substrate or bathymetry. Each object can be composed of pixels with similar digital values and is thus spectrally more homogeneous within the object than between neighbors (Yu et al., 2006). After segmentation, objects are classified according to a combination of various object features, such as mean, median, standard deviation, dissimilarity, homogeneity, texture, or spatial relationship to other objects (Blaschke, 2010; Yu et al., 2006).

Visual Interpretation

Visual interpretation techniques can be applied to any type of imagery (Donnellan & Foster, 1999), including images produced from transformed bands or indices (Casal et al., 2011). This method relies on a user to visually define and delineate the boundaries of kelp beds. While visual interpretation benefits from its simplicity, it is subjective and may therefore introduce error.

Furthermore, as a non-automated process, it may be more time-consuming and less repeatable than other classification techniques (Pfister et al., 2018).

Unsupervised Classification

Unsupervised classification algorithms do not require ground-truth information for training. A commonly used algorithm, cluster analysis, groups pixels into classes based on their spectral similarities, and then assigns all possible pixels to the nearest class (Tou & Gonzalez, 1974). A key consideration is the number of classes selected as an output, which will depend on the amount of variability in a survey area, where masked images with mostly kelp and water will need fewer classes than an area with other features such as rocks, boats, docks, etc. A small number of classes may group kelp with other spectrally similar features in the image, while a large number of classes may divide kelp into several clusters due to differences in density. Clustering algorithms have been effectively used for kelp classification of both aerial (Deysher, 1993) and satellite imagery (Casal et al., 2011)

Classification Adjustment

Often, the outputs from classifications contain errors caused by digital noise in the image, or classified artifacts that may need to be removed. For example, Cavanaugh et al. (2010) applied a filter wherein single isolated kelp pixels were assumed to be incorrect and reclassified as water. The applicability of this technique depends on the spatial resolution of the sensor and the size of the kelp beds, where errors in classifying small kelp beds will be more difficult to determine.

2.4.5 Validation and Accuracy Assessment

To evaluate the extent of errors associated with the classification step, an estimate of the overall accuracy is usually necessary, allowing the classification products to be used in decision-making processes (Richards & Congalton, 2001). In order to assess accuracy, ground-truth data must exist, which ideally should be collected at the same time as image acquisition. When data are not collected at the same time as image acquisition, close attention must be paid to differences in tide height, current, and season, as these factors can have major impacts on the mapped extent of macro algae (Britton-Simmons, Eckman, & Duggins, 2008).

The accuracy of a classification is generally reported in terms of Producers accuracy (errors of commission) and Users accuracy (errors of omission). These errors are defined based on comparison between classification outputs and validation data (i.e., ground-truth) and creating a

standard error matrix to report omission and commission errors (Congalton, 1991). The total accuracy is also commonly reported, and is found by dividing the total number of correctly classified pixels by the total number of pixels considered. A poor outcome from an error matrix may induce reiteration through the classification steps until a satisfactory outcome is achieved, if possible.

2.4.6 Products

The goals of a monitoring project may include kelp detection (presence/absence), quantification of the spatial extent of beds, change detection, or deriving biological parameters such as biomass, productivity, and physiological condition. Basic kelp detection products can be used for temporal analysis or for biomass estimates. For detecting temporal trends, multiple classification products derived from images collected at different times are used; however, care must be taken concerning differences in image quality and conditions at the time of imagery acquisition that may affect the accuracy of kelp classification between time periods. Differences in tide, water surface, and water column characteristics may create error in the classified extent of kelp that is not due to the full kelp extent (Britton-Simmons et al., 2008). To overcome some of these differences, images should be normalized when possible.

Monitoring initiatives that require biomass estimates can give more detailed insight into kelp forest productivity and response to environmental change (Bell, Cavanaugh, Reed, et al., 2015). To calculate biomass from imagery, physical data such as plant densities, lengths, and weights need to be collected at an appropriate scale (Cavanaugh et al., 2010). This information is then related to image derived indices such as NDVI values (Cavanaugh et al., 2010) or kelp fraction (Bell, Cavanaugh, & Siegel, 2015) through linear regression. Total or surface kelp biomass can then be calculated from the classified kelp area (Bell, Cavanaugh, Reed, et al., 2015; Cavanaugh et al., 2010; Stekoll et al., 2006). In California, biomass of giant kelp beds was derived from Landsat imagery using the MESMA method discussed above, where the percent cover of kelp in each 30m pixel was related to diver estimates of kelp density using a linear regression (Reed et al., 2011). Other measures such as sub-bulb diameter of bull kelp have been used to estimate plant weight, enabling a simpler method of field data collection for use in derived biomass estimates (Stekoll et al., 2006).

2.5 Case Study: Remote Sensing of Bull Kelp in the Salish Sea

This section presents a case study in which methods adapted from the macro algae studies discussed in sections 2 and 3 are adopted for mapping fringing beds of bull kelp in nearshore regions of the Salish Sea on the west coast of Canada.

2.5.1 Study Site

The study site covers approximately 100 km² in Cowichan Bay and Sansum Narrows in the Salish Sea, on the west coast of Canada (Figure 4). In this region, bull kelp is the dominant canopy forming algae often growing in narrow fringing beds along steep rocky shorelines, at depths between 0-20m (Mumford, 2007). Most growth occurs between April and early September, depending on water and light conditions (Mumford, 2007; Springer et al., 2007). Canopies may be maintained until fall or early winter depending on the sea and temperature conditions (Springer et al., 2007).

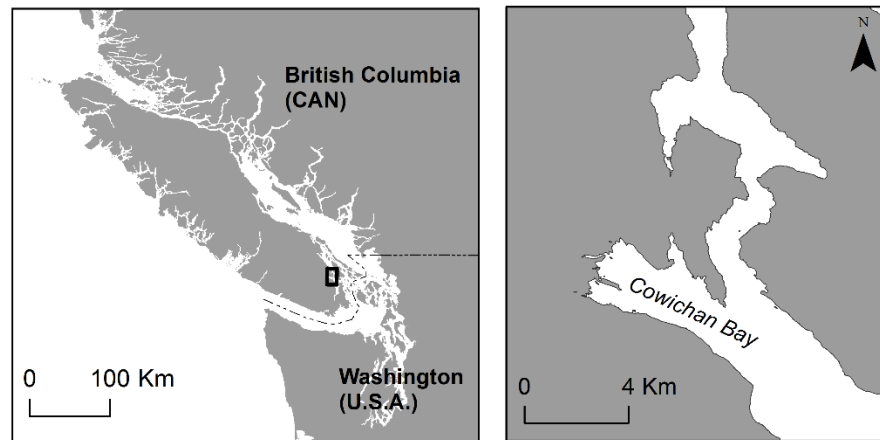


Figure 4. Left: Regional context of study area (black box) Cowichan Bay and Sansum Narrows on the east coast of Vancouver Island, British Columbia, Canada. Right: extent of study area, covering Cowichan Bay and Sansum Narrows.

2.5.2 Methods

Step 1: Imagery acquisition and ground-truthing

A WorldView 3 satellite image covering approximately 100 km² with four multispectral bands (480, 545, 660, 832nm) and 1.8 m spatial resolution was planned for acquisition by DigitalGlobe on August 30th, 2016. Conditions required for successful collection were: tide height lower than 1.2 m MLLW, specified by the ground-truth methods as the tide height where the majority of the

kelp canopy should be visible at the surface; sensor angle less than 15 degrees off nadir; minimal cloud cover (< 5% over shoreline); and low wind conditions (< 10m/s).

At the same time that image collection occurred, ground-truthing of kelp extent over a subset of the area was conducted using kayak and handheld GPS methods following Fretwell and Boyer(2010). Three teams of two person crews started from different locations and paddled kayaks along the shoreline for one hour before, during, and one hour after the low slack tide of 1.1m MLLW. Kelp location was recorded by handheld GPS (Garmin 64s) as either a point (single bulb, or several bulbs in close proximity <1m²), line (continuous kelp less than 5m wide), or polygon (continuous kelp more than 5m wide). Beds were considered distinct if there was a distance greater than 8m between kelp plants. All data was digitized in ArcGIS into shapefiles for use as training and validation data.

Step 2: Pre-processing

Initially, the acquired image was georectified in BC Albers NAD 83 with ArcGIS 10.5 using 30 ground control points, producing a final average root mean square error (RMSE) of 0.28m. Next, the raw digital numbers were converted to at-satellite radiance (L_λ in units of $\mu\text{W}/\text{cm}^{-2} \text{sr}^{-1} \text{nm}^{-1}$ equation 1), and an absolute atmospheric correction was applied using the FLAASH® (Fast Line of Sight using Hypercubes) tool in ENVI (Matthew et al., 2000).

$$L_\lambda = \text{Gain} * \text{Pixel value} + \text{Offset} \quad (1)$$

A land mask was created using object-based segmentation with Definiens eCognition to allow for separation of land from water; the NIR, Red, and Green bands were used as inputs, and spectral characteristics were given greater weight than spatial characteristics for defining objects. This method resulted in a more accurate definition of the coastline than the use of published coastline shapefiles, which do not reflect the tide level occurring at the time of image acquisition. A 4-metre buffer was added to the defined land mask to account for occurrence of nearshore vegetation such as *Fucus* and *Ulva*, as well as removal of adjacency effects and pixel mixing caused by the proximity of terrestrial vegetation to the shoreline. While this method produces a reliable mask of the exact shoreline location, and thus allows for effective masking of land classes that may influence the classification, it will also potentially mask kelp located within 4

meters of the shoreline. Kelp in such close proximity to the shoreline is not likely to be resolved from other algae species in the nearshore due to similarities in reflectance. It is preferable to mask this area rather than to misclassify the shoreline algae as kelp. Finally, a 30m deep-water mask was applied using bathymetry contours created from single and multi-beam sonar data acquired from the Canadian Hydrography Service for coastal British Columbia. This mask represents the depth at which kelp will not be found in this region (Springer et al., 2007). Together, the masks minimize erroneous classification introduced from land, shoreline algae, glint, waves, and water column constituents.

Step 3: Image processing

Index selection:

To explore the best possible bands and band ratios for separating kelp from other features, the Jeffries-Matusita Distance (JMD) statistical separability analysis (Swain & King, 1973) was applied to all the applicable indices and transformations available in the literature (Table 3). Some indices discussed in the literature could not be applied due to the limitations of band availability for the WorldView 3 image. The following products were analyzed: NDVI, GNDVI, SAI, EVI, simple ratios as well as PC outputs, and the Blue, Green, Red, and NIR reflectance bands. According to the JMD analysis, the products selected as best able to identify kelp - NDVI, GNDVI, and PC1 - were further linearly enhanced to maximize spectral differences and minimize noise, and then used as input for classification.

Step 4: Classification

To illustrate the feasibility of using different classification techniques with different levels of user input, four types of supervised methods, minimum distance (MD), decision tree threshold (DT), spectral un-mixing (SU), and object-based image analysis (OBIA), and one unsupervised method, ISODATA (ISO), were compared. All classifications used a composite of NDVI, GNDVI, and PC1 as input.

For the supervised methods, MD used training data derived from ground-truth and expert knowledge to define six classes (kelp, water, glint, shallow water, bright objects, and shadow) with at least 100 pixels each. The DT used thresholds defined by the mean of the same class samples ± 2 standard deviations. The SU was defined based on adapted methods from Cavanaugh et al.(2011), in which the *matched filtering* tool in ENVI was used to un-mix pixels. Spectral

endmembers for dense kelp (50 kelp endmembers) and water (120 water endmembers) were selected from the image based on ground-truth data and known reflectance characteristics of kelp and water. The result is a grey scale image for each endmember representing their approximate subpixel abundances, where a value of 1.0 would represent 100% kelp. Based on the ground-truthing data and known spectral reflectance of kelp and water, a kelp minimum fraction threshold of 0.142 was defined. All pixels with a fraction lower than 0.142 were classified as water. OBIA was applied using Definiens eCognition® Version 8. As commonly used in object-based classification, trials for different weights for parameters of scale, shape, and compactness were conducted to determine the optimal approach for the segmentation (Evans, Costa, Tomas, & Camilo, 2014). Defined parameters were considered acceptable if areas of known kelp beds were captured as a single object, rather than broken into several objects or combined with areas of non-kelp. The resulting image objects were classified using a supervised nearest-neighbor approach for the six classes defined above. For the unsupervised ISO method, multiple classification trials were performed to define the combination of parameters and number of classes needed to yield the best results.

Step 5: Accuracy assessment

The output product of each classification was converted into two binary classes, kelp and non-kelp, where all non-kelp classes defined through classification were combined into one class. A stratified random sample approach was used to define 500 validation pixels per class from the ground-truth data, and an error matrix was produced (Table 4). The selection of the validation pixels also considered the uncertainties in the ground-truth data due to the accuracy of the handheld GPS (± 9 m), displacement of kelp beds of up to 1m related to changes in tide and current and bias or inaccuracy of the kayak surveyors. A 10m buffer was added to the kelp ground-truth polygons (Figure 8) to accommodate for these possible uncertainties, and no samples in this region were used for either the kelp or the non-kelp classes, reducing the number of pixels for validation to a range between 400 and 485 for each class.

2.5.3 Results and Discussion

All five classification methods performed relatively well in detecting kelp beds. For total accuracy, MD (90.7%) and SU (88.5%) yielded the best results (Figure 5), followed by DT (87.9%), ISO (86.9%), and OBIA (82.5%), (Table 4). The classification products showed high

fidelity when visually compared to the shape and location of ground-truth maps (Figures 6 and 7), and the total accuracies are comparable to other studies which reported values between 74% and 94%, depending on the density of the kelp (Casal et al., 2011; Fyfe et al., 1999).

For all classification outputs, accuracy was generally the highest in areas where kelp was dense and beds were large, as illustrated in Figures 6 and 7. In these regions, the detected spectral signals better represent kelp due to less mixing with the spectral signal of water (see Figure 1 for spectral signal of dense kelp vs sparse kelp). Conversely, in areas where kelp was sparse, kelp detection was less reliable due to spectral signal mixing with water. The greatest error happened in areas in which submerged vegetation such as eelgrass was classified as kelp. The reflectance spectra of submerged kelp and eelgrass with high epiphytes loads are very similar when using only four spectral bands (O'Neill & Costa, 2013). Alternatives for minimizing this error include using hyperspectral data to improve the spectral separability between species and/or masking areas of soft substrate where kelp is unlikely to occur. Misclassification also occurred between the shadows of terrestrial vegetation on the water, as seen in Figure 6. Despite the 4m buffer, the shadow of terrestrial vegetation was not removed in some areas during the masking process, likely due to large shadows caused by the height of trees, sensors viewing angle, and sun illumination angle (Figure 7).

Among the supervised methods, the MD classification produced the best results due to its use of high-quality ground-truth data and consideration of the mean of training classes in the minimum distance algorithm. Similarly, the spectral un-mixing method yielded good results. In this method, the best results will occur when pure pixels of each class are used to establish the un-mixing algorithm. The decision tree classification applied user-defined thresholds to classify pixels, which can introduce bias on class definition. Adjusting threshold values or including additional classes where misclassifications occur may improve the results. The poorest results were obtained with the OBIA approach. The small size, irregular shape, and sparse nature of the kelp beds resulted in objects containing a range of kelp and water extents. In these conditions, the mean of each object mostly represents the mixing of spectral signals corresponding to water and kelp. Depending on ratio of kelp and water, image objects containing kelp may be classified as water, thus causing larger error compared to pixel-based classification. In areas where kelp beds are large and dense, OBIA will likely perform better as image objects will more accurately represent kelp spectral signatures and have a uniform nature. The unsupervised ISODATA

method performed well with both dense and sparse kelp beds, as the iterative clustering algorithm is most affected by the difference in spectral signals between cover types rather than their spatial relationship. This method is advantageous where there is a lack of ground-truth data, such as when analyzing historical imagery. However, knowledge of the site characteristics or spectral signature of cover types is still required to label the resulting classes.

Table 4. Error matrices for Minimum Distance (MD), ISODATA (ISO), Decision Tree (DT) spectral unmixing SU, and OBIA classification results for bull kelp in the Salish Sea.

		Ground-truth			User Accuracy	Total Accuracy	
		Kelp	Not Kelp	Total			
Classification	MD	Kelp	409	42	451	90.7	90.7
		Not Kelp	37	358	395	90.6	
		Total	446	400	846		
		Producers Accuracy	91.7	89.5			
	ISO	Kelp	376	83	459	81.9	86.9
		Not kelp	28	362	390	92.8	
		Total	404	445	849		
		Producers Accuracy	93.1	81.4			
	DT	Kelp	385	75	460	83.7	87.9
		Not Kelp	27	359	386	93.0	
		Total	412	434	846		
		Producers Accuracy	93.5	82.7			
	SU	Kelp	399	62	461	86.6	88.5
		Not Kelp	34	343	377	91.0	
		Total	433	405	838		
		Producers Accuracy	92.2	84.7			
	OBIA	Kelp	333	121	454	73.4	82.5
		Not Kelp	27	364	391	93.1	
		Total	360	485	845		
		Producers Accuracy	92.5	75.1			



Figure 5. Result of minimum distance (MD) supervised classification with total accuracy of 90.7.

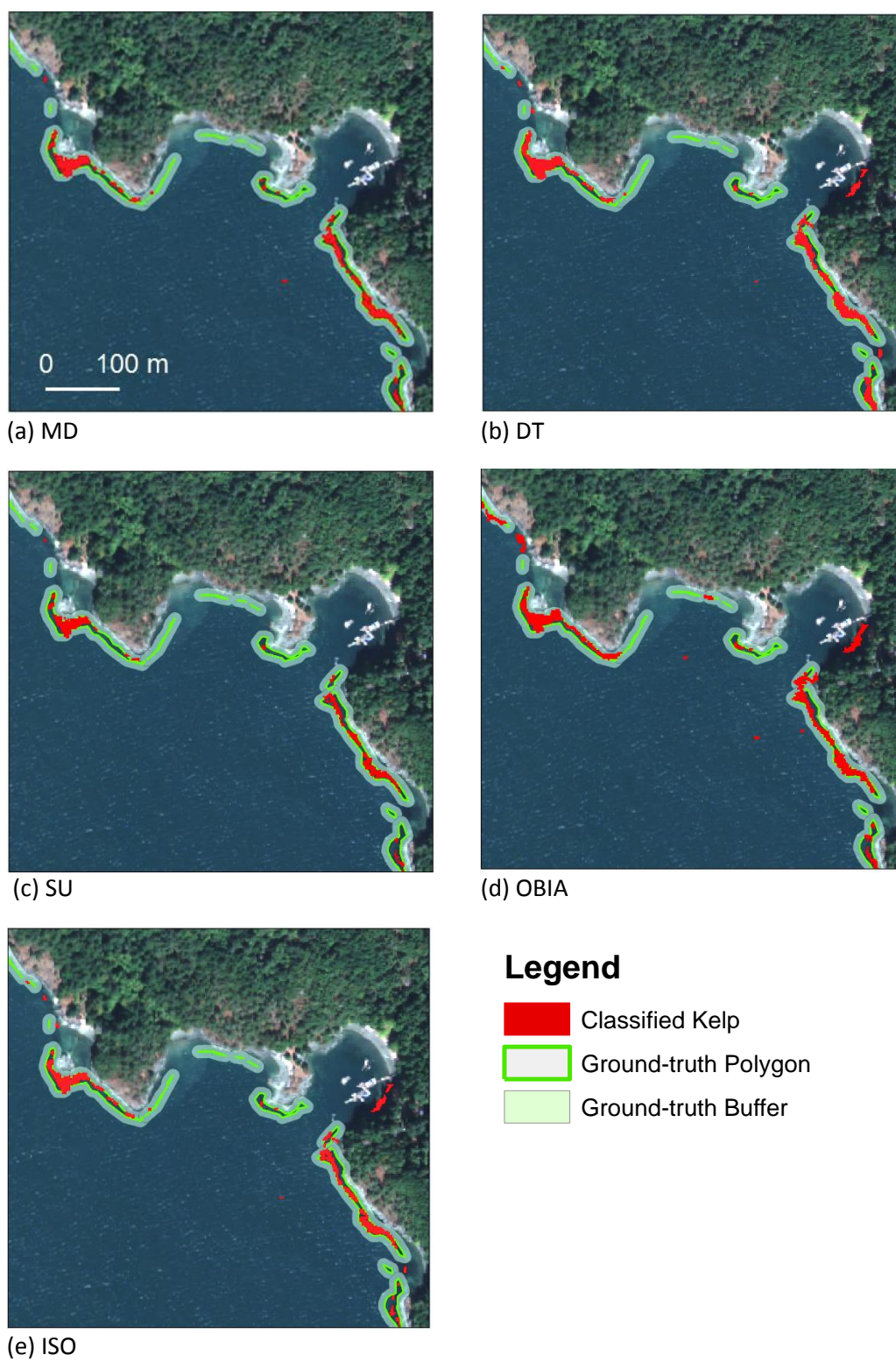


Figure 6. Classification results for the MD, DT, SU, OBIA, and ISO classifications on a subset of the true colour WorldView 3 image for bull kelp in the Salish Sea.

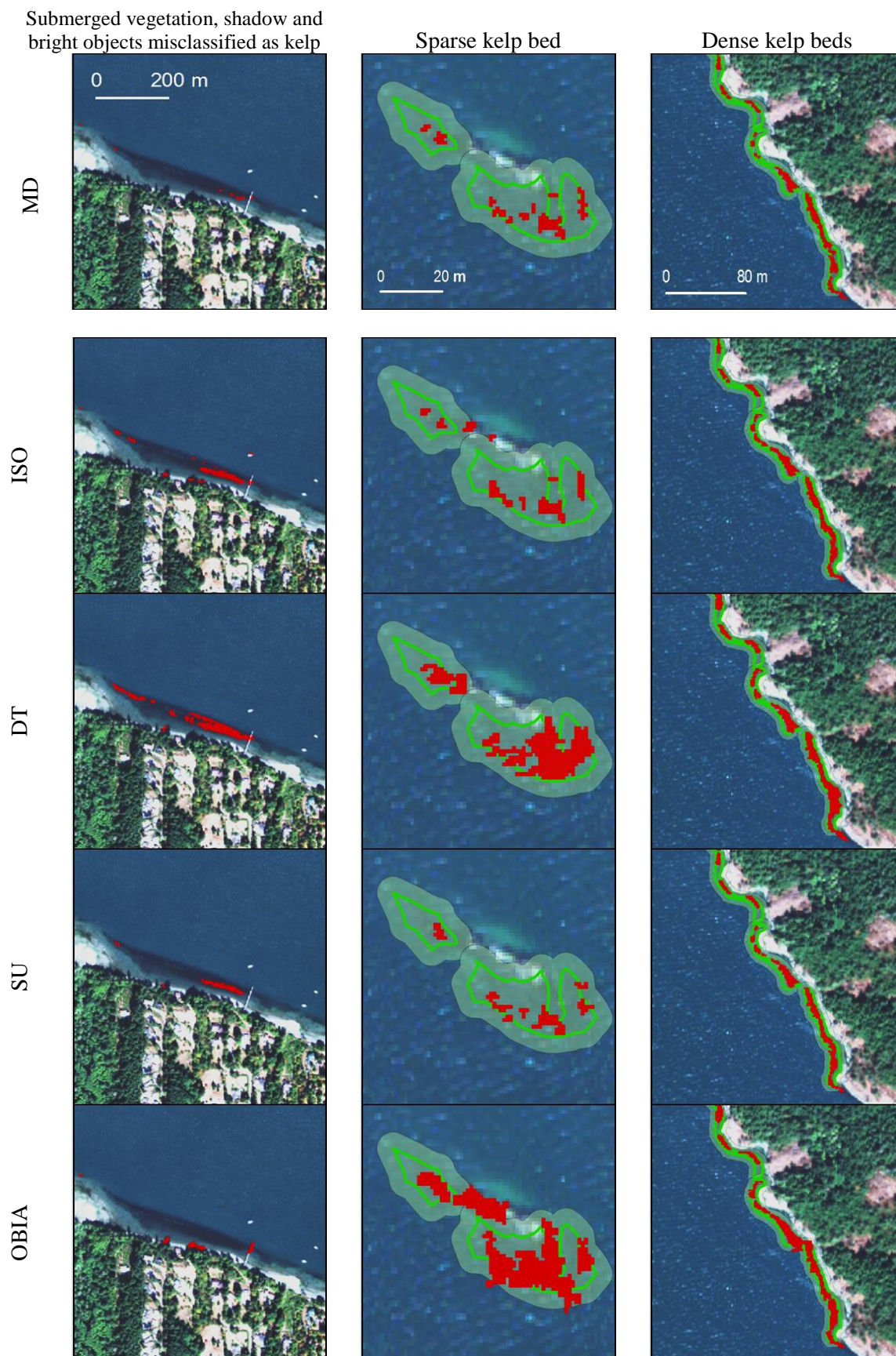



Figure 7. Errors in classification methods for submerged vegetation, shadow, bright objects, sparse kelp beds, and dense kelp beds in the Salish Sea. (Legend provided in Figure 6)

Table 5 summarizes the choice of image classification methods based on the characteristics of the study sites and available ground-truth information. Specifically, sensors will depend on the size and location of beds, where large offshore beds can be detected with medium resolution sensors and smaller nearshore beds will require higher resolution imagery. As kelp beds become sparse, fringing, or small, classification techniques such as supervised minimum distance yield the most robust results. Additionally, the quality of the ground-truth data affects the choice of classification method, with high quality data acquired concurrent to image acquisition being ideal for all classification techniques. If ground-truth data is unavailable, unsupervised ISODATA classification is the most appropriate choice. However, for any of the classification approaches, environmental conditions during the time of image acquisition, including tide height, currents, water surface roughness, turbidity, and sensor angle will also have effects on the accuracy of the classifications.

Table 5. Selection of classification methods based on quality of input parameters.

Data Quality	Study Site Characteristics	Ground-truth Data	Sensor Type and Resolution	Classification Type
Ideal  Poor	Large dense kelp beds, far from shoreline	Collected at same day and time as imagery	Mid-high resolution 30m-2m	OBIA, MD, SU, DT, ISO
	Large sparse beds, small beds, near shoreline	Collected during same season	High resolution (<10m)	MD, SU, DT, ISO
	Small beds, fringing, close proximity to shoreline	No ground-truth	High resolution 2m	ISO

2.6 Conclusion

Remote sensing technologies and imagery processing methods are continuously advancing, allowing for improvements in macro algae detection. Specifically, for kelp mapping and biomass indicators, ongoing research is developing new techniques for deriving ecological information from remotely sensed kelp beds. With increasing sources of high-quality data, automated classification methods are being developed for use with free data sources such as Landsat (Bell,

Reed, et al., 2018; Nijland et al., 2019), allowing for long term monitoring and detection of large kelp beds with global scale potential. Ultimately, these data sets are crucial to understanding environmental drivers of kelp distribution and abundance, and how they relate to ecosystem functions affecting biodiversity, community structure, and productivity.

With the growing availability of high spatial resolution images, such as WorldView, SPOT, and GeoEye sensors, the accuracy of detecting small patches of fringing kelp along nearshore zones has increased. However, for successful use of remote sensing, considerations concerning the environmental conditions at the time of image collection, such as tide height, currents, waves, kelp extent, and imagery analysis techniques are of utmost importance. Additionally, the scale of areas able to be studied may be limited by the smaller coverage and greater costs of higher resolution imagery. Here, we present a literature review and a case study demonstrating how high-resolution satellite imagery can be used effectively for mapping at regional scales by applying imagery-processing techniques adapted from the literature. By using appropriate methods suited to the characteristics of the area of interest, we are able to accurately detect floating kelp beds and create maps of kelp distribution for nearshore systems. Specifically, among the evaluated indices and classification methods, the supervised minimum distance classifier with input of NDVI, GNDVI, and PC1 produced the map with the highest accuracy (90.7%). For monitoring that requires temporal analysis without ground-truth data, unsupervised ISODATA can also produce accurate results. This case study illustrates a systematic method that can be transferred to others areas of the world where species form small or fringing beds.

3.0 Spatial and Temporal Persistence of Nearshore Kelp Beds on the West Coast of British Columbia, Canada using Satellite Remote Sensing.

3.1 Introduction

As one of the most productive ecosystems on the planet (Krumhansl & Scheibling, 2012; Steneck et al., 2002), kelp forests support high biodiversity, providing protection, habitat and foraging opportunities for invertebrates, fish, birds and mammals (Christie et al., 2009; Estes, Duggins, & Rathbun, 1989), and as such are an important indicator of ecosystem health (Claisse, Pondella, Williams, & Sadd, 2012; Uhl, Bartsch, & Oppelt, 2016). Further, the physical structure of kelp beds influence coastlines through dampening of waves and providing nutrient subsidies to shorelines as wrack (Teagle, Hawkins, Moore, & Smale, 2017).

Globally, kelp species are found growing on rocky reefs in temperate coastal regions, in response to abiotic drivers: temperature, nutrient, photosynthetically active radiation (PAR), substrate type, current and wave stress (Cavanaugh et al., 2011), and biotic: grazing and competition (D. O. Duggins, 1980). Optimum growth conditions happen in cool nutrient rich waters, associated with temperate coastal regions, however, prolonged periods of warmer than average temperatures ($>17^{\circ}\text{C}$) reduce spore production and cause kelp die-off (Schiel et al., 2004; Vadas, 1972). Beyond increased ocean temperatures, other stressors including increased storm frequency, direct harvest and the effects of overfishing contribute to collapse of kelp ecosystems (Halpern et al., 2006; Hernández et al., 2018; Lorentsen, Sjøtun, & Grémillet, 2010). The degree to which these stressors influence kelp varies, with regional differences playing a key role and an overall downward trend of abundance world wide (Krumhansl et al., 2016).

Specifically, run-off associated with anthropogenic activities such as agriculture and forestry increases sediment loads in river effluent and has strong negative impacts on kelp beds through the reduction of PAR and smothering of recruits (Carney, 2005; J. A. Shaffer & Parks, 1994). Disturbance caused by wave and current can also have large impacts on the abundance of kelp, where areas of low current may leave kelp more susceptible to herbivory and high current or wave exposure may limit growth due to physical removal (Reed et al., 2011). In regions where predators such as sea otters or predatory fish have been removed through over-fishing, herbivores such as urchins thrive and have significant impacts on kelp bed size and abundance

through unchecked grazing (Foster & Schiel, 2010; Steneck et al., 2002). Additionally, changes in environmental conditions, which are unfavourable for kelp growth, may give rise to dominance by other species, such as coralline and turf algae resulting in a shift to altered stable states (Filbee-Dexter & Wernberg, 2018). Increased herbivory and warmer ocean temperatures can combine to cause major declines in kelp forest abundance (Burt et al., 2018; California Department of Fish and Wildlife, 2016).

These different kelp stressors have been reported for several regions of the world. In the Salish Sea, on the West Coast of North America, one of the dominant canopy-forming kelps, bull kelp (*Nereocystis luetkeana*) (Druehl, 1968) has shown variability in abundance with most declines recorded in regions adjacent to dense urban areas (Pfister et al., 2018). Fluctuation in abundance has also been linked to both broad scale oceanic conditions such as the Pacific Decadal Oscillation and North Pacific Gyre Oscillation, and to local scale impacts on water quality, temperature and increased herbivory (Burt et al., 2018; Foster & Schiel, 2010; Pfister et al., 2018; Taylor & Schiel, 2005).

Differences between global and local scale changes in kelp abundance may reflect regionally dependant influences where the local effects of grazing pressure, water quality and possible resilient populations interact with large scale environmental fluctuations, which result in decline, reduced resilience, or alternative stable states depending on the combination of factors¹.

Understanding the drivers, their outcomes and effects on associated ecosystems requires both long term and large-scale maps of kelp abundance. Mapping kelp extent has been a requirement for conservation and monitoring initiatives including quality of salmon habitat (A. Shaffer, 2004), creation of marine protected areas (Aïramé et al., 2003), regulating harvest impacts (Sutherland et al., 2008), oil spill impact monitoring (Peterson et al., 2003) and climate change adaptation services programs (Duarte, Losada, Hendriks, Mazarrasa, & Marbà, 2013).

Satellite imagery has been successfully used to map spatial-temporal changes in canopy kelp (Deysher, 1993; Stekoll et al., 2006; Young et al., 2016). Many of these successful analyses focus on species that form large beds, such as giant kelp, *Macrocystis pyrifera*, allowing the use of lower spatial resolution imagery from Landsat (Cavanaugh et al., 2010). However, detecting bull kelp, which may form fringing beds adjacent to the shoreline, may require high spatial resolution satellite, aerial or drone images ranging from 0.2 m to 2-4 m in resolution (Deysher,

1993; Schroeder et al., 2019). This study uses a time series of high-resolution satellite imagery from 2004 to 2017 to map bull kelp beds on the West Coast of British Columbia, Canada, and provides an analysis of changes in kelp persistence and its relationship to global and local scale environmental conditions.

3.2 Methods

3.2.1 Study Area

The study area covers approximately 50 km of coastline in Cowichan Bay and Sansum Narrows, located in the Salish Sea on the West Coast of British Columbia, Canada (Figure 8). Tides in this semi-enclosed body of water are mixed semi-diurnal with exchange of water from the open ocean through the Straits of Georgia and Juan de Fuca. Freshwater inputs come from the Cowichan and Koksilah Rivers directly into Cowichan Bay ($450 \text{ m}^3\text{s}^{-1}$ during peak flow in winter) as well as input from the Fraser River to the east ($10,000 \text{ m}^3\text{s}^{-1}$ during spring freshet). In the summer months, warm ocean temperature and peak flow from the Fraser River create stratification in the water column in the Strait of Georgia, which leads to increased surface water temperature ($14\text{-}21^\circ\text{C}$) and decreased salinity (26-28PSU) (Chappell & Pawlowicz, 2018; Waldichuk, 1957). However, water flowing through the Southern Gulf Islands with localized regions of high currents due to the narrow channels between the islands, tends to have increased mixing than that in the Strait of Georgia, resulting in slightly lower temperatures and higher salinity (Waldichuk, 1957).

The coastline in this region consists of rocky cliffs, mixed gravel beaches, sand and mudflats on which several species of aquatic vegetation grow. These habitats support a number of commercially and ecologically important species including Chinook (*Oncorhynchus tshawytscha*) and Coho (*Oncorhynchus kisutch*) salmon, whose populations have declined precipitously in recent years and for whom loss of habitat including kelp may be a contributing factor (Waldichuk, 1957).

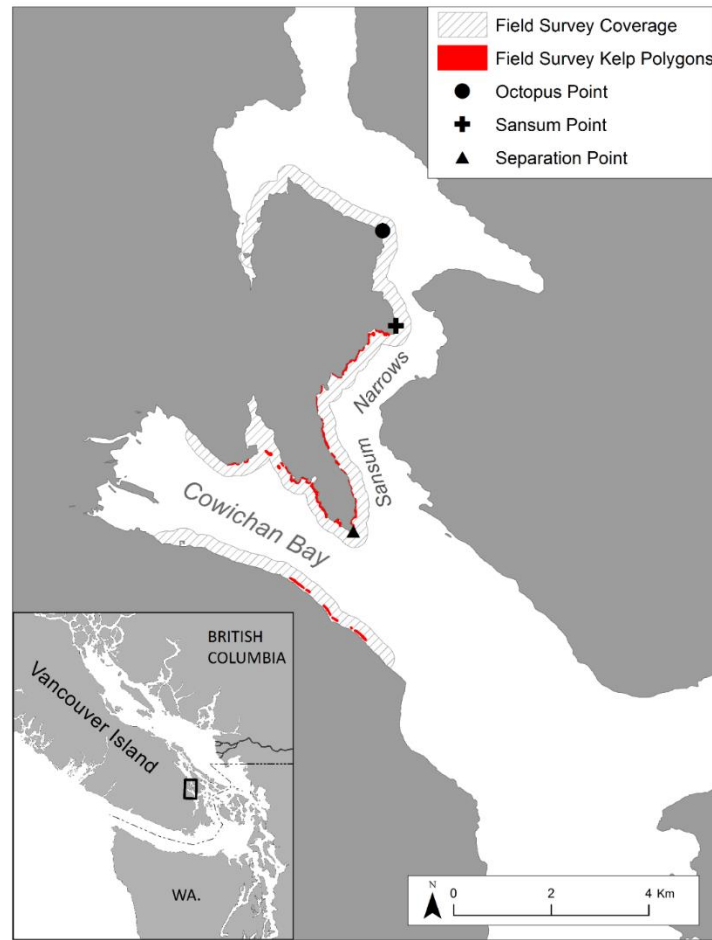


Figure 8. Study area including Cowichan Bay and Sansum Narrows on the East Coast of Vancouver Island, British Columbia, Canada. Red polygons are kelp beds delineated by a kayak-based field survey in August 2016. Hatched lines indicate the total area covered by the kayak-based field survey in August 2016.

3.2.2 Imagery database

A time series of high-resolution imagery from 2004 to 2017 were selected from the Digital Globe archives considering the preliminary criteria: spatial resolution of 2.5 m or higher, spectral resolution containing visible and near infrared (NIR) bands, minimal clouds and acquisition during peak kelp growth in summer. This selection resulted in eight images (Table 6). From these images, further criteria were developed to determine the reliability of the images for accurately mapping kelp. Similar to the methods by Nahirnick et al. (2019), each image was scored from 1 to 3 with one being the poorest condition, according to the following criteria: (1)

time of collection within the growing season; (2) tide height, where lower tides allow for better ability to detect kelp floating on the water surface; (3) intensity of glint on the water, where high glint obstructs the ability to detect kelp; (4) water surface roughness (WSR), which describes the texture of the water surface, where calm flat water is best for detecting kelp and breaking waves or white caps present difficult conditions (Table 7). The total score (maximum of 12) for each image was calculated and images with scores lower than seven were deemed too unreliable for kelp detection. Due to constraints in the overlap among all images, only five of the seven images meeting the quality criteria were used for further analysis (Table 6). This method resulted in selected images acquired in 2004, 2012, 2015, 2016 (tasked with concurrent field data), and 2017. Finally, the scores from the images, which qualified for analysis, were used to assess whether image quality played a role in the resulting kelp maps.

Table 6. Image Reliability scoring metrics. WSR = water surface roughness

Score	Season	Tide Height	Glint	WSR
Ideal (3)	Late July to Early September	≤ 1.2 m	No glint	Smooth calm water
Medium (2)	Mid June to Late July or Mid September to late September	1.3 – 2m	Some glint	Some surface texture
Poor (1)	Before mid June or After September	> 2	High glint throughout image	Breaking waves

Table 7. Quality Parameters for all images in database. WSR = Water surface roughness

Year	Date	Tide height	Glint	WSR	Score
2004*	Sept 24 th	1.8m	None	Minimal	10
2006	Sept 12 th	2.6m	Minimal	Medium	9
2011	June 8 th	2.4m	High	High	4
2012*	July 29 th	1.5m	Medium	Medium	9
2013	July 8 th	0.8m	Minimal	Minimal	10
2015*	August 27 th	1.2m	Minimal	Minimal	12
2016*	August 30 th	1.2m	Medium	Medium	10
2017*	July 27 th	1.5m	Minimal	Minimal	11

*images used for time series analysis

3.2.3 In situ dataset

The *in-situ* data set comprised of a kelp survey and above-water reflectance data acquisition. Field data acquisition was conducted during the time of the 2016 image acquisition using kayak and GPS methods following Fretwell & Boyer, (2010) covering North and South Cowichan Bay

and West Sansum Narrows to Maple Bay (Figure 8). Three teams of experienced mappers and volunteers with hand held GPSs paddled along the shoreline during the mapping window of one hour before and after low slack tide (1.1m). All canopy kelp floating on the waters surface was recorded as either a single bulb, multiple bulbs, line of kelp or a bed. The GPS points were digitized and used to create kelp polygons in ArcGIS for use as data in validation of classification methods. Possible uncertainties associated with this field data are: (1) error in the GPS units, which recorded accuracy between 1 and 9m, (2) errors in the kayakers' ability whereby points may not be exact due to the nature of collecting data in a moving platform with currents, waves and in close proximity to rocky outcrops, and (3) changes in the location of kelp between the time of the field survey and the acquisition of the image due to differences in tide height and current speed. Due to these issues, a 10m uncertainty buffer was added around the field-derived kelp polygons, and points extracted for use in training or validations of classification were not collected in this buffer.

Above-water *in situ* kelp and water spectra were collected in the field to record the spectral characteristics of different combinations of kelp and water for further analysis of the classification results. A calibrated hand held FieldSpec® spectroradiometer with a spectral range from 325-1075nm was used to collect spectra of various densities of floating kelp, deep water and kelp submerged within approximately 20 cm of the water surface in August of 2017. A sample number of n=10 was collected for each kelp-water combination of dense, sparse, submerged kelp and pure water under conditions of clear sky and calm water. Spectral measurements were acquired by boat within and beside kelp beds in the study area with a sensor viewing geometry of 1m from the water's surface, held at a 45° angle zenith, and 90° azimuth to incoming solar radiation to prevent specular reflection. Reflectance measurements were averaged, and four classes were defined as dense (>50% of the sensors field of view (FOV) covered with kelp), sparse (<50% of FOV), submerged and pure water (Figure 9). The spectral signature of kelp shows high reflectance in the near-infrared (NIR) and low reflectance in red bands, while sparse or submerged kelp beds show lower ratio of NIR to red due to the effect of water, which strongly absorbs NIR (detailed spectral analysis in Schroeder et al., 2019).

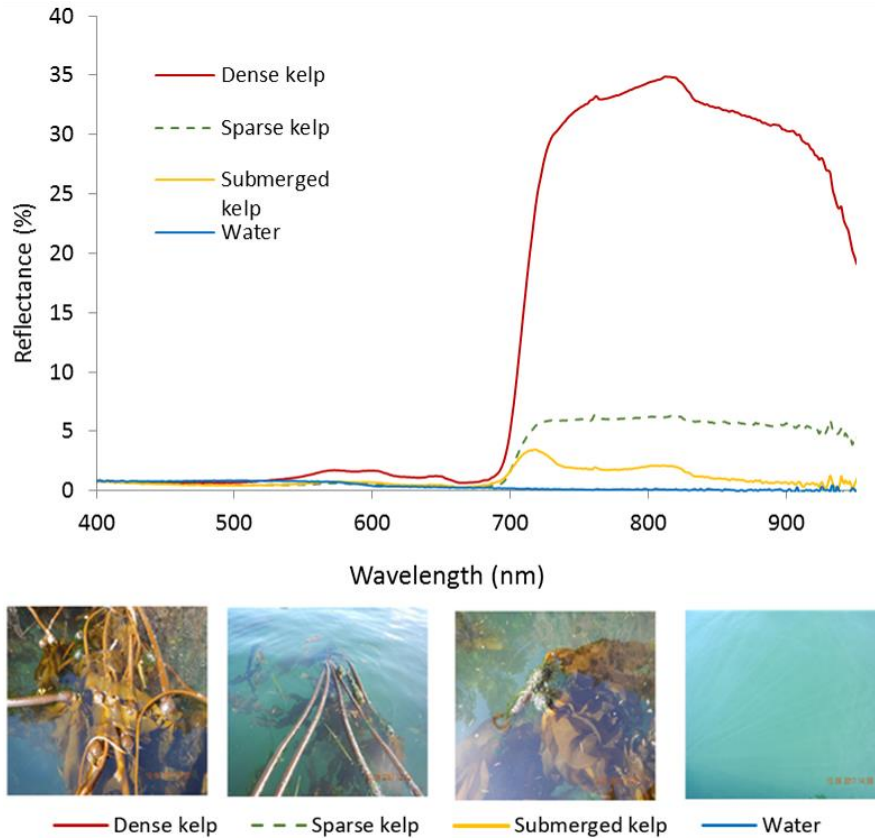


Figure 9. Representative reflectance of dense (>50% of FOV), sparse (<50% of FOV), submerged kelp and ocean water measured with a Fieldspec Pro® spectroradiometer in the coastal waters of British Columbia, Canada

3.2.4 Image Processing and Classification

Image processing methods included geometric, radiometric, and atmospheric correction, masking, image enhancement, transformation, and classification. First, historical images were georectified using the 2016 geometrically corrected image as reference, resulting in root mean square errors of less than 0.06m. Next, images were radiometrically corrected and atmospherically corrected (Adler-Golden et al., 1999) using the FLAASH module in ENVI v5.5, to minimize atmospheric effects and convert radiance signal to surface reflectance. To ensure reflectance values were comparable to the 2016 base image, all historical images were normalized using pseudo invariant features with the 2016 image as reference (Figure 10). This procedure allows for reflectance spectra of features of interest to be comparable for the different years, and therefore improving the performance of the classification results (Bao et al., 2012). Despite these corrections, water reflectance varied slightly from year to year likely due to

differences in characteristics of optical constituents in the water (Figure 10). This variability will be reflected in the spectral response of any image pixels containing kelp as the reflectance of each pixel is a product of the ratio of kelp and water as established in Figure 9.

Following normalization, a land mask was created for each image, using object-based image segmentation with Definiens eCognition® using the NIR (band 4), Red (band 3) and Green (band 2) bands as input to accentuate the contrast between the high reflectance of terrestrial vegetation and rocky shoreline compared to the low reflectance of water along the shoreline. A 4m buffer was added to the resulting land mask to eliminate adjacency effects from terrestrial vegetation and the presence of other nearshore algae such as *Fucus* spp. and *Ulva* spp. This masking method allowed precise delineation of the shoreline at the slightly different tide levels present between images. Next, a deep-water mask was applied using the 30m isobaths created using multibeam data acquired from the Canadian Hydrographic Service. This represents the maximum depth at which kelp generally grows in this region (Springer et al., 2007).

After applying the unique masks to each image, reflectance-based products were defined for optimizing input to the classification. A series of possible indices, reflectance transformations, and reflectance bands were tested for effectiveness in separating kelp from other cover types using the 2016 image and a subset of the field survey data. Using the Jefferies-Matusita distance statistical metric (Padma & Sanjeevi, 2014), NDVI (equation 1) and GNDVI (equation 2) were defined as best able to separate kelp from water, glint, shallow substrate and terrestrial vegetation in shadow. NDVI is the normalized difference vegetation index developed to enhance the detection of vegetation (Rouse et al., 1974) and is applicable to bull kelp due to kelp's similar reflectance properties (Figure 9); GNDVI or the green normalized vegetation index uses the green wavelengths instead of red, and is more sensitive to chlorophyll concentrations than NDVI (Goldberg, Kirby, & Licht, 2016).

$$NDVI = \frac{(NIR-Red)}{(NIR+Red)} \quad (1)$$

$$GNDVI = \frac{(NIR-Green)}{(NIR+Green)} \quad (2)$$

Additionally, a principal component analysis (Gupta et al., 2013) showed that PC1 was advantageous because of its ability to separate kelp from shadow over water that was not

previously masked due to its similar reflectance to kelp. These indices and transformations were combined as input for classification.

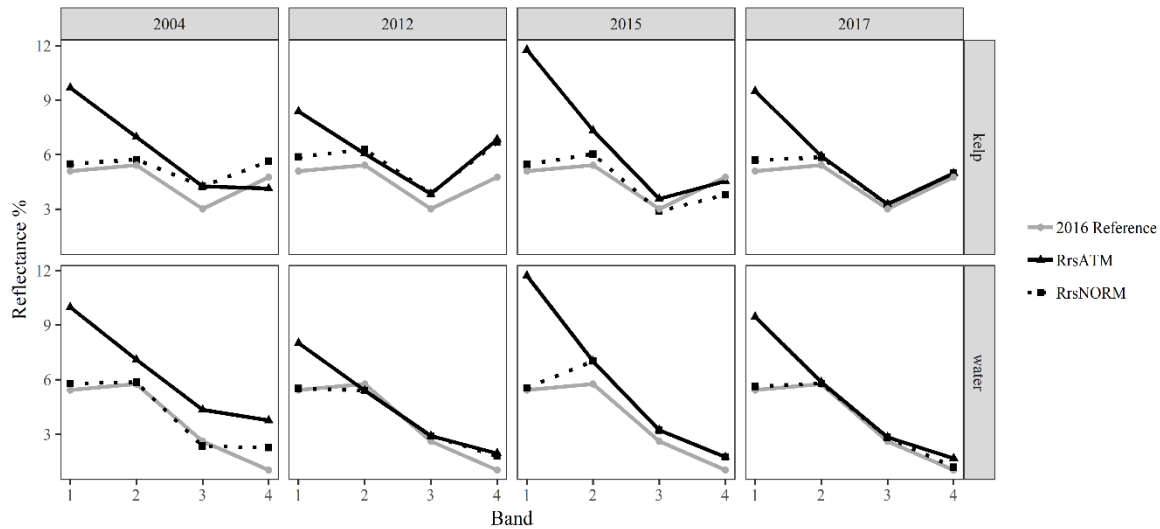


Figure 10. Example of normalization for water based on the 2016 corrected image (2016 Reference), and results before (RrsATM) and after normalization (RrsNorm) for each image year. Note the generalized decreased reflectance in band 1 (blue spectra) between RrsATM and RrsNORM showing improved Rayleigh correction, and the expected low and high band 4 (NIR) reflectance for water and kelp, respectively.

3.2.5 Classification

The unsupervised ISODATA classification method (Tou & Gonzalez, 1974) was deemed reliable for classification of historical imagery as it can be used without field survey data, which was unavailable for all years except 2016. This method was tested against several classification methods using the 2016 image and concurrent field survey data, and the results showed that the ISODATA approach performed similarly to supervised methods (Schroeder et al., 2019).

The ISODATA classification produced several classes for each image (8-12) and reflectance spectra for each class were compared to the known spectra for dense and sparse kelp derived from the 2016 image and *in situ* above-water spectra. These relationships were used to determine which of the defined classes should be categorized as kelp and then statistically confirmed in the validation step (Figure 11, Table 9). Finally, a filter to remove single isolated pixels identified as kelp that were separated by greater than eight pixels was applied; this situation may happen due to glint.

After the classification, the resulting kelp maps were validated following two distinct procedures due to availability of *in-situ* data: (1) 2016 image, accuracy assessment based on concurrent *in-situ* samples and (2) for the other years without concurrent field data, a statistical approach was taken. For the 2016 image, a confusion matrix was constructed using 849 randomly selected samples from the field data for accuracy assessment, and an error matrix was constructed to determine users, producers, and total accuracy. For the remaining images (2004, 2012, 2015, 2017), accuracy assessment was accomplished using the non-parametric Wilcoxon Signed Rank test (Taheri & Hesamian, 2013) to determine whether pixels classified as kelp in both, 2016 reference image vs. historical image, were spectrally statistically similar. First, a random sample of pixels ($n=500$) from the classification results was collected for each image and the spectral information from NDVI and GNDVI were extracted. PC1 values were not compared, as they are a function of the data within a scene and not expected to remain similar between images (Schowengerdt, 2012). The analysis takes into consideration that the output ranges of NDVI and GNDVI are a function of the proportion of highly reflective kelp in the NIR to highly absorbing water within each pixel.

3.2.6 Change Analysis

Several factors affect the accuracy of measuring changes in kelp extent derived using satellite-based methods, including:

- (1) Differences in the kelp extent in a given area from year to year. This may be caused by the dynamics of the environment during the growing season including temperature, nutrients, PAR and biotic interactions (Springer et al., 2007), as well as growing conditions in the previous year or years affecting the production and viability and settlement of spores (Cavanaugh et al., 2011; Pfister et al., 2018). This would be considered a true change in kelp extent.
- (2) Differences in the timing of peak kelp growth due to growing conditions from year to year. As bull kelp is an annual species, the timing of peak kelp growth may have natural variability from year to year depending on the growing conditions, including temperature, nutrient, and light availability. Extended periods of warm surface waters may also cause early die off in populations where peak growth is usually in late summer (Mumford, 2007; Simonson, Scheibling, & Metaxas, 2015). In this case, images collected prior to or after peak growth may underestimate maximum kelp extent.

(3) Differences in image quality due to environmental conditions at the time of acquisition including tide height, glint and water surface (Schroeder et al., 2019). Effects of currents can cause changes to surface kelp extent on an hourly and even minutely basis (Britton-Simmons et al., 2008). In this case, maximum kelp extent is present but is obscured by waves, glint or water column and is not detected in the image.

Together, these factors add complexity and uncertainty on how to define change in kelp extent based on area derived from image pixels. Satellite images offer a “snap-shot” of kelp extent, which may only represent a portion of the total kelp present in a given season depending on the conditions explained above. To overcome this problem, we adopted a method similar to that used in Pfister et al. (2018) in which shoreline units were used to analyze changes in kelp. We divided the study area into 100 m bins (shoreline units) taking into consideration the characteristics of the region, including the exposure, orientation and the average size of kelp beds data from the British Columbia Marine Conservation Analysis (BCMCA 2011), *in situ* observation, and field data. Within each bin, the number of times kelp was mapped over all the images was defined and expressed as a kelp persistence measure. For instance, a persistence of 100% indicates that kelp was present in a bin in all years analyzed. Note that due to the limited spatial coverage of the 2004 image, the east side of Sansum Narrows (Figure 12) was analyzed separately using the remaining four images (2012, 2015, 2016, and 2017); for this area, 100% persistence equals to kelp present in four years. Drivers of spatial and temporal kelp persistence were considered based on known factors that influence kelp growth and reproduction and data availability. High-resolution data of substrate and current strength allowed sub regional variation to be explored whereas sea surface temperature and climate indices were considered at a regional scale. Substrate type was identified through the ShoreZone coastal classes of “Rocky”, “Gravel”, “Sand”, and “Man-made”. Tidal current strength data Foreman (2004) was quantified using root mean square (RMS) of tidal speeds modelled over a number of tidal cycles, and is used as an indication of relative current speed. RMS analysis is used to indicate relative mixing within estuaries and enclosed areas such as fjords and narrows (Etherington, Hooze, Hooze, & Hill, 2007). Mixing is then used as an indicator of relative temperature and stratification conditions, where areas of high mixing indicate weak or no stratification, and therefore lower ocean temperature.

Multiple sources of sea surface temperature were considered including satellite derived SST anomalies for the Strait of Georgia from 2003-2016 (Suchy, Costa, & Perry, 2019) and SST data collected by a citizen science program as part of the Pacific Salmon Foundation's Salish Sea Marine Survival Project using CTD profiles collected in Cowichan Bay and Sansum Narrows from 2015-2017. The satellite-based data provides a broad scale picture of SST anomalies, which may have been modified to varying degrees across the subregions due to local scale driver such as mixing and river effluent. The limited time series of local scale data from the citizen science program corroborates this effect, as temperatures measured in the narrows were 1-3 degrees lower than the satellite data.

3.3 Results

3.3.1 Image Reliability

All images used for the persistence analysis showed high values for the reliability matrix, which was considered sufficient to detect presence or absence of kelp within a 100 m shoreline unit. The kelp maps (Figure 12) show similar patterns of kelp growth across years within the study areas. Specifically, the reliability matrix (Table 6) shows that the 2015 image exhibited the highest reliability (12) and the highest percentage of kelp (89.2%). The 2012 image had the lowest reliability (9) due to slightly poor environmental conditions, including tide height, glint, and water surface roughness (Table 1). The lowest kelp presence was detected in 2017 (45.7%), which had the second highest reliability (11) (Table 7).

Classification

The results of the accuracy assessment for the 2016 image with concurrent field data yielded total (86.9%), users' (81.9%) and producers' (93.1%) accuracies (Table 8). The largest errors occurred in areas where kelp corresponded to single bulbs or small clusters. These errors were a result of the greater proportion of water in these pixels dampening the high NIR reflectance of kelp. Similar results, with accuracies between 74-94%, were reported in other studies using satellite imagery to map floating algae where high-density beds had higher accuracy (Casal et al., 2011; Fyfe et al., 1999).

Table 8. Validation error matrix for the 2016 Image using a subset of concurrent field data.

		Field Data				
		Kelp	Non-Kelp	Total	User Accuracy	Total Accuracy
Classification	Kelp	376	83	459	81.9	86.9
	Non-kelp	28	362	390	92.8	
	Total	404	445	849		
	Producer Accuracy	93.1	81.4			

For the remaining image years of 2004, 2012, 2015, and 2017, the analysis of distribution and median values for kelp NDVI and GNDVI for all image samples are described in a boxplot in Figure 4. The Wilcoxon Signed Rank test shows that kelp NDVI values were the same as the 2016 reference pixels for all image years except 2004 and 2012 while the kelp GNDVI values were the same for all image years except 2012 (Table 9). The distribution of slightly higher NDVI and GNDVI values for 2004 and 2012 images are likely due to the presence of denser kelp beds than were present in the 2016 reference image rather than misclassification as spatial filtering and visual error adjustment would have removed any erroneous high NIR reflectance sources, such as glint or boats.

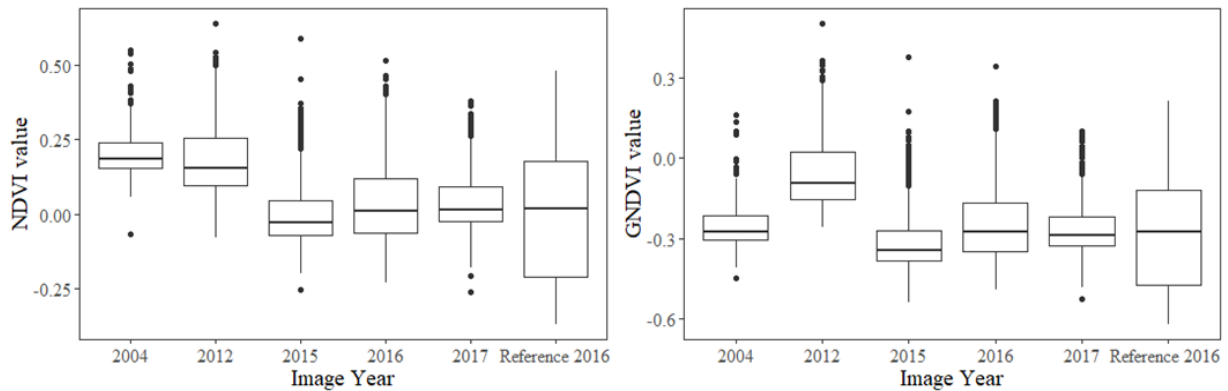


Figure 11. Boxplots of the relative distributions of sampled kelp pixels (n=500), for the classification results of each image year and the reference.

Table 9. Wilcoxon tests for differences between field data from 2016 base image and other imagery.

Image Year	NDVI			GNDVI		
	W stat	P value	Difference	W stat	P value	Difference
2004	11902	<0.001	yes	23901	0.0897	no
2012	15656	<0.001	yes	12028	<0.0	yes
2015	47028	0.988	no	48326	0.6571	no
2016	31482	0.1384	no	30384	0.1867	no
2017	24104	0.1029	no	24528	0.1683	no

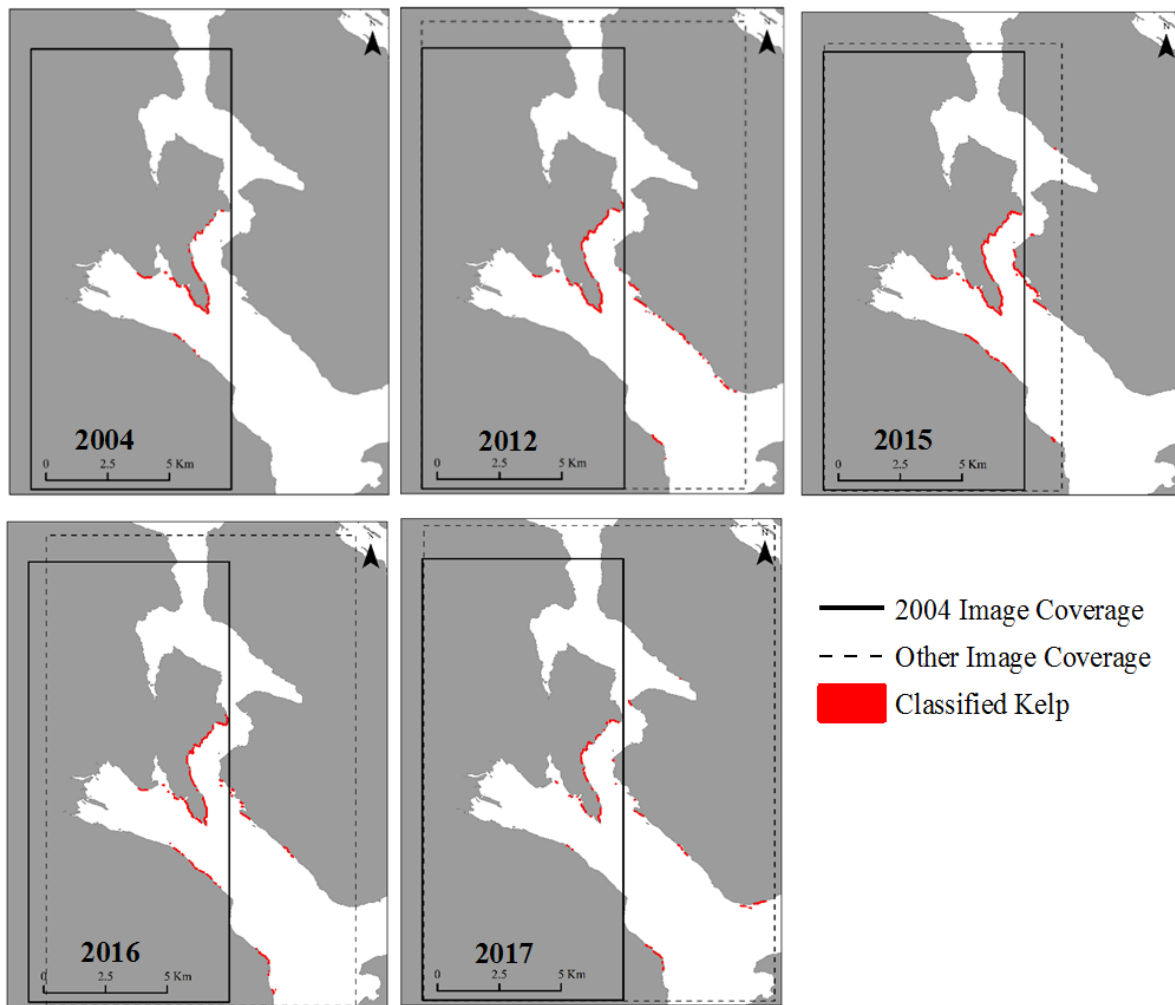


Figure 12. Classification results for the five images with each year's image extent shown in dashed lines. Note the difference in coverage area for the 2004 image which did not cover East Sansum.

3.3.2 Spatial Patterns of Persistence

Four hundred and forty-eight units were analysed, representing 48.8 km of coastline (Fig 13, 14). Of the 448 units, 37.1% (166 units) had kelp present in at least one year (persistence >0%). The regions north of Sansum Point (N, MB, OP), accounting for 31.2% (140) of all units, had kelp absent in all considered years (persistence= 0%). On the north side of Cowichan Bay (NC) and west side of Sansum Narrows (WS), persistence was generally high with 61.0% of units showing kelp present in at least one year. Specifically, in the WS region, 36.7% of shoreline units showed kelp present in all years and 54.4% in 4 or more years. In North Cowichan (NC), temporal presence of kelp was lower with 13.9% of units showing kelp in all years and 32.9% of units in 4 or more years, followed by even lower persistence measured on the south side of Cowichan Bay (SC), with no units having kelp in all years. The east side of Sansum Narrows (ES) also showed high persistence of kelp considering the 4 image years (excluding the 2004 image due to differences in image extents); kelp was present in about half of the 88 units and 50.0% of those kelp units had kelp present in at least 3 years.

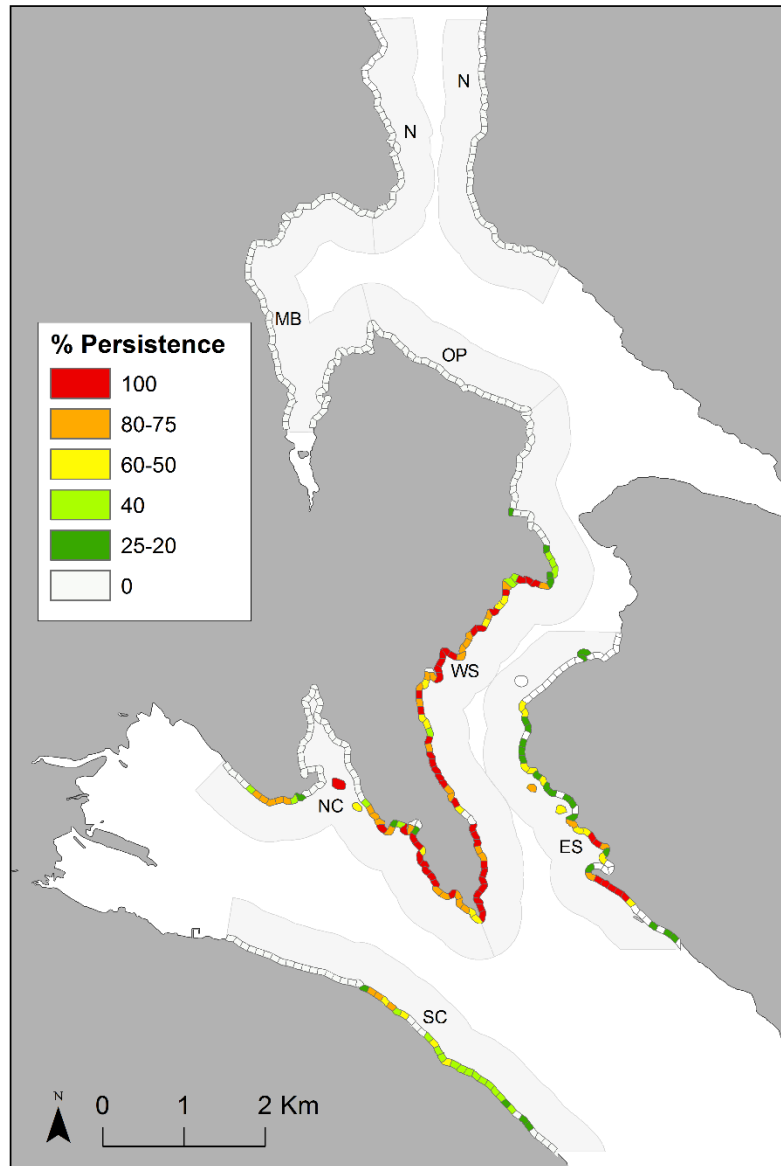


Figure 13. Persistence of kelp beds in Cowichan Bay and Sansum Narrows from 2004 to 2017. Shaded grey areas indicate the Sub regions of SC= South Cowichan, NC= North Cowichan, WS= West Sansum, ES= East Sansum, OP= Octopus point, MB= Maple Bay, N= North channel.

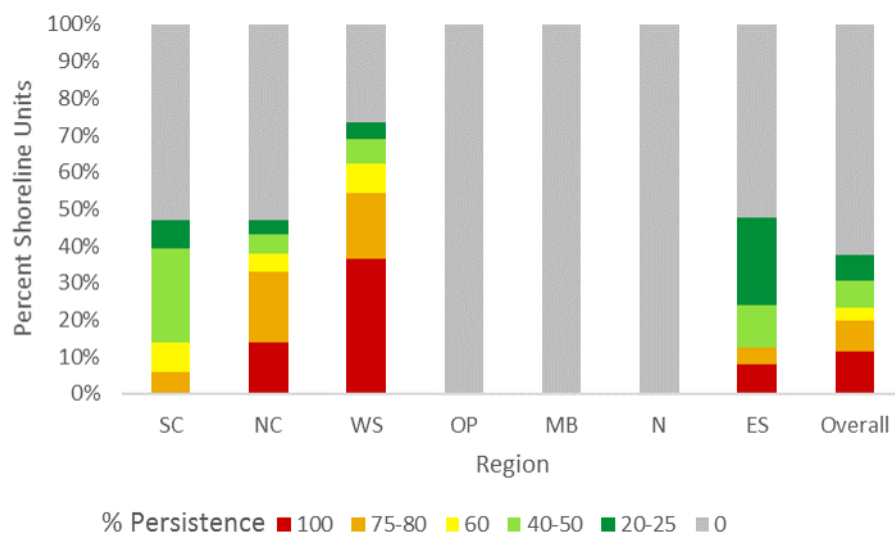


Figure 14. Percentage of total shoreline units with persistence of kelp by sub-region and entire region. East Sansum units are calculated from only four images (2012, 2015, 2016, and 2017) due to differences in number of images. For region definitions, see Figure 13.

3.3.3 Temporal Change

To understand change over time in kelp presence, the 166-shoreline units (37.1% of the total number of units), which showed kelp present in at least one year, referred to as “kelp units”, were used in the analysis. The kelp units were used with the understanding that units where persistence = 0 do not have suitable environmental conditions for kelp to grow and no change will have occurred over time.

We then used this set of kelp units (166) to calculate the yearly percentage of units with kelp present. Regionally, the highest kelp presence was in 2015 (89.2%), followed by 2016 (76.5%), 2004 (66.1%), 2012 (62.7%), and the lowest number was in 2017 (45.7%), (Figure 15). This indicates that there was an overall decrease in kelp presence from 2015-2017 of 48.6%, with a general increase from 2012 to 2015 of 42.9%. Similar trends are seen on a sub-regional scale, where all sub-regions experienced a loss of kelp from 2015-2017. However, this was least pronounced in West Sansum where the decrease was 20.3% compared to the greatest decrease in South Cowichan of 86.4% (Figure 15).

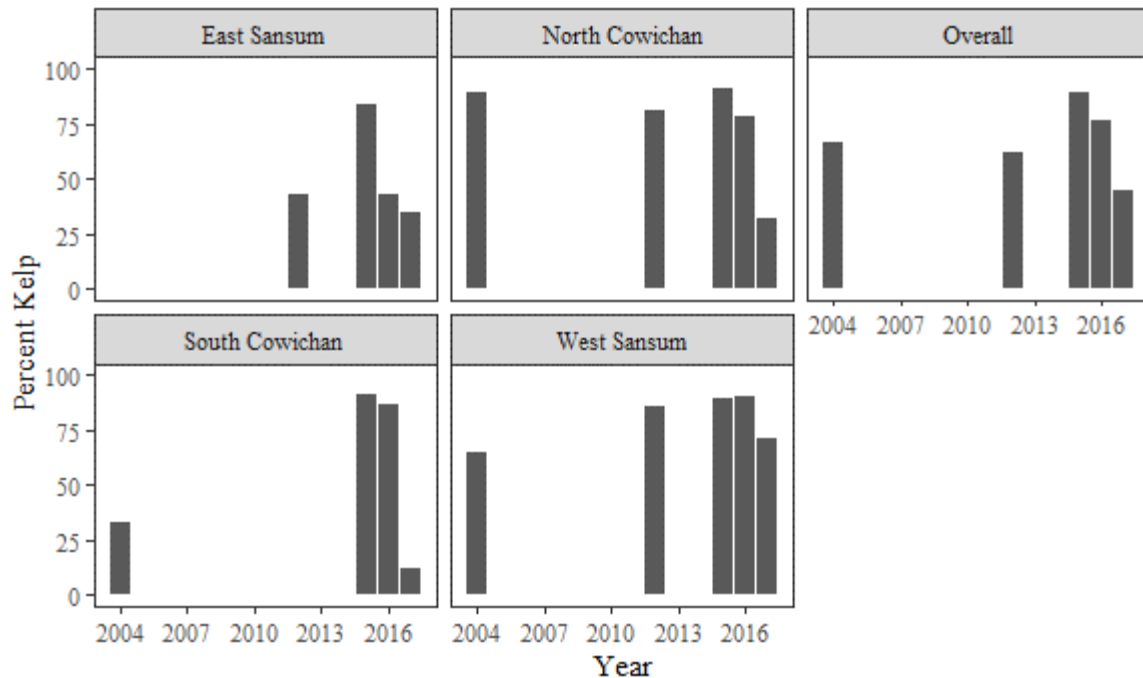


Figure 15. Percent of Kelp Units containing kelp each year by sub region and overall. Sub regions are: East Sansum (ES), North Cowichan (NC), South Cowichan (SC), and West Sansum (WS). Note OP, MB and N were not included as no units had kelp in any year. No data were available for ES in 2004 due to imagery coverage.

3.3.4 Spatial Drivers

Figure 16 shows the greatest persistence of kelp when the substrate is rocky and where RMS tide is either low, 0.1, or medium between 0.3-0.6, on a scale of 0-1 (M. G. Foreman, 1978). Figure 17 shows how East and West Sansum have both high proportions of rocky substrate and high RMS tide (>50% of area with values >0.5) and at the same time medium to high kelp persistence (Figure 14), while areas which had low kelp persistence in Maple Bay, Octopus Point and North region (Figure 14) had low RMS tide (values < 0.3).

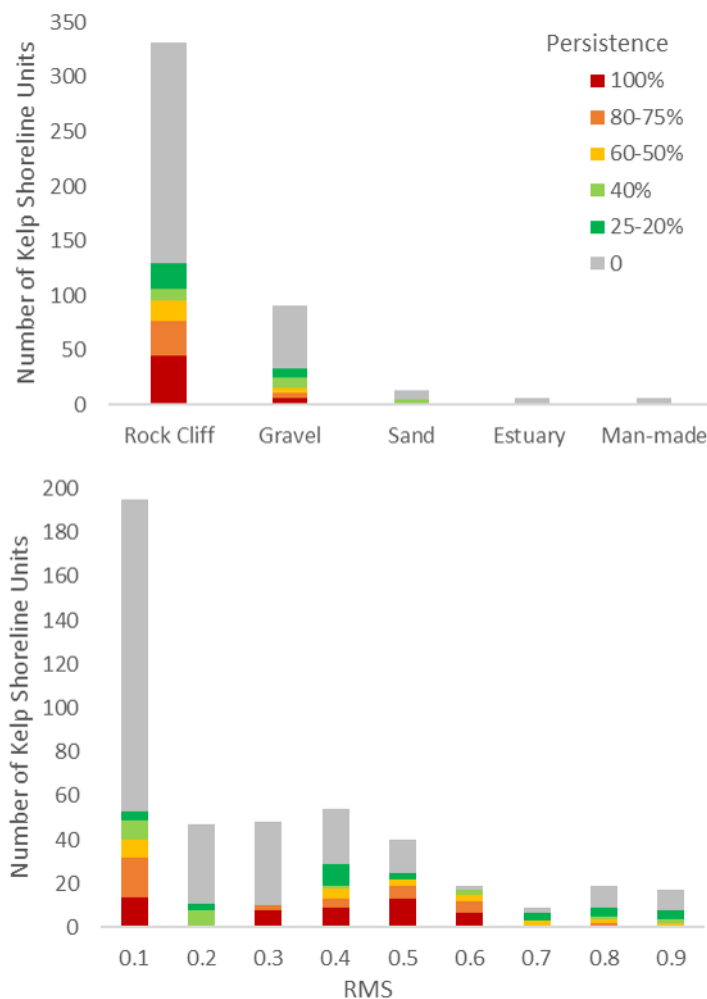


Figure 16. Kelp persistence across substrate types (top) and RMS tide (bottom), where RMS 0.1 is low current and 0.9 is high current.

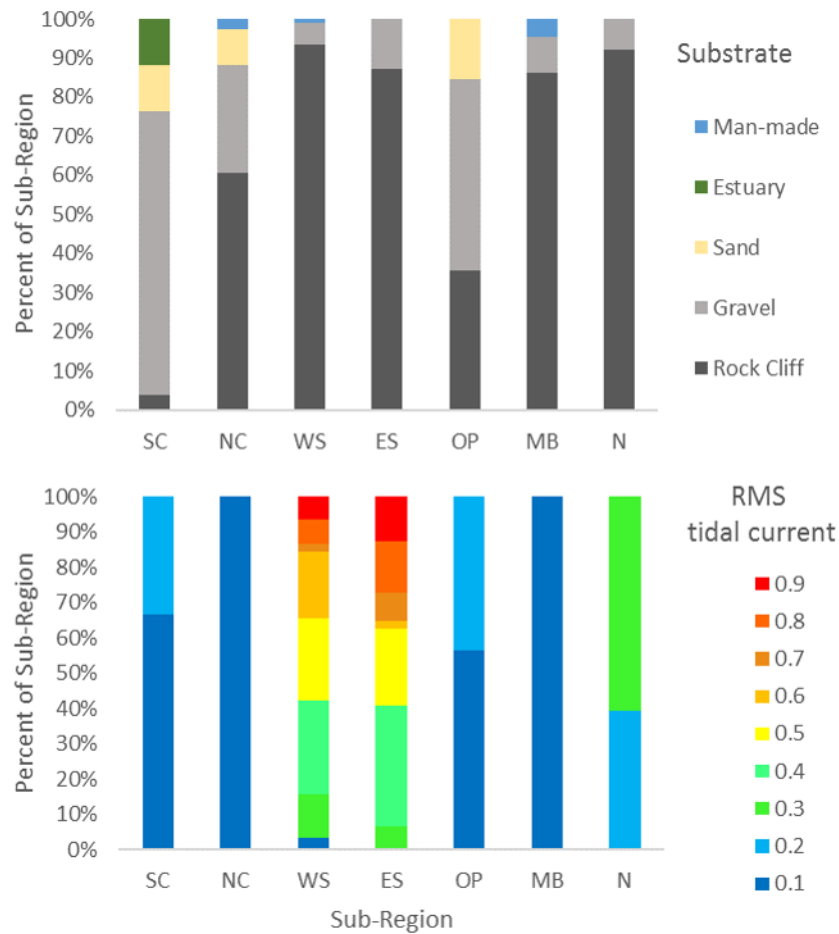


Figure 17. Coastal class (Top) and RMS tidal speeds (bottom) by Region. SC=South Cowichan, NC=North Cowichan, WS=West Sansum, ES=East Sansum, OP=Octopus Point, MB=Maple Bay, N=North.

3.4. Discussion

3.4.1 Limitations of Satellite Imagery

In a satellite imagery-based method, using kelp presence or absence within a shoreline unit helps to reduce the likelihood that no kelp is detected due to beds that are too small or sparse in relation to the imagery spatial resolution. Still, it is possible that only small patches of kelp are present in a given shoreline unit and thus not detected in which case the unit will be recorded as having no kelp. Further, the limited spatial and temporal extent of the dataset creates uncertainty in determining the drivers of kelp persistence. A longer time series of data with greater regional

coverage would allow better understanding of variability and its relationships to long and short-term local and global scale environmental conditions.

Other satellite platforms can be used for mapping kelp extent, each with their own strengths and weaknesses (Bennion, Fisher, Yesson, & Brodie, 2018; Schroeder et al., 2019). The use of commercial high-resolution satellite imagery as in this study allows the user to acquire images during optimal conditions of tide height, cloud cover, water conditions and kelp growth resulting in the highest quality imagery for mapping kelp. The high resolution allows small or fringing beds which are adjacent to the shoreline to be detected and may also be used to differentiate species (Botha, Brando, Anstee, Dekker, & Sagar, 2013) and estimate biomass (Andréfouët, Zubia, & Payri, 2004; Knudby & Nordlund, 2011). However, commercial platforms may be cost prohibitive as tasking imagery can cost up to \$30 USD/m (digitalglobe.com). However, free sources of imagery such as from the Landsat series with a 30m resolution much of the nearshore beds will be missed due to spectral mixing of pixels with land. Landsat is still a valuable source of imagery for mapping large kelp beds on a large scale where the use of an extensive historical time series can form composites of kelp extent seasonally and detect trends in kelp abundance and be averaged to account for areas covered by cloud and differences in tide. (Bell, Allen, Cavanaugh, & Siegel, 2018; Nijland et al., 2019) However, its application is limited to regions with large offshore beds of kelp (Nijland et al., 2019). Copernicus' Sentinel-2 is also a free source of imagery and with a spatial resolution of 10 m, it may be more appropriate for monitoring fringing kelp moving forward as the mission began in 2015. Additionally, free open source software such as Google's Earth Engine and QGIS are making the use of satellite imagery for environmental monitoring increasingly accessible to a wider user base and allow for the automated analysis of imagery for use in broad scale mapping and change analysis (Nijland et al., 2019; Traganos et al., 2018). These broad scale maps can then be used to inform the selection of representative or important sites for more rigorous surveys.

3.4.2 Spatial Drivers

The regions that had the highest kelp persistence were East and West Sansum (Figure 13 and 14). These areas provide optimal growth conditions in regards to substrate type (rocky) and relatively strong currents a result of the narrow passage (~0.5 to 1.0km) in Sansum Narrows (Mullan, 2017). These stronger currents result in higher mixing and reduced stratification, which

lead to lower temperature to which kelp is exposed compared to more stratified waters of Cowichan Bay.

The kelp persistence in Cowichan Bay may also be driven by substrate type and current strength. On the north side of Cowichan Bay there is a prevalence of rocky substrate, so despite the low currents recorded here (expressed as 0.1 RMS) kelp growth is supported (Figure 14 and 17). The lower persistence of kelp along the south side of Cowichan Bay is likely associated with substrate availability; here substrate consists of sand and gravel combined with lower currents, which allow for sediment deposition and less available substrate for kelp growth. Gravel and sand habitats typically indicate lower energy environments and favour species such as eelgrass, which attaches to substrate using root-like rhizomes (Mumford, 2007). Limited availability of hard rocky substrate will constrain the amount of kelp that can grow and the presence of sandy substrate indicates deposition of sediment, which can smother kelp recruits.

The sub regions north of Sansum Point (Octopus Point, Maple Bay and the North Channel) have similar predominantly rocky substrate types and current regimes (>0.3) to North Cowichan; however, kelp is absent in these regions whereas there are persistent beds in North Cowichan. Conditions north of Sansum Point may be less optimal for kelp growth due to warmer SST and higher turbidity when compared with North Cowichan. These regions may experience a stronger influence from warmer, turbid, stratified waters from the Fraser River (Suchy et al., 2019).

3.4.3 Temporal Change

The general detected change in kelp presence may represent a true decline from 2015-2017 or it may be within the natural bounds of variation given that presence in 2015 (62.6%) was not much higher than in 2017 (45.7%). However, on a sub-regional scale, it appears there are large variations in kelp, especially in South Cowichan; here we observed 91.9% in 2015 and 12.5% in 2017. In nearby Washington State, Pfister et al. (2018) showed that there was little significant change in kelp persistence over a period from 1911-2015, except for areas in close proximity to human populations where kelp populations showed declines. Further, Krumhansl et al. (2016) found a slight increasing trend in the Ecoregion containing Oregon, Washington, and Vancouver Island in studies spanning from 1983-2012, and suggested that local drivers including successful management practices, recovery of urchin predators and reduction in pollution are responsible for the differences from globally decreasing trends.

In the study area of Cowichan Bay and Sansum Narrows, environmental management has focused on the river and estuarine system including improving river levels, salt marsh and eelgrass bed restoration in support of creating habitat for juvenile salmon (<https://www.cowichanestuary.com/projects-2/>). More broadly, the provincial government has conducted limited inventories of coastal kelp resources for determining harvest quotas with the most recent in 2007, (Sutherland et al., 2008) however, kelp in the study is not harvested and the observed changes are likely associated with local environmental conditions.

The changes in persistence for the study region do not follow the expected trend in relation to large-scale climate indices. For instance, decreased kelp presence may occur during warm periods of the Pacific Decadal Oscillation (PDO) and El Nino Southern Oscillation (ENSO) as observed in Pfister (2018) and higher kelp presence during positive phases of the North Pacific Gyre Oscillation (NPGO) when salinity and nutrients are high (Di Lorenzo et al., 2008). Instead, for 2015, the year with the highest recorded regional temperature anomalies during a positive PDO, our data showed the highest presence of kelp. In Washington State, the PDO, NPGO, and ENSO indices were found to have significant correlations with kelp abundance (Pfister et al., 2018), whereas lower temperatures (negative PDO, ENSO, positive NPGO) were associated with higher nutrients and increased kelp abundance. Multiple studies have shown the inverse relationship between warm climate regimes and kelp abundance (Cavanaugh et al., 2011; Filbee-Dexter, Feehan, & Scheibling, 2016; Ronald E. Foreman, 1984; Krumhansl et al., 2016; Pfister et al., 2018), however, the impacts may be short-lived given a switch to colder, nutrient rich conditions, which can provide opportunities for kelp to recover relatively quickly (Pfister et al., 2018).

Several factors may explain the changes in kelp persistence described in this study. Poor environmental conditions such as the warm SSTs recorded from 2013-2016, may have had a lag in the effects on the persistence of kelp. In these conditions, prolonged periods of exposure to water temperatures greater than 17°C has been shown to reduce spore formation and germination success (Springer et al., 2007; Vadas, 1972). The warmer than average regional SSTs in 2015 and 2016 (Suchy et al., 2019), may be responsible for the lower presence of kelp in the subsequent years (2016, 2017) through reducing spore production and germination (Dayton, Tegner, Edwards, & Riser, 1998). Similarly, a one-year lag was shown to be the best predictor of

kelp growth and SST in Washington State (Pfister et al., 2018). Conversely, light availability, which also limits kelp growth, is more likely to cause within-year effects on kelp beds (Desmond, Pritchard, & Hepburn, 2015). In 2015, positive anomalies in photosynthetic light availability were recorded for the Strait of Georgia region, which may help to explain the high kelp presence for that year.

Furthermore, in situ measurements of SST from Cowichan Bay from 2015 to 2017 were on average 3°C cooler than those measured for the Strait of Georgia region, indicating that large-scale temperature anomalies were likely minimized due to the higher currents and stronger mixing in this sub-region. Because both nutrient availability and stratification are linked to temperature and mixing, this sub-region, particularly Sansum Narrows may experience better kelp growth conditions than the region as a whole. This is significant as the persistence of kelp populations here may be an important source of spores to adjacent areas and facilitate connectivity between habitats (Coleman et al., 2011; Olson, Hessing-Lewis, Haggarty, & Juanes, 2019; Reed, Schroeter, & Raimondi, 2004).

3.5. Conclusion

Using high spatial resolution satellite imagery, temporal and spatial persistence of kelp was determined in the coastal waters of British Columbia. In this region, bull kelp showed higher persistence in areas with rocky substrate and well-mixed waters. Temporal analysis showed declines from 2015-2017, which may be due to local scale effects related to a lag effect from anomalous warm temperatures from 2015-2016.

Limitations of using satellite images for kelp detection include access to images with the appropriate spatial, spectral, temporal and physical coverage of the areas of interest, and the environmental conditions during acquisition such as tide height, season, sun glint and water surface. By using only images with the highest reliability, the resulting classifications show higher accuracy (86.9% in relation to field surveys) and acceptable statistical performance compared to expected spectral characteristics of kelp for historical images.

Continuous and long-term mapping is needed to establish relationships between the measured persistence and environmental variables and to determine whether declines are long lasting or due to natural variability. By utilizing all available imagery sources such as new sensors like Sentinel-2 and developing automated processes for detecting kelp, a greater understanding of

spatial and temporal drivers can be gained. Monitoring efforts may want to combine large scale mapping for broad scale spatial temporal distribution and use this data to select representative sites for yearly collection of more detailed data for validation of imagery and biological data. This will allow conservation and management initiatives to better understand and mitigate impacts to kelp ecosystems.

4.0 Investigating the Use of Kelp Habitat by Juvenile Salmon during Early Marine Residency

4.1 Introduction

On the West Coast of North America, Pacific Salmon (*Oncorhynchus* spp.) are a significant source of prey for many species of birds, fish and mammals across a range of ecosystems from rivers and lakes, through estuaries, nearshores habitats and the open ocean (Schindler et al., 2003). Salmon also serve an important role as suppliers of nutrients to terrestrial systems (Gresh, Lichatowich, & Schoonmaker, 2000). Further, there are large economic, cultural, and social values of these important species with commercial and sport fisheries earning on average \$850-1996 million USD annually for Canada and the United States, respectively (Gislason et al., 2017). However, anthropogenic related activities are also the source of many adverse impacts to salmon populations, including overfishing (Finney, Gregory-Eaves, Sweetman, & Smol, 2007; Gresh et al., 2000), habitat degradation (David et al., 2016; Dethier et al., 2016), pollution (Macneale, Kiffney, & Scholz, 2010), introduction of parasites (Krkošek et al., 2007), disease (Di Cicco et al., 2018), and impacts of climate change (Finney et al., 2007). Together, this has contributed to declines in many Pacific salmon populations along the coast over the past decades (Beamish, Sweeting, Beacham, Lange, & Neville, 2010; Labelle, 2009; Ruff et al., 2017)

While mortality risks are present for salmon at every life stage, recent research has identified that early marine survival is an important predictor of overall survival (Lange, Neville, & Sweeting, 2011) as a result of bottom up and top down effects. Bottom up effects include habitat degradation (Beamish et al., 2010; Riche et al., 2014) and changes in oceanic conditions such as temperature, light and nutrients, which lead to decreased prey abundance and salmon fitness (Ruff et al., 2017). Top down effects include increased predation by fish, birds and mammals (Lance, Chang, Jeffries, Pearson, & Acevedo-Gutiérrez, 2012).

As juvenile salmon exit natal rivers and enter the marine environment, the quality of habitat encountered is essential for providing adequate food sources and refuge from predators allowing for growth, which is one of the main indicators of survival (David et al., 2016; Duffy & Beauchamp, 2011). During this phase of growth and transition to marine conditions, salmon

disperse from estuarine saltmarshes, traveling along the nearshore where eelgrass and kelp beds are the prevalent vegetative aquatic habitats. Where substrate is sandy and currents are weak, eelgrass beds in tidal flats provide opportunities for foraging and refuge (Kennedy, Juanes, & El-Sabaawi, 2018). Along the nearshore region where rocky coastlines dominate, sub-tidal and canopy forming macro-algae such as kelp create a three-dimensional habitat providing foraging opportunities and refuge from predators and currents (Shaffer, 2004; Teagle et al., 2017). Bull kelp (*Nereocystis luetkeana*) and giant kelp (*Macrocystis pyrifera*) are two dominant canopy-forming kelps on the West Coast of North America with distributions ranging from California to Alaska. These foundation species form important habitat and have been shown to increase faunal diversity and provide important services to nearshore ecosystems (Schiel & Foster, 2015; Springer et al., 2007). Anecdotal reports and a few studies indicate juvenile salmon use kelp habitats as either refuge, a feeding source, or both (Shaffer, 2004). However, these studies are limited due to the inherent difficulties in sampling within kelp beds. This research aims to investigate the use of kelp habitat by juvenile salmon in nearshore areas in the Salish Sea, West Coast of Canada. Specifically, we aim to detect potential differences in the density of juvenile salmon in kelp-associated areas compared to adjacent areas not associated with kelp, using non-invasive, non-lethal sampling methods of visual counts via snorkel transects and remote underwater video.

4.2 Methods

4.2.1 Study Area

The study area is located in Cowichan Bay, on the East Coast of Vancouver Island in British Columbia, Canada (Figure 18). Flowing into Cowichan Bay, the Cowichan River supports wild populations of Chinook (*O. tshawytscha*), Coho (*O. kisutch*) and Chum (*O. keta*) salmon. Fisheries and Oceans Canada identifies the Cowichan Chinook population as an indicator stock, resulting in comprehensive monitoring data including in-river counts, biological sampling in the bay using beach and purse seines, and tagging programs used for tracking migration and survival rates (Beamish, McCaughran, King, Sweeting, & McFarlane, 2000; Neville, Beamish, & Chittenden, 2015). Additionally, hatchery raised Chinook are released in late spring so that the timing of juvenile migration from the river is recorded and predictable (Schmidt, Pearsall, Riddell, Sucic, & Ewanciw, 2018).

Cowichan Bay and the surrounding inter-island narrow passages support a corridor of bull kelp beds extending from the north side of the Bay and into Sansum Narrows (Schroeder et al., 2019) where several tagging and seining projects have recorded juvenile salmon throughout the summer (Beamish et al., 2000; Neville et al., 2015). This region is characterised by salt marsh and eelgrass habitat in the tidal flats of the estuary with rocky shorelines on the north side of the bay supporting persistent kelp beds, and gravel and sand shoreline on the southern shores with some thin fringing kelp with variable persistence (Schroeder et al. submitted).

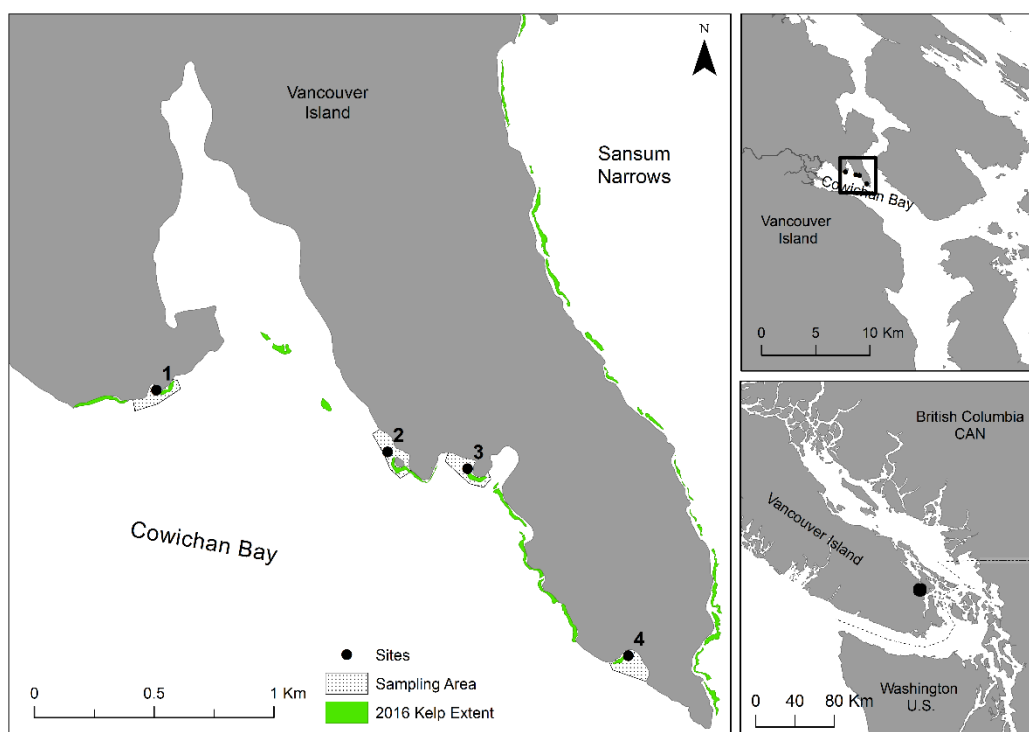


Figure 18. Location of sampling sites on the north side of Cowichan Bay, East Coast of Vancouver Island, British Columbia, Canada. Green polygons indicate kelp beds mapped by kayak in 2016.

4.2.2 Field Methods

Four sampling sites were chosen based on the location of kelp in maps derived from satellite and kayak-based methods conducted in August 2016 (Schroeder, Dupont, Boyer, Juanes, & Costa, 2019) and knowledge gained from tagging programs of where salmon were likely to be found (Schmidt et al., 2018). Within each of the four sites, one “kelp” area and one “no-kelp” area was designated (Figure 19). Specifically, kelp areas (Kelp) were defined as areas that had been mapped with kelp beds at least 60m long and 5m wide. No-kelp areas (Nok) were areas adjacent to the kelp area that had a similar rocky shoreline type but where there was no kelp recorded in

the 2016 map (Schroeder et al., 2019). Pairing the areas within-site allowed for differences in salmon counts caused by sampling conditions, such as exposure to waves, tide height, and time of day and physical characteristics to be minimized (Dethier et al., 2016).

Due to accessibility, tide and weather conditions, each site was sampled by snorkeling and remote stationary underwater video, on average once per week from May to August 2017. The sample timing was planned to coincide with the known migration of salmon from the Cowichan River and the release of hatchery Chinook on April 17th and May 24st. However, kelp beds in this region were not present at any of the selected areas until June, and thus the kelp and no-kelp areas were sampled during the period before any kelp was present and during growth of the plants. The data analysis was therefore separated into two periods (1) “pre-kelp” where both Kelp and Nok areas did not contain kelp, from week 1-6 (May 1-June20), (2) “With kelp” defined as the time when “kelp areas” had at least 15 plants reaching the water surface which occurred at all sites by June 21st (week 7-13).

4.2.3 Snorkel Data

Snorkel transects were conducted at each site in the kelp and no-kelp areas along a line running through the center of the kelp area parallel to the shore and at the same bathymetry contour for the no-kelp area; these are referred to as the middle transects. Additional transects on the inner and outer sides of the kelp area were swum, as well as the corresponding bathymetry contours of the no-kelp area (Figure 19). Each transect was approximately 80-90m in length depending on the site and was swum at a slow speed of approximately 0.2 m/s to reduce disturbance to fish (Smith, 1988). Following established methodology (Granneman & Steele, 2015; Millar, Babcock, & Willis, 2000), all salmon encountered, the approximate fish size, and other observations, such as behaviour, were recorded on a dive slate. Other species present were also recorded, including invertebrates and other fish. The snorkeler also carried a digital underwater camera to aid in fish identification, post survey.

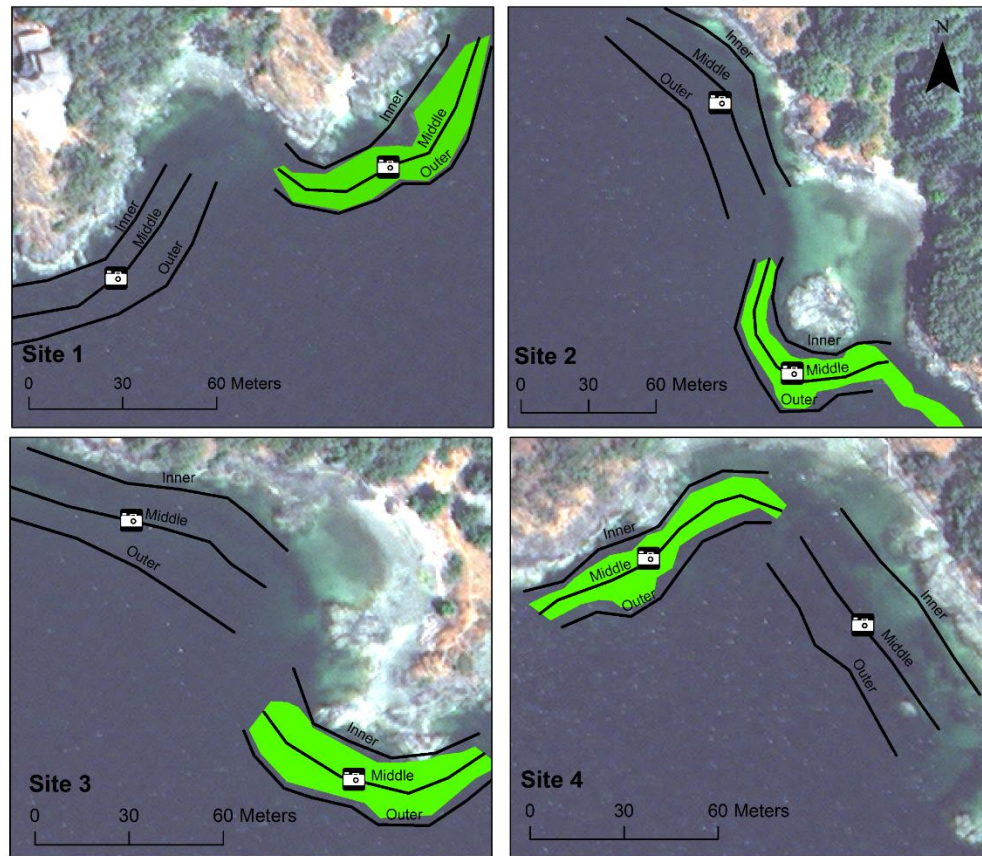
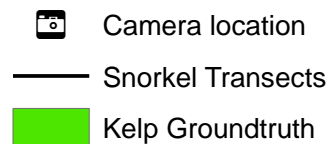


Figure 19. Location of snorkel transects, remote camera's and kelp and no-kelp areas within the four sampling sites.



4.2.4 Video Data

As very few studies had attempted to record salmon in kelp beds (but see Shaffer, 2004), an additional method using stationary underwater video was employed to (1) understand the effects of snorkeler visual counts on fish behaviour (Dearden, Theberge, & Yasué, 2010) and (2) determine if video is a feasible method for studying highly mobile species in the changing conditions of kelp beds by comparing video results to snorkel counts. Cameras attached to weighted tripods were placed in the center of the kelp and no-kelp middle transects. Each tripod was adjustable for the height of the tide on a given day (max 3.5m) and mounted with two Sony HS-A50 underwater cameras, one rear, and one front facing. These cameras could also be rotated and moved up or down depending on the conditions when deployed (Figure 20). Camera height was adjusted so that they were approximately 45cm below the water surface, as preliminary

observations determined juvenile salmon were primarily found within the top of the water column. Cameras were deployed upon arrival to each site and data recorded for approximately 60 minutes per deployment, which included the time before, during and after the snorkeler was in the water allowing for visual analysis of the effect of the snorkeler on the behaviour of the fish (Cappo, Harvey, & Shortis, 2006; Mallet & Pelletier, 2014).

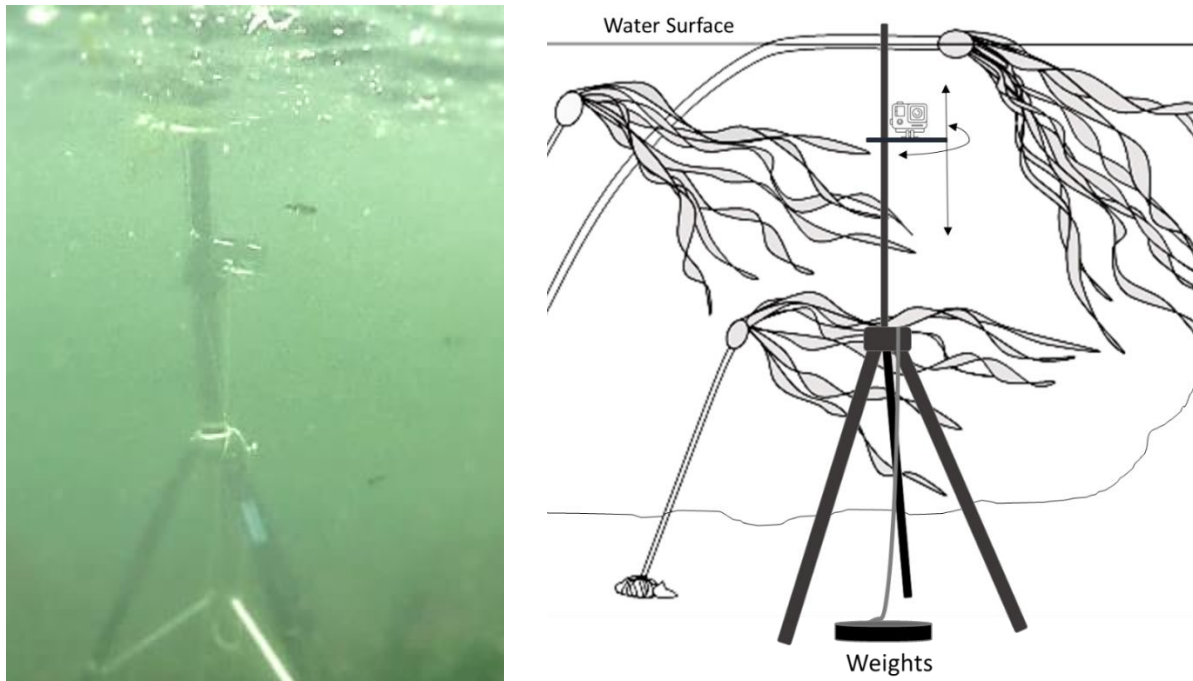


Figure 20. Image and diagram of remote underwater video tripod. Two cameras facing opposite directions adjustable up to 3.5m vertically and 360 degrees depending on orientation of kelp and direction of sun.

4.3 Data Analysis

4.3.1 Snorkel Data

First, salmon count data from the snorkel transects were converted to salmon density in m^3 given the number of salmon counted per meter of transect, following methods by Shaffer, (2004).

Subsequently, salmon density data were tested for differences between Kelp and Nok area overall, before and with kelp presence, and by transect according to the Paired Wilcoxon Signed Rank test with the significance threshold set at 0.05 (Taheri & Hesamian, 2013).

4.3.2. Video Data

In total more than 240 hours of video were recorded and analysed by trained personnel. Using methods developed by Ellis and DeMartini (1995), the maximum number (maxN) of fish in a given frame was determined by analysing twenty-five minutes of video, from the one hour sampling period for each kelp and no-kelp area. Any time fish were in frame, the time, species and number of fish was recorded. If the snorkeler appeared in frame, counts were paused for one minute before and one minute after to allow any disturbance to be minimized. Additionally, frames where kelp obstructed the view by more than 20% were not analyzed. The final maxN values are the maximum number of salmon counted in a single frame per sampling period. While this method is extremely conservative as it defines the minimum number of fish known to occur in a recording, it eliminates the potential for the same fish to be counted multiple times. Using the maxN for the paired kelp and no-kelp areas, a relative comparison of the two habitat types can be accomplished. Additionally, the use of relative comparisons reduces the effects of the visibility, tide and current, which are assumed to be constant between kelp and no-kelp areas within a site during a given sampling period, but will change from day to day and over a season. Video data were analyzed similarly to snorkel data, except only for the middle transect.

4.4 Results

Average salmon density overall and by site, transects and week is summarized in Figure 21. All salmon observed in the inner and middle transects and on the video were estimated to be between 60-100 mm with the exception of the outer transects later in the season (July, August) where several fish greater than 120 mm were observed. Other species recorded included shiner perch (*Cymatogaster aggregata*), kelp perch (*Brachyistius frenatus*), striped sea perch (*Embiotoca lateralis*), bay pipefish (*Syngnathus leptorhynchus*), tube snout (*Aulorhynchus flavidus*), sculpin (*Oligocottus spp.*), red rock crab (*Cancer productus*), kelp crab (*Pugettia producta*), harbour seals (*Phoca vitulina*), and river otter (*Lontra canadensis*).

4.4.1 Snorkel Data

In total, 2092 juvenile salmon were counted using the snorkel method, of which 1685 were recorded in the Kelp areas and 407 in the Nok areas. Paired Wilcoxon Signed Rank tests showed that overall there was a significant difference ($\alpha = 0.05$; $P < .0001$) between salmon density in the Kelp and Nok areas. Kelp areas had an average density of 0.15 (0.040) salmon/m³ (mean and

SE), while no-kelp areas had an average density of 0.036 (0.012) salmon/m³. Before kelp was present, an average salmon density of 0.27 (0.12) salmon/m³ in Kelp and 0.066 (0.34) salmon/m³ in Nok was recorded. With kelp beds present, there was an average of 0.089 (0.20) salmon/m³ Kelp and 0.021 (0.0067) salmon/m³ Nok. Specifically, by transect, average densities of salmon were 0.18 (0.057) salmon/m³ in the inner (0.32 [0.11] Kelp, 0.036 [0.013] Nok), 0.060 [0.018] in the middle (0.070 [0.021] Kelp, 0.050 [0.028] Nok) and 0.030 (0.013) salmon/m³ in the outer (0.044 [0.023] Kelp, 0.016[0.011] Nok). The inner transects densities were significantly different ($P < .001$), whereas the middle and outer transects were not significantly different between Kelp and Nok areas ($P = .18$ and $P = .53$, respectively, Table 10).

Considering only the data before kelp beds were present (May 4th- June 21st, Weeks 1-6), there was a significant difference in overall salmon density between the Kelp and Nok areas ($P < .01$) and the inner transects accounted for this difference ($P < .01$), while the middle and outer were not significantly different. The data collected during the period when kelp beds were present show similar results where Kelp and Nok areas were different and this was driven by the inner transect (Table 10).

The average salmon density were greatest at site 3 0.14 (0.066) salmon/m³ (0.24 [0.13] Kelp, 0.039 [0.016] Nok) followed by sites 1: 0.097 (0.039) salmon/m³ (0.11 [0.045] Kelp, 0.079 [0.064] Nok), site 4: 0.085 salmon/m³ (0.15 [0.063] Kelp, 0.017 [0.011] Nok) and the lowest density at site 2: 0.052 (0.013) salmon/m³ (0.077 [0.023] Kelp, 0.026 [0.012] Nok).

The salmon density by week (Figure 21d) follows the expected trends in salmon migration as defined by the timing of hatchery fish release and recorded from other surveys. Peak densities were recorded in week three corresponding to the release of hatchery fish (Figure 21 D) with 0.64 (0.41) salmon/m³ in kelp areas and 0.19 (0.13) salmon/m³ in Nok. As sampling progressed through the season, lower salmon densities were measured in both Kelp and Nok areas (0.00088 [0.00088] salmon/m³ Kelp and Nok, week 13).

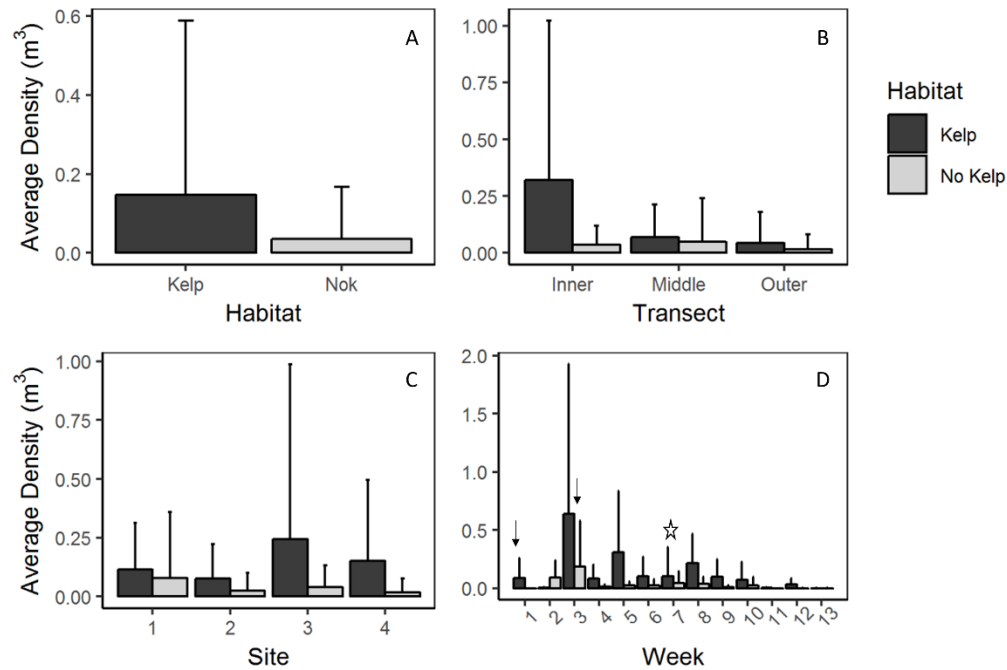


Figure 21. Snorkel data for average salmon density per m³ error bars indicate one standard deviation by a) Habitat, and Habitat by b) Transect, c) Site and d) Week. Star indicates time when kelp was present at surface. Arrows indicate weeks of hatchery salmon release. April 17th and May 24th. Note: The different scales for the y-axis due to the range of values included with the error bars.

Table 10. Results of Paired Wilcoxon Signed Rank Test for Salmon Density measured by Snorkel Survey

	P value	Significance ($\alpha = 0.05$)
<i>Overall</i>		
All Transects	5.029e-06	Yes
Inner	4.958e-06	Yes
Middle	0.1836	No
Outer	0.5268	No
<i>Before Kelp Growth</i>		
All Transects	0.005624	Yes
Inner	0.003857	Yes
Middle	0.5049	No
Outer	1	No
<i>After Kelp Growth</i>		
All Transects	0.0002797	Yes
Inner	0.0005901	Yes
Middle	0.169	No
Outer	0.4388	No

4.4.2 Video Data

For the Kelp areas maxN ranged from 0 to 113 and the Nok areas maxN ranged from 0 to 45. Peak maxN values occurred in week 1 (May 1-7) for both Kelp and Nok areas, with a mean maxN of 62.0 (51.0) [mean and SE] for Kelp and 19.0 (19.0) for Nok areas. Before kelp was present, the mean maxN for Kelp was 14.1 (7.4) and the mean for Nok areas was 9.0 (3.7). With kelp present, the mean maxN for Kelp was 2.6 (0.74) and the mean for Nok areas was 2.5 (0.86). Wilcoxon tests of the difference between maxN found a significant difference between Kelp and Nok areas overall ($P = .038$) (Table 11). Further, there was a difference measured before kelp beds were present ($P = .037$) but no significant difference with kelp present ($P = .49$, Table 11).

MaxN values by site also show a trend similar to the snorkel data, where site 3 had the highest maxN 10.3 [5.3], (14.4 [10.1] Kelp, 6.09 [3.48] Nok). Sites 2 showed the opposite effect with an average maxN of 2.25 (0.75), (1.42 [0.37] Kelp and 3.08 [1.45] Nok, Figure 22 B). By week the peak maxN was recorded in week 1 at the beginning of May with an average maxN of 40.5 (25.5), (62.0 [51.0] Kelp, 19.0 [19.0] Nok), which may correspond to the first release of fish from the hatchery in late April (Figure 22 C).

Comparing the video data to the analogous snorkel data from the middle transect, a similar pattern was observed. Both methods of observation found higher salmon counts in the Kelp areas and peaks in salmon number during the “before kelp” phase of the survey in week 1 (video) and 4 (snorkel) (Figure 22).

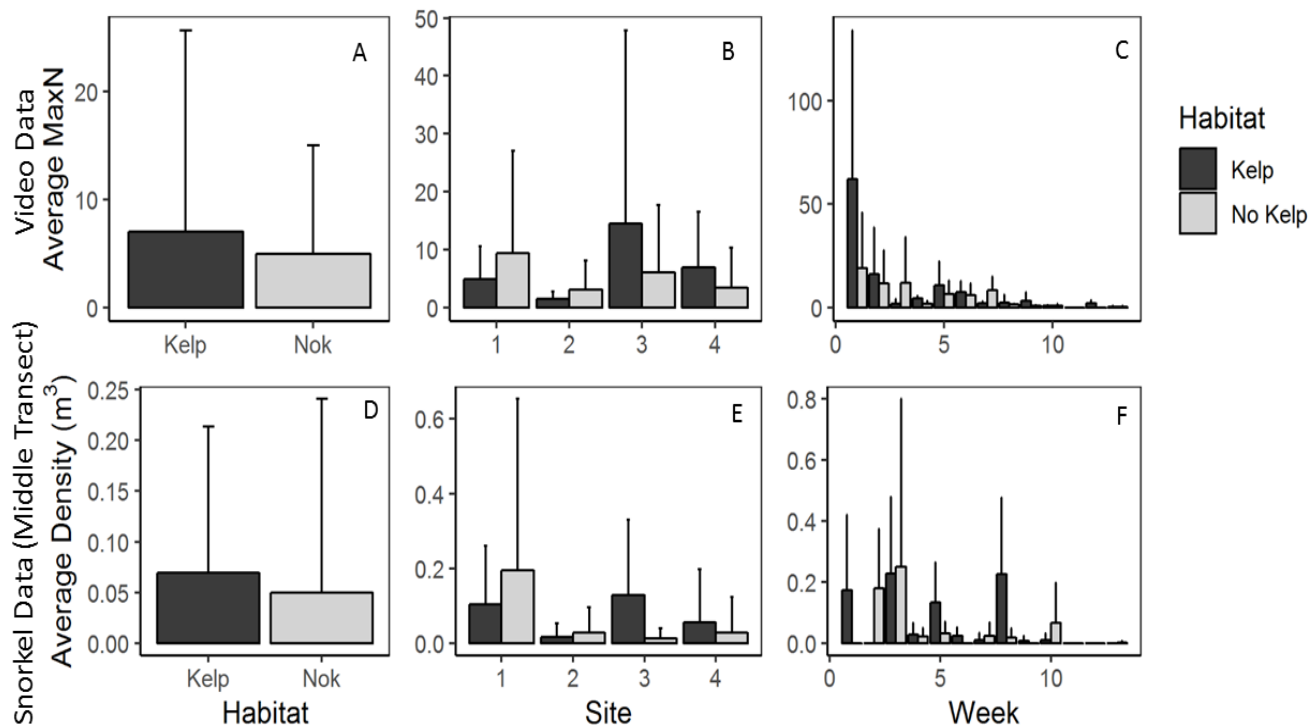


Figure 22. Average MaxN and one standard deviation by habitat type (A, D), site (B, E) and week (C, D) for video data and the analogous average salmon density from the middle transect of snorkel data. Note: Different scales are used for the y-axis due to the range in values when including error bars.

Table 11. Results of Paired Wilcoxon Signed Rank Test for maxN of Kelp and Nok areas calculated from stationary video data.

	P-value	Significance ($\alpha = 0.05$)
Overall	0.03777	yes
Before kelp	0.03727	yes
With Kelp	0.4934	no

4.5 Discussion

4.5.1 Snorkel vs video survey

There are advantages of using snorkel surveys in kelp beds, including the ability to maneuver through dense plants and decrease disturbance and impacts to both the kelp beds and fish. However, several factors must be considered in the analysis of the resulting data. The effect of the snorkeler on salmon behaviour was observed through review of the stationary video data. Salmon were observed moving away from the snorkeler but returned to their original positions within seconds of the snorkeler leaving the video frame. It is possible that due to the displacement caused by the snorkeler, the same fish could be recorded multiple times in different transects and across the kelp and no-kelp areas. Dearden et al. (2010) found the presence of

snorkelers conducting visual fish counts in coral reefs reduced the total fish count; however, this was species dependent. Brignon et al. (2011) also found that snorkeler presence disturbed juvenile salmon in rivers and resulted in altered fish behaviour but did not change the number of fish in the field of view. In our methods, we accounted for the effect of snorkeler disturbance by pairing habitat areas with the assumption that the effect would remain the same across the kelp and no-kelp areas. By randomizing the order in which transects were swum, the possibility of displacing fish to other transects was equalized across transects and habitat areas. Visual count methods may also suffer from bias due to the observer's ability to see and accurately identify species at varying distances due to the obstruction by kelp (Weaver, Kwak, & Pollock, 2014).

Both the snorkel surveys and stationary video surveys may have been impacted by differences in the observable area between the kelp and no-kelp areas, where the presence of kelp can obscure the frame or reduce the distance and area that can be observed. For the videos, no frames where kelp was directly obstructing the view, or frames one minute before, during or one minute after the snorkeler entered the FOV were analysed to reduce the impacts of obstruction and disturbance on counts. However, the smaller area able to be observed due to the presence of kelp may have affected the counts of salmon by both snorkeler and video methods and the counts in the kelp areas may be lower as a result.

While both methods of observation have limitations, snorkel and video techniques are widely used in fisheries science (Brignon et al., 2011; Cappo et al., 2006; Duffy et al., 2018; Ellis & DeMartini, 1995). For this research, the added complication of sampling within the physical structure of kelp beds, which can unpredictably alter the field of view, results in greater difficulty determining the difference in habitat types. Snorkel methods seem to be more robust as an individual observer can determine their field of view and adjust accordingly, whereas, the camera system is static and cannot control for its surroundings. The influence of snorkeler presence on fish behaviour is assumed equivalent across habitat types and thus using relative differences as a metric rather than absolute abundance should reduce this effect.

4.5.2 Juvenile salmon: kelp vs no-kelp habitat

The overall greater salmon density found within kelp areas compared to no-kelp (0.15 salmon/m³ in Kelp, 0.036 salmon/m³ in Nok) is mostly attributed to the inner transects, which were immediately adjacent to the rocky shoreline, indicating this may be a preferential habitat for

juvenile salmon. Several studies have found that fish behaviour within kelp habitats varies between species, with edges and interiors being preferential to different fish assemblages (Efird & Konar, 2013). Shaffer (2004) found that juvenile salmon preferred kelp beds compared to un-vegetated areas, with the highest salmon density in the middle of beds as it provides a higher potential as refuge from predators. Differences in the use of habitat found in this survey may be linked to the size and age of salmon, as larger fish tend to be found further from shore and in deeper water (Lange et al., 2011). The majority of salmon observed were approximately 100 mm in length and located within the top 2 m of the water column. When larger fish (>120mm) were observed they were located in deeper water in the outer transects.

The sampling methods may have contributed to uncertainties in the results, as both snorkel and video methods were conducted during daylight hours and calm conditions. Habitats may be utilized differently by salmon throughout the day or depending on environmental conditions. All surveys were conducted during the day (between 9:30 -18:00), as sampling was constrained by the need for adequate light conditions to observe salmon without the use of artificial light. It has been shown that using artificial light can affect fish behaviour as either an attractant or deterrent depending on the species and may have attracted unwanted predators in this case (Cappo et al., 2006; Rooper, Williams, De Robertis, & Tuttle, 2015; Ryer, Stoner, Iseri, & Spencer, 2009). Additionally, an exploratory snorkel survey conducted at varying hours and light conditions (from 6 am to 9 pm) to determine the utility of using artificial light for sampling showed that due to the high amounts of particulates in the water, a reduced field of view and an inability to observe any fish during low light conditions. Salmon behaviour has been shown to change according to the time of day where foraging activities may be limited during daylight hours due to higher predation risk, salmon may become more active during nocturnal or twilight hours when foraging is less efficient but predation risk is lower (Bradford & Higgins, 2001; Metcalfe, Fraser, Burns, & Burns, 1999).

The horizontal visibility in the water column in the nearshore region sampled during this study was recorded from less than 1 m to greater than 6 m in the top 2 m of the water column. This visibility changed based on tide direction with incoming tides having higher turbidity, and could be patchy within a site. During sampling it was noted that there were often higher levels of turbidity near to the shoreline, in those areas where the inner transects occurred. The spatial

patterns of turbidity may partially explain the preference for the inner transects by juvenile salmon. Many studies on diel activity have been conducted in river systems where increased water turbidity has been shown to reduce predation on juvenile salmon and allow increased activity during the day (Gregory & Levings, 2004).

There may also be an effect of seasonal timing on the patterns described where the highest densities of salmon were measured in May (Week 3 May 19-26: 0.64 salmon/m³ in Kelp; 0.19 salmon/m³ in Nok) and subsequently declined throughout the summer (0.00088 salmon/m³ in kelp, 0.00088 salmon/m³ in Nok, week 13 August 18-24) (Figure 21, 22). This is consistent with multiple sampling programs in the region that describe the transition of juvenile salmon from the nearshore towards deeper water as fish grow and consume larger prey (Duffy & Beauchamp, 2011). Throughout the sampling period, salmon observed in the inner transects were of consistently similar size (estimated 60-100mm), indicating that new juveniles were entering the area rather than the same fish remaining in place.

While peak salmon density occurred in May for both kelp and no-kelp areas, substantial kelp presence did not occur until mid June (Week 7, June 15-21st, Kelp 0.10 salmon/m³, 0.045 salmon/m³). This indicates a potential mismatch in timing, as there were no substantial kelp beds when the majority of salmon were present in the nearshore areas. In other areas of the coast, kelp beds are observed much earlier in the season and thus may have a greater impact on migrating salmon (Pfister et al., 2018). Additionally, beds in Cowichan Bay tend to be small and fringing compared with larger beds observed in some areas of the Southern Gulf Islands and on the outer coast of Vancouver Island. These areas experience conditions of cooler temperatures and higher nutrients (Nijland et al., 2019; Schroeder et al., submitted). The small size of kelp beds in Cowichan Bay may reduce the quality of potential habitat and limit effects of kelp on provisioning of suitable refuge, nutrient entrainment or dampening of currents (Eckman, Duggins, & Sewell, 1989; Teagle et al., 2017).

There are inherent differences in the physical and environmental characteristics of the kelp and no-kelp areas, which likely influence whether kelp will successfully grow in each location. Kelp areas were more exposed to waves and exhibited rugose rocky shorelines. Areas of no-kelp also occurred beside rocky shorelines, however, wave action in these regions was observed to be

lower, and substrate adjacent to the shoreline had sandy substrate. The higher wave exposure in the kelp areas is consistent with the biology of bull kelp, as it tends to grow in areas with the appropriate rocky substrate and high wave energy which favours the tensile strength of bull kelp over other species of algae (Burrows, 2012; Duggins et al., 2001). The higher wave exposure and energy here may reduce the vulnerability of salmon to predators that hunt from above, such as birds by reducing visibility (Efird & Konar, 2013; Gregory & Levings, 2004). The inner transects of the kelp areas were also associated with higher rugosity than the no-kelp areas. Areas with structural complexity, such as highly rugose rocks with creases and crevices were found to support greater abundances of small fish and lower abundances of large fish which may indicate lower numbers of potential predators or more opportunities for refuge in these areas (Trebilco et al., 2015).

4.6 Conclusion

Understanding how juvenile salmon interact with kelp beds is the first step in assessing the role of these habitats and their importance to salmon survival during the critical early marine growth period. This study provides important insight on the potential for sampling salmon in kelp beds, finding that it is possible to observe and quantify small juvenile salmon within complex habitats. However, methods for quantifying species use of kelp habitats remain challenging to apply due to the difficulties of sampling a mobile species within a complex biogenic habitat. Snorkel methods provided greater flexibility for sampling in a fluctuating environment, allowing adjustments to be made as tides, currents, kelp position, and visibility changed, however the presence of the snorkeler may have had an effect on fish behaviour, resulting in lower or inaccurate counts. Results of the stationary underwater video methods were limited by inherent differences in the area observed caused by the presence of kelp in the camera. The results of this study show that there may be preferential use of shorelines bordering kelp beds, which may experience higher wave energy due to differences in exposure and offer greater opportunities for refuge in the complex rocky outcrops. The use of kelp habitat in this study area may also be atypical due to differences in the timing of peak salmon migration and maximum kelp growth as well as the small size of kelp beds compared to those in other regions. Further development of methods should include the consideration of the size and characteristics of the kelp beds where fringing beds may have different effects compared to larger reefs. Future surveys should also

consider the timing of kelp bed growth in spring compared to the migration peaks of juvenile salmon through selection of appropriate study sites.

5.0 Summary and Conclusions

The goal of this research project was to understand how nearshore kelp habitats are changing and how these changes may affect the species, which rely on them, specifically juvenile salmon.

Methods were developed to detect floating kelp beds using satellite imagery, and kelp beds within Cowichan Bay, Sansum Narrows were mapped and changes in persistence were assessed. Based on the satellite-mapped kelp extents, non-invasive in-situ surveys of paired kelp and no-kelp areas were employed to evaluate if juvenile salmon were preferentially using kelp habitats.

The case study presented in chapter two defines methods for detecting floating kelp canopy using satellite imagery based on techniques adapted from other macro-algal studies. The methods allowed for mapping small, nearshore, and fringing bull kelp beds through using high-resolution imagery (~2.5 m) and optimizing image collection for ideal conditions of low tides, peak seasonal growth, minimal sun-glint and water surface roughness. Spectral indices were statistically explored in relation to how effective they were in detecting kelp floating on water and NDVI, GNDVI and PC1 were found to be the best for separating kelp from other objects in the images. Additionally, multiple methods of classification were tested for accuracy in classifying kelp with the most accurate results from the supervised minimum distance classifier with an accuracy of 90.7%. However, all classifications performed well, resulting in accuracies of 82.0% or higher.

Chapter 3 used the best methods defined in chapter 2, and a time series of imagery from 2004-2017 was collected from the DigitalGlobe Foundation's historical database for defining the kelp extent for each year. Due to differences in environmental conditions during acquisition of historical satellite imagery, an image reliability index was created whereby parameters including tide height, water surface roughness, sun glint, and season were rated. Imagery used for change analysis was required to meet a minimum reliability value, reducing the number of images used to the years of 2004, 2012, 2015, 2016, 2017. Presence of kelp beds within a defined unit area was then developed as a metric for quantifying persistence of kelp over time. Finally, spatial and temporal drivers were examined with regard to kelp persistence. Rocky substrate and areas with high current had the most persistent kelp beds. Temporally, there was a decline in kelp from 2015 to 2017, which showed the lowest kelp presence. This decline may have been related to anomalous warm sea surface temperatures in 2015 and 2016 resulting in a lag effect where kelp

growth in the following years was reduced due to lower spore production or germination. As the time series of imagery had a limited span and incomplete coverage, it is difficult to determine whether the measured decline is anomalous or within the natural bounds of variation for this annual species.

Chapter 4 utilized the kelp bed extents mapped in chapters 2 and 3 to identify sampling sites for evaluating the use of kelp beds by juvenile salmon. These areas were defined as having a kelp bed of at least 80 m in length and an adjacent area, which did not have kelp. Paired surveys of kelp and no-kelp areas using visual counts by snorkeler were evaluated showing higher densities of salmon in kelp associated areas (0.15 salmon/m^3) compared to the no-kelp areas (0.036 salmon/m^3). Stationary video was also utilized in order to monitor the effect of snorkeler on salmon behaviour and compare the feasibility of evaluating salmon's use of kelp habitats between the two methods. Video methods also found a greater number of salmon in kelp areas compared with no-kelp (7.0, 5.0 mean maxN); however, the results of this method have uncertainties due to differences in the size of the areas the cameras observed. Interpretation of the data is complicated by the seasonal trend in kelp growth since when sampling began in spring no areas contained kelp. During this period, the kelp-associated areas still had a greater density of salmon compared to the no-kelp areas, suggesting other factors may be driving the trends in habitat use. The snorkel surveys found the greatest density of juvenile salmon close to the shoreline on the inside edge of kelp beds. This kelp associated area had shorelines that were more exposed and contained complex rocky outcrops.

The results of this research contribute to the growing literature on the importance of nearshore habitats to marine species. Understanding how these habitats are distributed and how they are changing is key to their management and conservation. Ongoing efforts should be made to monitor kelp extent and distribution at various spatial scales and over longer periods to understand the bounds of variation and trends of kelp bed growth in response to natural and anthropogenic disturbances. Further research should seek to define more clearly the role of the nearshore zone and kelp associated areas as a resource for juvenile salmon. The results of the juvenile salmon surveys are a foundation to build better understanding of the connections between kelp habitats and salmon. The ways in which salmon are interacting with kelp, whether for refuge, forage or otherwise should be evaluated as well as the impacts that loss of kelp may

have. Improvements will come from using additional techniques such as stable isotope analysis and eDNA (Kennedy et al., 2018; Tillotson et al., 2018) to help define the how kelp-based food webs are linked to salmon, and expand surveys of salmon habitat use to include crepuscular and nocturnal hours.

6.0 References

- Adler-Golden, S. M., Matthew, M. W., Bernstein, L. S., Levine, R. Y., Berk, A., Richtsmeier, S. C., ... Burke, H. K. (1999). Atmospheric correction for shortwave spectral imagery based on MODTRAN4. *Imaging Spectrometry V*, 3753, 61–69. <https://doi.org/10.1117/12.366315>
- Airamé, S., Dugan, J. E., Lafferty, K. D., Leslie, H., McArdle, D. A., & Warner, R. R. (2003). Applying ecological criteria to marine reserve design: A case study from the California Channel Islands. *Ecological Applications*, 13(1), 170–184. [https://doi.org/10.1890/1051-0761\(2003\)013\[0170:aectmr\]2.0.co;2](https://doi.org/10.1890/1051-0761(2003)013[0170:aectmr]2.0.co;2)
- Amsler, C. D., & Neushul, M. (1989). Diel periodicity of spore release from the kelp *Nereocystis luetkeana* (Mertens) Postels et Ruprecht. *Journal of Experimental Marine Biology and Ecology*, 134(2), 117–127. [https://doi.org/10.1016/0022-0981\(90\)90104-K](https://doi.org/10.1016/0022-0981(90)90104-K)
- Anderson, J. M., Barrett, J., Wolstenhome, G. E. W., & Fitzsimons, D. W. (1979). Chlorophyll-Protein Complexes of Brown Algae: P700 Reaction Centre and Light-Harvesting Complexes. In *Chlorophyll Organization and Energy Transfer in Photosynthesis* (Vol. 61, pp. 81–104). <https://doi.org/10.1002/9780470720431.ch4>
- Anderson, R. J., Rand, A., Rothman, M. D., Share, A., & Bolton, J. J. (2007). Mapping and quantifying the South African kelp resource. *African Journal of Marine Science*, 29(3), 369–378. <https://doi.org/10.2989/AJMS.2007.29.3.5.335>
- Andréfouët, S., Zubia, M., & Payri, C. (2004). Mapping and biomass estimation of the invasive brown algae *Turbinaria ornata* (Turner) J. Agardh and *Sargassum mangarevense* (Grunow) Setchell on heterogeneous Tahitian coral reefs using 4-meter resolution IKONOS satellite data. *Coral Reefs*, 23(1), 26–38. <https://doi.org/10.1007/s00338-003-0367-5>
- Augenstein, E. W., Stow, D. A., & Hope, A. S. (1991). Evaluation of Spot Hrv-Xs Data for Kelp Resource Inventories. *Photogrammetric Engineering and Remote Sensing*, 57(5), 501–509.
- Babin, M., Stramski, D., Ferrari, G. M., Claustre, H., Bricaud, A., Obolensky, G., & Hoepffner, N. (2003). Variations in the light absorption coefficients of phytoplankton, nonalgal particles, and dissolved organic matter in coastal waters around Europe. *Journal of Geophysical Research*, 108(C7), 3211. <https://doi.org/10.1029/2001jc000882>
- Bao, N., Lechner, A. M., Fletcher, A., Mellor, A., Mulligan, D., & Bai, Z. (2012). Comparison of relative radiometric normalization methods using pseudo-invariant features for change detection studies in rural and urban landscapes. *Journal of Applied Remote Sensing*, 6(1), 063578–1. <https://doi.org/10.1117/1.jrs.6.063578>
- Beamish, R J, McCaughran, D., King, J. R., Sweeting, R. M., & McFarlane, G. A. (2000). Estimating the abundance of juvenile coho salmon in the Strait of Georgia by means of surface trawls. *North American Journal of Fisheries Management*, 20(2), 369–375. [https://doi.org/10.1577/1548-8675\(2000\)020<0369:ETAOJC>2.3.CO;2](https://doi.org/10.1577/1548-8675(2000)020<0369:ETAOJC>2.3.CO;2)
- Beamish, R J, Sweeting, R. M., Neville, C. M., & Lange, K. (2005). Changing trends in the rearing capacity of the Strait of Georgia ecosystem for juvenile Pacific salmon. NPAFC Doc. 875.

- Beamish, Richard J, Sweeting, R. M., Beacham, T. D., Lange, K. L., & Neville, C. M. (2010). A late ocean entry life history strategy improves the marine survival of chinook salmon in the Strait of Georgia. *North Pacific Anadromous Fish Commission*, 1282, 14pp.
- Bell, T. W., Allen, J. G., Cavanaugh, K. C., & Siegel, D. A. (2018). Three decades of variability in California's giant kelp forests from the Landsat satellites. *Remote Sensing of Environment*, 110811. <https://doi.org/10.1016/j.rse.2018.06.039>
- Bell, T. W., Cavanaugh, K. C., Reed, D. C., & Siegel, D. A. (2015). Geographical variability in the controls of giant kelp biomass dynamics. *Journal of Biogeography*, 42(10), 2010–2021. <https://doi.org/10.1111/jbi.12550>
- Bell, T. W., Cavanaugh, K. C., & Siegel, D. A. (2015). Remote monitoring of giant kelp biomass and physiological condition: An evaluation of the potential for the Hyperspectral Infrared Imager (HypIRI) mission. *Remote Sensing of Environment*, 167, 218–228. <https://doi.org/10.1016/j.rse.2015.05.003>
- Bell, T. W., Reed, D. C., Nelson, N. B., & Siegel, D. A. (2018). Regional patterns of physiological condition determine giant kelp net primary production dynamics. *Limnology and Oceanography*, 63(1), 472–483. <https://doi.org/10.1002/lno.10753>
- Bennion, M., Fisher, J., Yesson, C., & Brodie, J. (2018). Remote Sensing of Kelp (Laminariales, Ochrophyta): Monitoring Tools and Implications for Wild Harvesting. *Reviews in Fisheries Science & Aquaculture*, 1–15. <https://doi.org/10.1080/23308249.2018.1509056>
- Berry, H. D., Mumford, T. F., & Dowty, P. (2005). Using Historical Data to Estimate Changes in Floating Kelp (*Nereocystis luetkeana* and *Macrocystis integrifolia*) in Puget Sound, Washington. In *Proceedings of the 2005 Puget Sound George Basin Research Conference. Puget Sound Action Team, Olympia, Washington (Vol. 9)*.
- Blaschke, T. (2010). Object based image analysis for remote sensing. *ISPRS Journal of Photogrammetry and Remote Sensing*, 65(1), 2–16. <https://doi.org/10.1016/j.isprsjprs.2009.06.004>
- Botha, E. J., Brando, V. E., Anstee, J. M., Dekker, A. G., & Sagar, S. (2013). Increased spectral resolution enhances coral detection under varying water conditions. *Remote Sensing of Environment*, 131, 247–261. <https://doi.org/10.1016/j.rse.2012.12.021>
- Bradford, M. J., & Higgins, P. S. (2001). Habitat-, season-, and size-specific variation in diel activity patterns of juvenile chinook salmon (*Oncorhynchus tshawytscha*) and steelhead trout (*Oncorhynchus mykiss*). *Canadian Journal of Fisheries and Aquatic Sciences*, 58(2), 365–374. <https://doi.org/10.1139/f00-253>
- Brezonik, P. L., Olmanson, L. G., Finlay, J. C., & Bauer, M. E. (2015). Factors affecting the measurement of CDOM by remote sensing of optically complex inland waters. *Remote Sensing of Environment*, 157, 199–215. <https://doi.org/10.1016/j.rse.2014.04.033>
- Brignon, W. R., Davis, M. B., Olson, D. E., Schaller, H. A., & Schreck, C. B. (2011). Snorkelers' in-water observations can alter salmonid behavior. *Journal of Fish and Wildlife Management*, 2(1), 90–98. <https://doi.org/10.3996/052010-JFWM-012>
- Britton-Simmons, K., Eckman, J. E., & Duggins, D. O. (2008). Effect of tidal currents and tidal

- stage on estimates of bed size in the kelp *Nereocystis luetkeana*. *Marine Ecology Progress Series*, 355, 95–105. <https://doi.org/10.3354/meps07209>
- Burrows, M. T. (2012). Influences of wave fetch, tidal flow and ocean colour on subtidal rocky communities. *Marine Ecology Progress Series*, 445, 193–207. <https://doi.org/10.3354/meps09422>
- Burt, J. M., Tinker, M. T., Okamoto, D. K., Demes, K. W., Holmes, K., & Salomon, A. K. (2018). Sudden collapse of a mesopredator reveals its complementary role in mediating rocky reef regime shifts. *Proceedings of the Royal Society B: Biological Sciences*, 285, 20180553. <https://doi.org/10.1098/rspb.2018.0553>
- Byrnes, J. E., Reed, D. C., Cardinale, B. J., Cavanaugh, K. C., Holbrook, S. J., & Schmitt, R. J. (2011). Climate-driven increases in storm frequency simplify kelp forest food webs. *Global Change Biology*, 17, 2513–2524. <https://doi.org/10.1111/j.1365-2486.2011.02409.x>
- California Department of Fish and Wildlife. (2016). “Perfect Storm” Decimates Northern California Kelp Forests. Retrieved June 25, 2019, from <https://cdfwmarine.wordpress.com/2016/03/30/perfect-storm-decimates-kelp/>
- Cappo, M., Harvey, E. S., & Shortis, M. (2006). Counting and measuring fish with baited video techniques - an overview. In *Australian Society for Fish Biology Workshop Proceedings* (p. Vol. 1, pp. 101–114). https://doi.org/10.1007/978-1-62703-724-2_1
- Carney, L. T. (2005). Restoration of the bull kelp *Nereocystis luetkeana*. *Marine Ecology Progress Series*, 302, 49–61. <https://doi.org/10.3354/meps302049>
- Casal, G., Kutser, T., Domínguez-Gómez, J. A., Sánchez-Carnero, N., & Freire, J. (2013). Assessment of the hyperspectral sensor CASI-2 for macroalgal discrimination on the Ría de Vigo coast (NW Spain) using field spectroscopy and modelled spectral libraries. *Continental Shelf Research*, 55, 129–140. <https://doi.org/10.1016/j.csr.2013.01.010>
- Casal, G., Sánchez-Carnero, N., Sánchez-Rodríguez, E., & Freire, J. (2011). Remote sensing with SPOT-4 for mapping kelp forests in turbid waters on the south European Atlantic shelf. *Estuarine, Coastal and Shelf Science*, 91, 371–378. <https://doi.org/10.1016/j.ecss.2010.10.024>
- Cavanaugh, K. C., Siegel, D. A., Kinlan, B. P., & Reed, D. C. (2010). Scaling giant kelp field measurements to regional scales using satellite observations. *Marine Ecology Progress Series*, 403, 13–27. <https://doi.org/10.3354/meps08467>
- Cavanaugh, K. C., Siegel, D. A., Reed, D. C., & Dennison, P. E. (2011). Environmental controls of giant-kelp biomass in the Santa Barbara Channel, California. *Marine Ecology Progress Series*, 429, 1–17. <https://doi.org/10.3354/meps09141>
- Chappell, R., & Pawlowicz, R. (2018). *Atlas of Oceanographic Conditions in the Strait of Georgia (2015-2017) based on the Pacific Salmon Foundation Citizen Science Dataset*. Department of Earth, Ocean and Atmospheric Sciences, University of British Columbia. Retrieved from http://soggy.zoology.ubc.ca:8080/geonetwork/srv/api/records/ab455d82-59c5-4d8a-9c9f-bbc9636144b5/attachments/sogatlas_citsci2018.pdf
- Charrier, B., Le Bail, A., & de Reviers, B. (2012). Plant Proteus: brown algal morphological

- plasticity and underlying developmental mechanisms. *Trends in Plant Science*, 17(8), 468–477. <https://doi.org/10.1016/J.TPLANTS.2012.03.003>
- Christie, H., Norderhaug, K. M., & Fredriksen, S. (2009). Macrophytes as habitat for fauna. *Marine Ecology Progress Series*, 396, 221–233. <https://doi.org/10.3354/meps08351>
- Claissse, J. T., Pondella, D. J., Williams, J. P., & Sadd, J. (2012). Using GIS Mapping of the Extent of Nearshore Rocky Reefs to Estimate the Abundance and Reproductive Output of Important Fishery Species. *PLoS ONE*, 7(1), e30290. <https://doi.org/10.1371/journal.pone.0030290>
- Coleman, M. A., Chambers, J., Knott, N. A., Malcolm, H. A., Harasti, D., Jordan, A., & Kelaher, B. P. (2011). Connectivity within and among a network of temperate marine reserves. *PLoS ONE*, 6(5), e20168. <https://doi.org/10.1371/journal.pone.0020168>
- Congalton, R. G. (1991). A review of assessing the accuracy of classifications of remotely sensed data. *Remote Sensing of Environment*, 37(1), 35–46. [https://doi.org/10.1016/0034-4257\(91\)90048-B](https://doi.org/10.1016/0034-4257(91)90048-B)
- Cui, T. W., Zhang, J., Sun, L. E., Jia, Y. J., Zhao, W., Wang, Z. L., & Meng, J. M. (2012). Satellite monitoring of massive green macroalgae bloom (GMB): imaging ability comparison of multi-source data and drifting velocity estimation. *International Journal of Remote Sensing*, 33(17), 5513–5527. <https://doi.org/10.1080/01431161.2012.663112>
- David, A. T., Simenstad, C. A., Cordell, J. R., Toft, J. D., Ellings, C. S., Gray, A., & Berge, H. B. (2016). Wetland Loss, Juvenile Salmon Foraging Performance, and Density Dependence in Pacific Northwest Estuaries. *Estuaries and Coasts*, 39(3), 767–780. <https://doi.org/10.1007/s12237-015-0041-5>
- Dayton, P. K., Tegner, M. J., Edwards, P. B., & Riser, K. L. (1998). Sliding Baselines, Ghosts, and Reduced Expectations in Kelp Forest Communities. *Ecological Applications*, 8, 309–322. [https://doi.org/10.1890/1051-0761\(1998\)008\[0309:SBGARE\]2.0.CO;2](https://doi.org/10.1890/1051-0761(1998)008[0309:SBGARE]2.0.CO;2)
- Dearden, P., Theberge, M., & Yasué, M. (2010). Using underwater cameras to assess the effects of snorkeler and SCUBA diver presence on coral reef fish abundance, family richness, and species composition. *Environmental Monitoring and Assessment*, 163(1–4), 531–538. <https://doi.org/10.1007/s10661-009-0855-3>
- Deiman, M., Iken, K., & Konar, B. (2012). Susceptibility of *Nereocystis luetkeana* (Laminariales, Ochrophyta) and *Eualaria fistulosa* (Laminariales, Ochrophyta) spores to sedimentation. *Algae*, 27(2), 115–123. <https://doi.org/10.4490/algae.2012.27.2.115>
- Desmond, M. J., Pritchard, D. W., & Hepburn, C. D. (2015). Light limitation within southern New Zealand kelp forest communities. *PLoS ONE*, 10(4), 1–18. <https://doi.org/10.1371/journal.pone.0123676>
- Dethier, M. N., Raymond, W. W., McBride, A. N., Toft, J. D., Cordell, J. R., Ogston, A. S., ... Berry, H. D. (2016). Multiscale impacts of armoring on Salish Sea shorelines: Evidence for cumulative and threshold effects. *Estuarine, Coastal and Shelf Science*, 175, 106–117. <https://doi.org/10.1016/j.ecss.2016.03.033>
- Deysher, L. E. (1993). Evaluation of remote sensing techniques for monitoring giant kelp

- populations. *Hydrobiologia*, 260/261, 307–312. <https://doi.org/10.1007/BF00049033>
- Di Cicco, E., Ferguson, H. W., Kaukinen, K. H., Schulze, A. D., Li, S., Tabata, A., ... Miller, K. M. (2018). The same strain of Piscine orthoreovirus (PRV-1) is involved in the development of different, but related, diseases in Atlantic and Pacific Salmon in British Columbia. *FACETS*, 3(1), 599–641. <https://doi.org/10.1139/facets-2018-0008>
- Di Lorenzo, E., Schneider, N., Cobb, K. M., Franks, P. J. S., Chhak, K., Miller, A. J., ... Rivière, P. (2008). North Pacific Gyre Oscillation links ocean climate and ecosystem change. *Geophysical Research Letters*, 35(8), 6. <https://doi.org/10.1029/2007GL032838>
- Dierssen, H. M., Chlus, A., & Russell, B. (2015). Hyperspectral discrimination of floating mats of seagrass wrack and the macroalgae Sargassum in coastal waters of Greater Florida Bay using airborne remote sensing. *Remote Sensing of Environment*, 167, 247–258. <https://doi.org/10.1016/j.rse.2015.01.027>
- Donnellan, M. D., & Foster, M. S. (1999). *Effects of small-scale kelp harvesting on giant kelp surface canopy dynamics in the Ed Ricketts Underwater Park region. Final Report to the Monterey Bay National Marine Sanctuary and the Cities of Monterey and Pacific Grove.*
- Druehl, L. D. (1968). Taxonomy and Distribution of Northeast Pacific Species of Laminaria. *Canadian Journal of Botany*, 46(5), 539–547.
- Druehl, L. D. (1970). The pattern of Laminariales distribution in the northeast Pacific. *Phycologia*, 9, 237–247. <https://doi.org/10.2216/i0031-8884-9-3-237.1>
- Duarte, C. M., Losada, I. J., Hendriks, I. E., Mazarrasa, I., & Marbà, N. (2013). The role of coastal plant communities for climate change mitigation and adaptation. *Nature Climate Change*, 3(11), 961–968. <https://doi.org/10.1038/nclimate1970>
- Duffy, E. J., & Beauchamp, D. A. (2011). Rapid growth in the early marine period improves the marine survival of Chinook salmon (*Oncorhynchus tshawytscha*) in Puget Sound, Washington. *Canadian Journal of Fisheries and Aquatic Sciences*, 68(2), 232–240. <https://doi.org/10.1139/F10-144>
- Duffy, E. J., Beauchamp, D. A., Sweeting, R. M., Beamish, R. J., & Brennan, J. S. (2010). Ontogenetic Diet Shifts of Juvenile Chinook Salmon in Nearshore and Offshore Habitats of Puget Sound. *Transactions of the American Fisheries Society*, 139(3), 803–823. <https://doi.org/10.1577/T08-244.1>
- Duffy, J. P., Pratt, L., Anderson, K., Land, P. E., & Shutler, J. D. (2018). Spatial assessment of intertidal seagrass meadows using optical imaging systems and a lightweight drone. *Estuarine, Coastal and Shelf Science*, 200, 169–180. <https://doi.org/10.1016/j.ecss.2017.11.001>
- Duggins, D., Eckman, J. E., Siddon, C. E., & Klinger, T. (2001). Interactive roles of mesograzers and current flow in survival of kelps. *Marine Ecology Progress Series*, 223, 143–155. <https://doi.org/10.3354/meps223143>
- Duggins, D. O. (1980). Kelp Beds and Sea Otters: An Experimental Approach. *Ecology*, 61(3), 447–453. <https://doi.org/10.2307/1937405>

- Duggins, D. O. (1988). The Effects of Kelp Forests on Nearshore Environments: Biomass, Detritus, and Altered Flow. In G. R. VanBaricom & J. A. Estes (Eds.), *The Community Ecology of Sea Otters. Ecological Studies (Analysis and Synthesis)* (vol 65, pp. 192–201). Berlin, Heidelberg: Springer. https://doi.org/10.1007/978-3-642-72845-7_9
- Eckman, J. E., Duggins, D. O., & Sewell, A. T. (1989). Ecology of under story kelp environments. I. Effects of kelps on flow and particle transport near the bottom. *Journal of Experimental Marine Biology and Ecology*, 129, 173–187. [https://doi.org/10.1016/0022-0981\(89\)90055-5](https://doi.org/10.1016/0022-0981(89)90055-5)
- Efird, T. P., & Konar, B. (2013). Habitat characteristics can influence fish assemblages in high latitude kelp forests. *Environmental Biology of Fishes*, 97(11), 1253–1263. <https://doi.org/10.1007/s10641-013-0211-x>
- Ellis, D. M., & DeMartini, E. E. (1995). Evaluation of a video camera technique for indexing abundances of juvenile pink snapper, *Pristipomoides filamentosus*, and other Hawaiian insular shelf fishes. *Fishery Bulletin*, 93(1), 67–77.
- Estes, J. A., Duggins, D. O., & Rathbun, G. B. (1989). The Ecology of Extinctions in Kelp Forest Communities. *Conservation Biology*, 3(3), 252–264. <https://doi.org/10.1111/j.1523-1739.1989.tb00085.x>
- Etherington, L. L., Hooge, P. N., Hooge, E. R., & Hill, D. F. (2007). Oceanography of Glacier Bay, Alaska: Implications for biological patterns in a glacial fjord estuary. *Estuaries and Coasts*, 30(6), 927–944. <https://doi.org/10.1007/BF02841386>
- Evans, T. L., Costa, M., Tomas, W. M., & Camilo, A. R. (2014). Large-scale habitat mapping of the Brazilian Pantanal wetland: A synthetic aperture radar approach. *Remote Sensing of Environment*, 155, 89–108. <https://doi.org/10.1016/j.rse.2013.08.051>
- Filbee-Dexter, K., Feehan, C. J., & Scheibling, R. E. (2016). Large-scale degradation of a kelp ecosystem in an ocean warming hotspot. *Marine Ecology Progress Series*, 543, 141–152. <https://doi.org/10.3354/meps11554>
- Filbee-Dexter, K., & Wernberg, T. (2018). Rise of Turfs: A New Battlefield for Globally Declining Kelp Forests. *BioScience*, 68(2), 64–76. <https://doi.org/10.1093/biosci/bix147>
- Finney, B. P., Gregory-Eaves, I., Sweetman, J., & Smol, J. P. (2007). Impacts of climatic change and fishing on Pacific salmon abundance of the past 300 years. *Science*, 290(27), 795–798.
- Foreman, M. G. (1978). Manual for tidal currents analysis and prediction. Revised 2004. *Pacific Marine Science Report 78-6*, (2004), 57pp.
- Foreman, R.E. (1975). *KIM-1: a method for inventory of floating kelps and its application to selected areas of kelp license area 12*. In. *Federal Fisheries and Marine Service and B.C. Marine Resources Branch*. 1-81. Retrieved from <http://waves-vagues.dfo-mpo.gc.ca/waves-vagues/search-recherche/display-afficher/280247>
- Foreman, Ronald E. (1984). Studies on *Nereocystis* growth in British Columbia, Canada. *Hydrobiologia*, 116–117(1), 325–332. <https://doi.org/10.1007/BF00027696>
- Foster, M. S., & Schiel, D. R. (2010). Loss of predators and the collapse of southern California

- kelp forests (?): Alternatives, explanations and generalizations. *Journal of Experimental Marine Biology and Ecology*, 393, 59–70. <https://doi.org/10.1016/j.jembe.2010.07.002>
- Fyfe, J. E., Israel, S. A., Chong, A., Ismail, N., Hurd, C. L., & Probert, K. (1999). Mapping marine habitats in Otago, Southern New Zealand. *Geocarto International*, 14(3), 17–28. <https://doi.org/10.1080/10106049908542113>
- Garcia, R. A., Fearn, P., Keesing, J. K., & Liu, D. (2013). Quantification of floating macroalgae blooms using the scaled algae index. *Journal of Geophysical Research: Oceans*, 118(1), 26–42. <https://doi.org/10.1029/2012JC008292>
- Gaydos, J. K., Dierauf, L., Kirby, G., Brosnan, D., Gilardi, K., & Davis, G. E. (2008). Top 10 principles for designing healthy coastal ecosystems like the Salish Sea. *EcoHealth*, 5(4), 460–471. <https://doi.org/10.1007/s10393-009-0209-1>
- Gislason, G., Lam, E., Gunnar, K., & Guettabi, M. (2017). *Economic Impacts of Pacific Salmon Fisheries*. Pacific Salmon Commission, Vancouver, Canada.
- Goldberg, S., Kirby, J., & Licht, S. (2016). *Applications of Aerial Multi-spectral Imagery for Algal Bloom Monitoring in Rhode Island*. SURFO Technical Report No. 16-01. Retrieved from http://digitalcommons.uri.edu/surfo_tech_reports/
- Gower, J., Hu, C., Borstad, G., & King, S. (2006). Ocean Color Satellites Show Extensive Lines of Floating Sargassum in the Gulf of Mexico. *IEEE Transactions on Geoscience and Remote Sensing*, 44(12), 3619–3625. <https://doi.org/10.1109/TGRS.2006.882258>
- Gower, Jim, & King, S. (2008). Satellite Images Show the Movement of Floating Sargassum in the Gulf of Mexico and Atlantic Ocean. *Nature Precedings*, 1–13. <https://doi.org/10.101/npre.2008.1894.1>
- Gregory, R. S., & Levings, C. D. (2004). Turbidity Reduces Predation on Migrating Juvenile Pacific Salmon. *Transactions of the American Fisheries Society*, 127(2), 275–285. [https://doi.org/10.1577/1548-8659\(1998\)127<0275:trpomj>2.0.co;2](https://doi.org/10.1577/1548-8659(1998)127<0275:trpomj>2.0.co;2)
- Gresh, T., Lichatowich, J., & Schoonmaker, P. (2000). An Estimation of Historic and Current Levels of Salmon Production in the Northeast Pacific Ecosystem: Evidence of a Nutrient Deficit in the Freshwater Systems of the Pacific Northwest. *Fisheries*, 25(1), 15–21. [https://doi.org/10.1577/1548-8446\(2000\)025<0015:aeohac>2.0.co;2](https://doi.org/10.1577/1548-8446(2000)025<0015:aeohac>2.0.co;2)
- Gupta, R. P., Reet, T. K., Saini, V., & Srivastava, N. (2013). A Simplified Approach for Interpreting Principal Component Images. *Advances in Remote Sensing*, 2, 111–119. <https://doi.org/10.4236/ars.2013.22015>
- Halpern, B. S., Cottenie, K., & Broitman, B. R. (2006). Strong top-down control in Southern California kelp forest ecosystems. *Science*, 312(5777), 1230–1232. <https://doi.org/10.1126/science.1128613>
- Hardin, P. J., & Jensen, R. R. (2011). Small-Scale Unmanned Aerial Vehicles in Environmental Remote Sensing: Challenges and Opportunities. *GIScience & Remote Sensing*, 48(1), 99–111. <https://doi.org/10.2747/1548-1603.48.1.99>
- Hedley, J. D., Harborne, A. R., & Mumby, P. J. (2005). Simple and robust removal of sun glint

- for mapping shallow-water benthos. *International Journal of Remote Sensing*, 26(10), 2107–2112. <https://doi.org/10.1080/01431160500034086>
- Hernández, C. A., Sangil, C., Fanai, A., & Hernández, J. C. (2018). Macroalgal response to a warmer ocean with higher CO₂ concentration. *Marine Environmental Research*, 136, 99–105. <https://doi.org/10.1016/J.MARENRES.2018.01.010>
- Hogland, J., Billor, N., & Anderson, N. (2017). Comparison of standard maximum likelihood classification and polytomous logistic regression used in remote sensing. *European Journal of Remote Sensing*, 46(1), 623–640. <https://doi.org/10.5721/EuJRS20134637>
- Hu, C. (2009). A novel ocean color index to detect floating algae in the global oceans. *Remote Sensing of Environment*, 113, 2118–2129. <https://doi.org/10.1016/j.rse.2009.05.012>
- Hu, C., Feng, L., Hardy, R. F., & Hochberg, E. J. (2015). Spectral and spatial requirements of remote measurements of pelagic Sargassum macroalgae. *Remote Sensing of Environment*, 167, 229–246. <https://doi.org/10.1016/j.rse.2015.05.022>
- Huete, A. R., Justice, C., & Van Leeuwen, W. (1999). *MODIS Vegetation Index (MOD 13). EOS MODIS Algorithm-Theoretical Basis Document*. NASA Goddard Space Flight Center, Greenbelt, Maryland. Retrieved from http://modis.gsfc.nasa.gov/data/atbd/land_atbd.html.
- Jensen, J. R. (2005). *Introductory digital image processing: a remote sensing perspective* (3rd ed.). Upper Saddle River, N.J.: Pearson, Prentice Hall.
- Jensen, J. R., Estes, J. E., & Tinney, L. (1980). Remote Sensing Techniques for Kelp Surveys. *Photogrammetric Engineering and Remote Sensing*, 46(6), 743–755.
- Kay, S., Hedley, J. D., & Lavender, S. (2009). Sun glint correction of high and low spatial resolution images of aquatic scenes: A review of methods for visible and near-infrared wavelengths. *Remote Sensing*, 1, 697–730. <https://doi.org/10.3390/rs1040697>
- Keesing, J. K., Liu, D., Fearn, P., & Garcia, R. A. (2011). Inter- and intra-annual patterns of *Ulva prolifera* green tides in the Yellow Sea during 2007–2009, their origin and relationship to the expansion of coastal seaweed aquaculture in China. *Marine Pollution Bulletin*, 62, 1169–1182. <https://doi.org/10.1016/j.marpolbul.2011.03.040>
- Kemp, I. M. (2014). *Spatial-temporal patterns in distribution and feeding of juvenile salmon and herring in Puget Sound, WA. (MSc. Thesis). University of Washington.*
- Kennedy, L. A., Juanes, F., & El-Sabaawi, R. (2018). Eelgrass as Valuable Nearshore Foraging Habitat for Juvenile Pacific Salmon in the Early Marine Period. *Marine and Coastal Fisheries*, 10(2), 190–203. <https://doi.org/10.1002/mcf2.10018>
- Kim, A. M., Olsen, R. C., Lee, K., & Jablonski, D. (2010). Using panchromatic imagery in place of multispectral imagery for kelp detection in water. *Proceedings of SPIE: Ocean Sensing and Monitoring II*, 7678, 12. <https://doi.org/10.1117/12.850352>
- Kislik, C., Dronova, I., & Kelly, M. (2018). UAVs in Support of Algal Bloom Research: A Review of Current Applications and Future Opportunities. *Drones*, 2(4), 35. <https://doi.org/10.3390/drones2040035>

- Knudby, A., & Nordlund, L. (2011). Remote sensing of seagrasses in a patchy multi-species environment. *International Journal of Remote Sensing*, 32(8), 2227–2244. <https://doi.org/10.1080/01431161003692057>
- Kotta, J., Remm, K., Vahtmäe, E., Kutser, T., & Orav-Kotta, H. (2014). In-air spectral signatures of the Baltic Sea macrophytes and their statistical separability. *Journal of Applied Remote Sensing*, 8, 83634–83748. <https://doi.org/10.1117/1.JRS.8.083634>
- Krkošek, M., Ford, J. S., Morton, A., Lele, S., Myers, R. A., & Lewis, M. A. (2007). Declining Wild Salmon Populations in Relation to Parasites from Farm Salmon. *Science*, 318(5857), 1772–1775. <https://doi.org/10.1126/science.1149887>
- Krumhansl, K. A., Okamoto, D. K., Rassweiler, A., Novak, M., Bolton, J. J., Cavanaugh, K. C., ... Byrnes, J. E. K. (2016). Global patterns of kelp forest change over the past half-century. *Proceedings of the National Academy of Sciences of the United States of America*, 113(48), 13785–13790. <https://doi.org/10.1073/pnas.1606102113>
- Krumhansl, K. A., & Scheibling, R. E. (2012). Production and fate of kelp detritus, 467, 281–302. <https://doi.org/10.3354/meps09940>
- Labelle, M. (2009). *Status of Pacific Salmon Resources in Southern British Columbia and the Fraser River Basin*. Pacific Fisheries Resource Conservation Council. Retrieved from www.fish.bc.ca
- Lance, M. M., Chang, W. Y., Jeffries, S. J., Pearson, S. F., & Acevedo-Gutiérrez, A. (2012). Harbor seal diet in northern Puget Sound: Implications for the recovery of depressed fish stocks. *Marine Ecology Progress Series*, 464, 257–271. <https://doi.org/10.3354/meps09880>
- Lange, K. L., Neville, C.-E. M., & Sweeting, R. M. (2011). Structural patterns in the distribution of ocean- and stream-type juvenile chinook salmon populations in the Strait of Georgia in 2010 during the critical early marine period. *North Pacific Anadromous Fish Commission*, 1354, 27.
- Liew, O., Chong, P., Li, B., & Asundi, A. (2008). Signature Optical Cues: Emerging Technologies for Monitoring Plant Health. *Sensors*, 8(5), 3205–3239. <https://doi.org/10.3390/s8053205>
- Ling, S. D., Johnson, C. R., Frusher, S. D., & Ridgway, K. R. (2009). Overfishing reduces resilience of kelp beds to climate-driven catastrophic phase shift. *Proceedings of the National Academy of Sciences*, 106(52), 22341–22345. <https://doi.org/10.1073/pnas.0907529106>
- Loretsen, S. H., Sjøtun, K., & Grémillet, D. (2010). Multi-trophic consequences of kelp harvest. *Biological Conservation*, 143(9), 2054–2062. <https://doi.org/10.1016/j.biocon.2010.05.013>
- Ma, L., Li, Y., Lan, G., & Li, C. (2009). Large-sized seaweed monitoring based on MODIS. *Proceedings of SPIE*, 7498, 749824. <https://doi.org/10.1117/12.832916>
- Macneale, K. H., Kiffney, P. M., & Scholz, N. L. (2010). Pesticides, aquatic food webs, and the conservation of Pacific salmon. *Frontiers in Ecology and the Environment*, 8(9), 475–482. <https://doi.org/10.1890/090142>

- Mallet, D., & Pelletier, D. (2014). Archimer Underwater video techniques for observing coastal marine biodiversity: A review of sixty years of publications (1952 – 2012). *Fisheries Research*, 154(June), 44–62. <https://doi.org/10.1016/j.fishres.2014.01.019>
- Marmorino, G. O., Miller, W. D., Smith, G. B., & Bowles, J. H. (2011). Airborne imagery of a disintegrating Sargassum drift line. *Deep-Sea Research Part I: Oceanographic Research Papers*, 58(3), 316–321. <https://doi.org/10.1016/j.dsr.2011.01.001>
- McCoy, R. M. (2005). *Field methods in remote sensing* (1st ed.). New York: Guilford Press.
- Metcalfe, N. B., Fraser, N. H. C., Burns, M. D., & Burns, D. (1999). Food availability and the nocturnal vs. diurnal foraging in juvenile salmon. *Journal of Animal Ecology*, 68(2), 371–381. <https://doi.org/10.1046/j.1365-2656.1999.00289.x>
- Mobley, C. (1994). *Light and Water: Radiative Transfer in Natural Waters Inverse methods for estimating inherent optical properties from radiometric measurements*. San Diego, California: Academic. Retrieved from <http://www.oceanopticsbook.info/view/references/publications>
- Mullan, S. (2017). *Tidal sedimentology and geomorphology in the central Salish Sea straits , British Columbia and Washington State. (PhD Thesis)*. University of Victoria, Canada.
- Mumford, T. F. (2007). *Kelp and Eelgrass in Puget Sound. Puget Sound Nearshore Partnership Report No. 2007-05* (U.S. Army Corps of Engineers). Seattle, Washington. Retrieved from http://www.pugetsoundnearshore.org/technical_papers/kelp.pdf
- Murfitt, S. L., Allan, B. M., Bellgrove, A., Rattray, A., Young, M. A., & Ierodiaconou, D. (2017). Applications of unmanned aerial vehicles in intertidal reef monitoring. *Scientific Reports*, 7(1). <https://doi.org/10.1038/s41598-017-10818-9>
- Nahirnick, N. K., Reshitnyk, L., Campbell, M., Hessing-Lewis, M., Costa, M., Yakimishyn, J., & Lee, L. (2019). Mapping with confidence; delineating seagrass habitats using Unoccupied Aerial Systems (UAS). *Remote Sensing in Ecology and Conservation*, 5(2), 121–135. <https://doi.org/10.1002/rse2.98>
- Neville, C. M., Beamish, R. J., & Chittenden, C. M. (2015). Poor Survival of Acoustically-Tagged Juvenile Chinook Salmon in the Strait of Georgia, British Columbia, Canada. *Transactions of the American Fisheries Society*, 144(1), 25–33. <https://doi.org/10.1080/00028487.2014.954053>
- Nezlin, N. P., Kamer, K., & Stein, E. D. (2007). Application of color infrared aerial photography to assess macroalgal distribution in an eutrophic estuary, Upper Newport Bay, California. *Estuaries and Coasts*, 30(5), 855–868. <https://doi.org/10.1007/BF02841339>
- Nijland, W., Reshitnyk, L., & Rubidge, E. (2019). Satellite remote sensing of canopy-forming kelp on a complex coastline: A novel procedure using the Landsat image archive. *Remote Sensing of Environment*, 220, 41–50. <https://doi.org/10.1016/j.rse.2018.10.032>
- North, W. J., James, D. E., & Jones, L. G. (1993). History of kelp beds (Macrocystis) in Orange and San Diego Counties, California. *Hydrobiologia*, 260–261(1), 277–283. <https://doi.org/10.1007/BF00049029>

- O'Neill, J. D., & Costa, M. (2013). Mapping eelgrass (*Zostera marina*) in the Gulf Islands National Park Reserve of Canada using high spatial resolution satellite and airborne imagery. *Remote Sensing of Environment*, 133, 152–167. <https://doi.org/10.1016/j.rse.2013.02.010>
- Olson, A. M., Hessing-Lewis, M., Haggarty, D., & Juanes, F. (2019). Nearshore seascape connectivity enhances seagrass meadow nursery function. *Ecological Applications*, 29(5), e01897. <https://doi.org/10.1002/eap.1897>
- Padma, S., & Sanjeevi, S. (2014). Jeffries Matusita based mixed-measure for improved spectral matching in hyperspectral image analysis. *International Journal of Applied Earth Observation and Geoinformation*, 32, 138–151. <https://doi.org/10.1016/j.jag.2014.04.001>
- Peterson, C. H., Rice, S. D., Short, J. W., Esler, D., Bodkin, J. L., Ballachey, B. E., & Irons, D. B. (2003). Long-Term Ecosystem Response to the Exxon Valdez Oil Spill. *Science*, 302, 2082–2086. <https://doi.org/10.1126/science.277.5325.509>
- Pfister, C. A., Berry, H. D., & Mumford, T. (2018). The dynamics of Kelp Forests in the Northeast Pacific Ocean and the relationship with environmental drivers. *Journal of Ecology*, 1–14. <https://doi.org/10.1111/1365-2745.12908>
- Preikshot, D., Beamish, R. J., Sweeting, R. M., Neville, C. M., & Beacham, T. D. (2012). The residence time of juvenile Fraser river sockeye salmon in the strait of Georgia. *Marine and Coastal Fisheries*, 4(1), 438–449. <https://doi.org/10.1080/19425120.2012.683235>
- Reed, D. C., Rassweiler, A., Carr, M. H., Cavanaugh, K. C., Malone, D. P., & Siegel, D. A. (2011). Wave disturbance overwhelms top-down and bottom-up control of primary production in California kelp forests. *Ecology*, 92(11), 2108–2116. <https://doi.org/10.1890/11-0377.1>
- Reed, D. C., Schroeter, S. C., & Raimondi, P. T. (2004). Spore supply and habitat availability as sources of recruitment limitation in the giant kelp *Macrocystis pyrifera* (Phaeophyceae). *Journal of Phycology*, 40(2), 275–284. <https://doi.org/10.1046/j.1529-8817.2004.03119.x>
- Richards, G., & Congalton, R. G. (2001). Accuracy assessment and validation of remotely sensed and other spatial information. *International Journal of Wildland Fire*, 10, 321–328. <https://doi.org/10.1071/WF01031>
- Richards, J. A. (2013). *Remote sensing digital image analysis: An introduction*. *Remote Sensing Digital Image Analysis: An Introduction*. Berlin, Heidelberg: Springer. <https://doi.org/10.1007/978-3-642-30062-2>
- Riche, O., Johannessen, S. C., & Macdonald, R. W. (2014). Why timing matters in a coastal sea: Trends, variability and tipping points in the Strait of Georgia, Canada. *Journal of Marine Systems*, 131, 36–53. <https://doi.org/10.1016/j.jmarsys.2013.11.003>
- Roesler, C. S., & Perry, M. J. (1995). In situ phytoplankton absorption, fluorescence emission, and particulate backscattering spectra determined from reflectance. *Journal of Geophysical Research*, 100(C7), 279–294. <https://doi.org/10.1029/95JC00455>
- Rooper, C. N., Williams, K., De Robertis, A., & Tuttle, V. (2015). Effect of underwater lighting on observations of density and behavior of rockfish during camera surveys. *Fisheries*

- Research*, 172, 157–167. <https://doi.org/10.1016/j.fishres.2015.07.012>
- Rouse, J., Haas, R., Schell, J., & Deering, D. (1974). Monitoring vegetation systems in the Great Plains with ERTS. In *Third ERTS Symposium, NASA SP-351* (pp. 309–317). Washington, DC. <https://doi.org/10.1002/mrm.26868>
- Ruff, C. P., Anderson, J. H., Kemp, I. M., Kendall, N. W., Mchugh, P. A., Velez-Espino, A., ... Rawson, K. (2017). Salish Sea Chinook salmon exhibit weaker coherence in early marine survival trends than coastal populations. *Fisheries Oceanography*, 26(6), 625–637. <https://doi.org/10.1111/fog.12222>
- Ryer, C. H., Stoner, A. W., Iseri, P. J., & Spencer, M. L. (2009). Effects of simulated underwater vehicle lighting on fish behavior. *Marine Ecology Progress Series*, 391, 97–106. <https://doi.org/10.3354/meps08168>
- Schiel, D. R., & Foster, M. S. (2015). *The biology and ecology of giant kelp forests* (1st ed.). Oakland, California: University of California Press.
- Schiel, D. R., Steinbeck, J. R., & Foster, M. S. (2004). Ten Years of Induced Ocean Warming Causes Comprehensive changes in marine benthic communities. *Ecology*, 85(7), 1833–1839. <https://doi.org/10.1890/03-3107>
- Schindler, D. E., Scheuerell, M. D., Moore, J. W., Gende, S. M., Francis, T. B., & Palen, W. J. (2003). Pacific salmon and the ecology of coastal ecosystems. *Frontiers in Ecology*, 1(1), 31–37.
- Schmidt, M., Pearsall, I., Riddell, B., Sucic, T., & Ewanciw, M. (2018). 2016 Year-end Report to the Pacific Salmon Commission and their Southern Fund Committee, 1–112. Retrieved from marinesurvivalproject.com
- Schowengerdt, R. A. (2012). *Remote sensing models and methods for image processing* (3rd ed.). San Diego: Academic Press.
- Schroeder, S. B., Dupont, C., Boyer, L., Juanes, F., & Costa, M. (2019). Passive remote sensing technology for mapping bull kelp (*Nereocystis luetkeana*): A review of techniques and regional case study. *Global Ecology and Conservation*, 19, e00683. <https://doi.org/10.1016/j.gecco.2019.e00683>
- Shaffer, A. (2004). *Preferential use of Nearshore Kelp Habitats by Juvenile Salmon and Forage Fish. Proceedings of the 2003 Georgia Basin/Puget Sound Research Conference*. Retrieved from http://www.caseinlet.org/uploads/SalmonKelp_Shaffer__1_.pdf
- Shaffer, J. A., & Parks, D. S. (1994). Seasonal Variations in and Observations of Landslide Impacts on the Algal Composition of a Puget Sound Nearshore Kelp Forest. *Botanica Marina*, 37(4), 315–324. <https://doi.org/10.1515/botm.1994.37.4.315>
- Shi, W., & Wang, M. (2009). Green macroalgae blooms in the Yellow Sea during the spring and summer of 2008. *Journal of Geophysical Research*, 114, C12010. <https://doi.org/10.1029/2009JC005513>
- Simonson, E. J., Scheibling, R. E., & Metaxas, A. (2015). Kelp in hot water: I. Warming seawater temperature induces weakening and loss of kelp tissue. *Marine Ecology Progress Series*,

- 537, 89–104. <https://doi.org/10.3354/meps11438>
- Smith, L. (1988). Effects of observer swimming speed on sample counts of temperate rocky reef fish assemblages. *Marine Ecology Progress Series*, 43, 223–231. <https://doi.org/10.3354/meps043223>
- Springer, Y., Hays, C., Carr, M., & Mackey, M. (2007). Ecology and Management of the bull kelp, (*Nereocystis luetkeana*): A synthesis with recommendations for future research. Lenfest Ocean Program, Washington, D.C., USA. Retrieved from https://www.lenfestocean.org/-/media/legacy/lenfest/pdfs/springer_underlying_report_0.pdf
- Stekoll, M. S., Deysher, L. E., & Hess, M. (2006). A remote sensing approach to estimating harvestable kelp biomass. *Journal of Applied Phycology*, 18, 323–334. <https://doi.org/10.1007/s10811-006-9029-7>
- Steneck, R. S., Graham, M. H., Bourque, B. J., Corbett, D., Erlandson, J. M., Estes, J. A., & Tegner, M. J. (2002). Kelp forest ecosystems: biodiversity, stability, resilience and future. *Environmental Conservation*, 29(4), 436–459. <https://doi.org/10.1017/s0376892902000322>
- Suchy, K., Costa, M., & Perry, I. (2019). Influence of environmental drivers on satellite-derived chlorophyll a in the Strait of Georgia. *Progress in Oceanography*, 176, 102134. <https://doi.org/10.1016/j.pocean.2019.102134>
- Sutherland, I. R., Karpouzi, V., Mamoser, M., & Carswell, B. (2008). *Kelp Inventory, 2007: Areas of the British Columbia Central Coast from Hakai Passage to the Bardswell Group*. Ministry of Environment, Oceans and Marine Fisheries Branch. Retrieved from <http://www.env.gov.bc.ca/omfd/reports/Kelp2007-HakaiPass.pdf>
- Swain, P. H., & King, R. C. (1973). *Two Effective Feature Selection Criteria for Multispectral Remote Sensing. Laboratory for Applications of Remote Sensing (LARS) Technical Reports* (Vol. 39).
- Taheri, S. M., & Hesamian, G. (2013). A generalization of the Wilcoxon signed-rank test and its applications. *Statistical Papers*, 54(2), 457–470. <https://doi.org/10.1007/s00362-012-0443-4>
- Taylor, D. I., & Schiel, D. R. (2005). Self-replacement and community modification by the southern bull kelp (*Durvillaea antarctica*). *Marine Ecology Progress Series*, 288, 87–102. <https://doi.org/10.3354/meps288087>
- Taylor, D. I., & Schiel, D. R. (2018). Algal populations controlled by fish herbivory across a wave exposure gradient on southern temperate shores. *Ecology*, 91(1), 201–211.
- Teagle, H., Hawkins, S. J., Moore, P. J., & Smale, D. A. (2017). The role of kelp species as biogenic habitat formers in coastal marine ecosystems. *Journal of Experimental Marine Biology and Ecology*, 492, 81–98. <https://doi.org/10.1016/j.jembe.2017.01.017>
- Thom, R. M., & Hallum, L. (1990). *Long-term changes in the areal extent of tidal marshes, eelgrass meadows and kelp forests of Puget Sound. Final Report to Office of Puget Sound, Region 10 U.S. Environmental Protection Agency*.
- Tillotson, M. D., Kelly, R. P., Duda, J. J., Hoy, M., Kralj, J., & Quinn, T. P. (2018). Concentrations of environmental DNA (eDNA) reflect spawning salmon abundance at fine

- spatial and temporal scales. *Biological Conservation*, 220, 1–11.
<https://doi.org/10.1016/j.biocon.2018.01.030>
- Tou, J. T., & Gonzalez, R. C. (1974). *Pattern recognition principles*. Reading, Mass: Addison-Wesley.
- Traganos, D., Aggarwal, B., Poursanidis, D., Topouzelis, K., Chrysoulakis, N., & Reinartz, P. (2018). Towards global-scale seagrass mapping and monitoring using Sentinel-2 on Google Earth Engine: The case study of the Aegean and Ionian Seas. *Remote Sensing*, 10(8), 1–14.
<https://doi.org/10.3390/rs10081227>
- Trebilco, R., Dulvy, N. K., Stewart, H., & Salomon, A. K. (2015). The role of habitat complexity in shaping the size structure of a temperate reef fish community. *Marine Ecology Progress Series*, 532, 197–211. <https://doi.org/10.3354/meps11330>
- Uhl, F., Bartsch, I., & Oppelt, N. (2016). Submerged kelp detection with hyperspectral data. *Remote Sensing*, 8(6), 487. <https://doi.org/10.3390/rs8060487>
- Uhl, F., Oppelt, N., & Bartsch, I. (2013). Spectral mixture of intertidal marine macroalgae around the island of Helgoland (Germany, North Sea). *Aquatic Botany*, 111, 112–124.
<https://doi.org/10.1016/j.aquabot.2013.06.001>
- Vadas, R. L. (1972). Ecological Implications of Culture Studies on *Nereocystis luetkeana*. *Journal of Phycology*, 8(2), 196–203. <https://doi.org/10.1111/j.0022-3646.1972.00196.x>
- Van Wagenen, R. F. (2015). *Washington coastal kelp resources: Port Townsend to the Columbia River, Summer 2014. Final report*. Washington Department of Natural Resources. Olympia, WA.
- Vergés, A., Doropoulos, C., Malcolm, H. A., Skye, M., Garcia-Pizá, M., Marzinelli, E. M., ... Steinberg, P. D. (2016). Long-term empirical evidence of ocean warming leading to tropicalization of fish communities, increased herbivory, and loss of kelp. *Proceedings of the National Academy of Sciences*, 113(48), 13791–13796.
<https://doi.org/10.1073/pnas.1610725113>
- Volent, Z., Johnsen, G., & Sigernes, F. (2007). Kelp forest mapping by use of airborne hyperspectral imager. *Journal of Applied Remote Sensing*, 1, 011503.
<https://doi.org/10.1117/1.2822611>
- Waldichuk, M. (1957). Physical Oceanography of the Strait of Georgia, British Columbia. *Fisheries Research Board of Canada*, 14(3), 321–486.
- Wang, M., & Hu, C. (2016). Mapping and quantifying Sargassum distribution and coverage in the Central West Atlantic using MODIS observations. *Remote Sensing of Environment*, 183, 350–367. <https://doi.org/10.1016/j.rse.2016.04.019>
- Watson, J., & Estes, J. A. (2011). Stability, resilience, and phase shifts in rocky subtidal communities along the west coast of Vancouver Island, Canada. *Ecological Monographs*, 81(2), 215–239. <https://doi.org/10.1890/10-0262.1>
- Weaver, D. M., Kwak, T. J., & Pollock, K. H. (2014). Sampling Characteristics and Calibration of Snorkel Counts to Estimate Stream Fish Populations. *North American Journal of*

- Fisheries Management*, 34(6), 1159–1166. <https://doi.org/10.1080/02755947.2014.951808>
- Wheeler, W. N., Smith, R. G., & Srivastava, L. M. (1984). Seasonal Photosynthetic Performance of *Nereocystis luetkeana*. *Canadian Journal of Botany*, 62(4), 664–670.
- Young, M., Cruz, S., Cavanaugh, K., Angeles, L., Bell, T., Barbara, S., & Raimondi, P. (2016). Environmental controls on spatial patterns in the long-term persistence of giant kelp. *Ecology*, 86(1), 45–60.
- Yu, Q., Gong, P., Clinton, N., Biging, G., Kelly, M., & Schirokauer, D. (2006). Object-based Detailed Vegetation Classification with Airborne High Spatial Resolution Remote Sensing Imagery. *Photogrammetric Engineering & Remote Sensing*, 72(7), 799–811. <https://doi.org/10.14358/PERS.72.7.799>